Alma Mater Studiorum - Università di Bologna

FACOLTÀ DI SCIENZE MATEMATICHE, FISICHE E NATURALI

Scuola di Dottorato in
Biologia cellulare, molecolare e industriale

Progetto Biologia e Fisiologia Cellulare
Ciclo XXI
Settore scientifico disciplinare BIO/18 Genetica

Coordinatore: Prof.ssa Michela Rugolo

Morphogenesis of follicular epithelium in *Drosophila melanogaster*: function of *von Hippel-Lindau* tumour suppressor gene

Presentata da:
Dott.ssa Serena Duchi

Tutore:
Prof. Giuseppe Gargiulo

Anno Accademico 2007 - 2008

INDEX

1. INTRODUCTION

During my PhD research program I've been involved in several projects regarding the analysis of follicular epithelium morphogenesis during *Drosophila melanogaster* oogenesis. This process represents a powerful model system for investigating many aspects of cell and developmental biology. Its usefulness can be attributed partly to the genetic tractability of *Drosophila* as a model system; however, it is also one of the most intensively and successfully studied stages in the development of this model organism. The development of a single stem cell into a mature egg requires almost every cellular processes that can occur during development from cell cycle control and fate specification to cell polarization and epithelial morphogenesis. Hence a system that appears relatively simple on the surface can provide insights applicable to more complex processes, such as vertebrate development and disease progression.

Another useful facet of *Drosophila* oogenesis is practical. The ovary is the single largest organ in the female fly and the oocyte the single largest cell. A single ovary contains every stage of development from stem cell to mature egg, and each egg chamber contains both somatic (follicle cells) and germline cells (oocyte and nurse cells), allowing easy comparison and extensive manipulation.

1.1. Overview of *Drosophila melanogaster* oogenesis

The female reproductive system, occupying the posterior two-thirds of abdomen, consists of two ovaries which are joined by two short lateral oviducts to a common median oviduct, and this in turn enters the uterus. The latter opens to the exterior through the vulva, situated between the gonopods, which form the retractile ovipositor. Opening into the genital chamber are a ventral seminal receptacle, a pair of spermathecae and a pair of accessory glands (Fig. 1).

The ovaries are compact and pyriform and lie bilaterally in the third, fourth and fifth abdominal segments, surrounded by adipose tissue. The size of the ovaries varies with the extent of the development of the eggs and with the nature of the individual. The abdomen is distended by their growth. Each ovary consists of a compact group of parallel egg tubes or ovarioles which ordinarily vary in number from 10 to 20, each containing a string of developing egg chambers of progressive age. The ovarioles are held together by a thin connective-tissue envelope, the peritoneal sheath, and converge basally where they are attached to the calyx of the lateral oviduct.

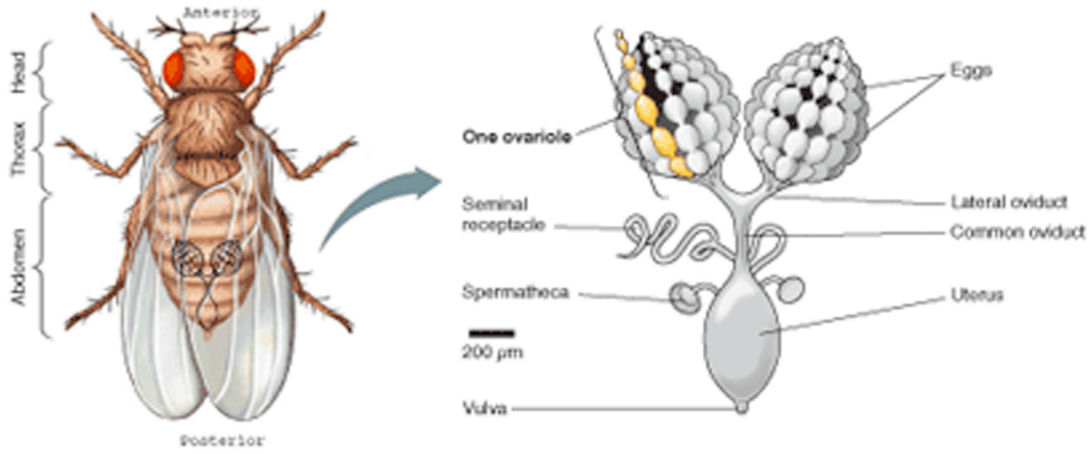

Figure 1. The Reproductive System of the *Drosophila* female.
A dorsal view indicating where the reproductive system is located in the abdomen. The enlargement on the right shows the basic parts of the gonad, the tracts, and some of the accessory organs, including the seminal receptacle and spermatheca, where sperm is stored.

The event of oogenesis takes place in the egg chamber, which consists of the oocyte and 15 nurse cells, surrounded by a monolayer of approximately 1.000 follicle cells. Based on the morphology of the maturing egg chamber, oogenesis has been divided into 14 stages (Fig. 2) (King, 1970; Spradling, 1993) temporally well determined. The ovariole is considered the morphological and functional unit of the

ovary and is structurally divided into two different regions: a proximal one, called vitellarium, where egg chambers develop into mature eggs, and a distal one, called germarium, characterized by the presence of germline and somatic stem cell populations.

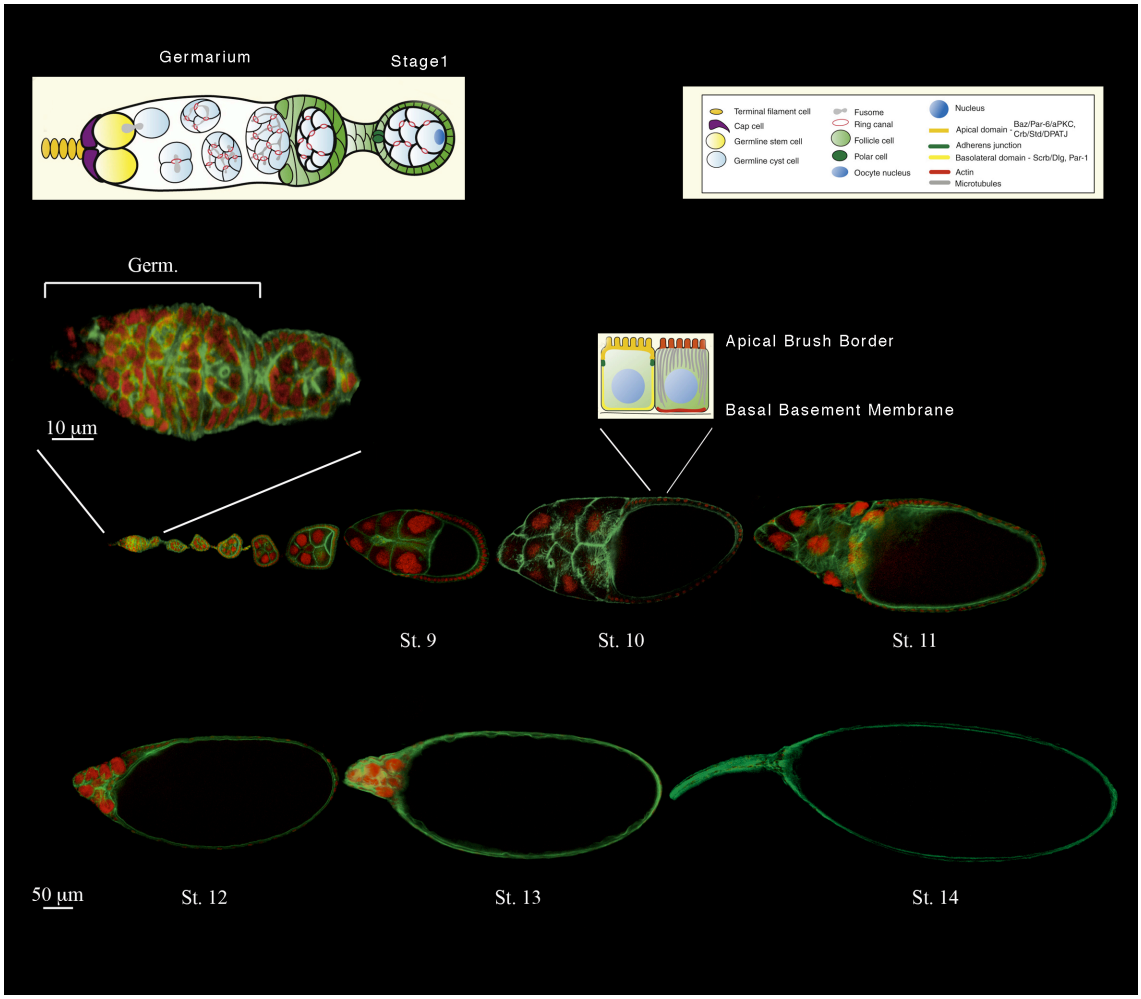

Figure 2. Stages of egg chamber development.
Confocal cross-sections of wild-type egg chambers. Staining of *Drosophila* egg chambers is facilitated with labelling with FITC-phalloidin (green) that reveals F-actin cytoskeleton and with nuclear dye propidium iodide (red). A high magnification and a schematic representation of the germarium and of a stage-1 egg chamber are shown (top left). During mid-oogenesis (stages 9-11), the rearrangement of follicle cells and the increasing size of the oocyte become evident. In the late stages (stages 12-14), oocyte growth continues and the nurse cells, after carrying out their function, undergo death. In the inset is shown the schematic representation of follicle cells morphology at stage 10B. germ., germarium; st., stage. (Modified from Cavaliere et al., 2008)

1.2. The germarium

The germline stem cells lie at the far anterior of the germarium in contact with a somatic structure known as the terminal filament (Fig. 2, see inset at the top left). These cells divide asymmetrically to produce another stem cell and a daughter cell, which begins to differentiate. The daughter cell undergoes four mitotic divisions with incomplete cytokinesis to form a cyst of 16 cells interconnected by cytoplasmic bridges known as ring canals. The orientation of these divisions is controlled by the fusome, a branched structure composed of a continuous endoplasmic reticulum surrounded by cortical cytoskeletal components and microtubules. This ensures that each cyst contains eight cells with one ring canal, four with two, two with three and two with four ring canals. One of these 16 cells will differentiate as the oocyte, while the others become polyploid nurse cells, synthetizing nutrients and cytoplasmic components to be transported into the oocyte (Lin and Spradling, 1993). The oocyte is the only cell within the cyst that will progress through meiosis; it arrests during prophase I before exiting the germarium and does not continue until the mature egg is laid and activated. Nearby, somatic stem cells give rise to precursor follicle cells and about 16 of them invade between adjoining cysts, cease division, and become pre-polar cells, which ultimately become polar cells and stalk cells. Inward migration of polar, stalk, and epithelial cells separate individual germline cysts into discrete egg chambers (Horne-Badovinac and Bilder, 2005). As the cyst exits the germarium, the other somatic cells covering each chamber, the epithelial follicle cells, remain undifferentiated. Determination of the oocyte occurs gradually as the cyst travels through the germarium. Cell-fate markers, along with markers of meiotic chromosome pairing, become restricted to the two cells containing four ring canals known as pro-oocytes. By the time the cyst has been

enveloped by somatic follicle cells, these markers have been restricted to a single cell, which will become the oocyte. When the cyst then enters region II it flattens and centrosomes, mitochondria, golgi vesicles, various proteins and RNA coalesce at the anterior of the oocyte to form a Balbiani body. As the follicle cells migrate inwards to envelope the cyst it rounds up, with the oocyte always coming to rest at the posterior. Finally, the oocyte itself polarizes, with the centrosomes and a subset of proteins and RNAs specifically localized to the posterior (Grünert and St Johnston, 1996). At the same time the DNA within the oocyte nucleus condenses into a compact structure known as the karyosome (Huynh and St Johnston, 2004).

1.3. Follicular epithelium

Studies in cultured cells have driven our understanding of mechanisms that regulate cell shape and migration. The application of this mechanistic information to living tissues remains a challenge. Genetic studies in the model invertebrate *Drososphila melanogaster* have been instrumental for illuminating how cell biological mechanisms are orchestrated during tissue morphogenesis. An important tissue for such studies is the follicular epithelium that surrounds the maturing fly oocyte, a single monolayer epithelium with a pronounced apicobasal polarity (Fig. 2, inset over stage 10B). Elegant developmental and genetic studies have revealed that this epithelium develops coordinately with the oocyte and establishes the body axes of the resultant embryo. Cell–cell communication coordinates the morphogenesis of the follicular epithelium with the associated germ cells, in much the same way as epithelial–mesenchymal interactions drive tissue formation in vertebrates.

Follicle cells that surround the egg chamber undergo mitotic divisions to follow the increase in size of the germline cells. By stage 7, the epithelial follicle cells cease proliferation and enter endocycles, a change in cell cycle triggered by Notch signalling (Shcherbata et al., 2004; Horne-Badovinac and Bilder, 2005). Afterwards, these cells begin to show morphological and molecular signs of differentiation into the five main epithelial fates: border, stretched, centripetal, posterior, and main body follicle cells (Fig. 3).

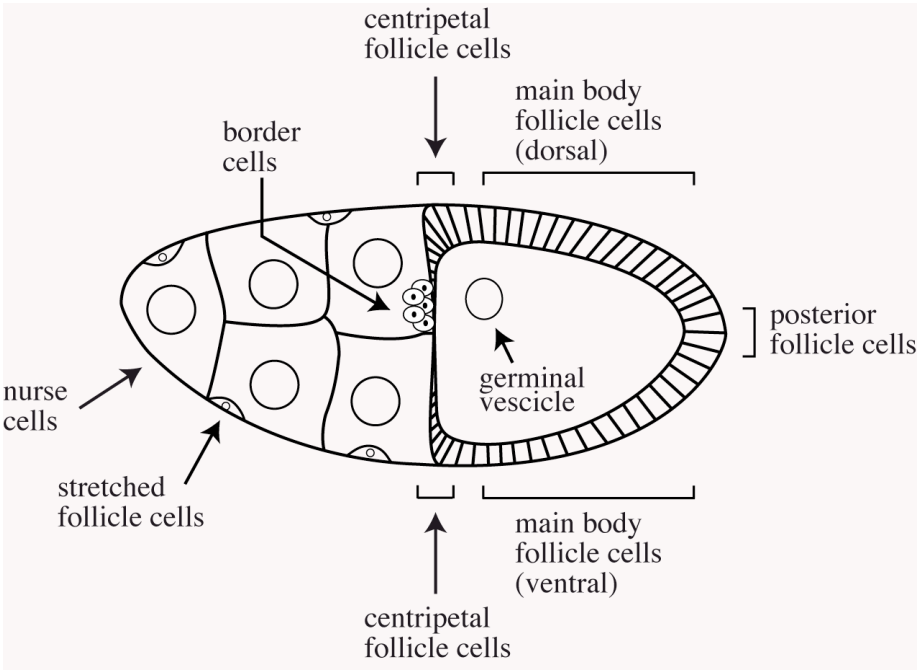

Figure 3. Schematic view of different cell populations in the stage 10B egg chamber.

Each of these follicle cell subpopulations has a specific function with respect to the production of a mature egg, such as the correct number and position of each type which is critical to ultimate egg morphogenesis. These functions influence the production of structures that are essential to the egg, such as the dorsal respiratory

appendages and the micropyle. These functions are also critical for proper anterior-posterior organization of the oocyte and, therefore, also for the resulting embryo (Xi et al., 2003). Follicle cells form a cuboidal epithelium until stage 8, but at the beginning of stage 9 they reorganize in a series of migrations. The 6-10 anterior-most follicle cells, the border cells, migrate through the nurse cells to the oocyte anterior end. Another 50 anterior cells, the stretched cells, form a flattened epithelium overlying the nurse cells. Polar cells reside at the anterior and posterior termini of egg chamber and organize follicle cell fates throughout oogenesis. They provide cues for axial patterning of the embryo, create a porthole for sperm entry, and organize the specialized eggshell domains thought to enhance embryonic survival (Beccari et al., 2002; Xi et al., 2003; Grammont and Irvine, 2002). Coincidently with these events in the soma, the oocyte itself is busy re-arranging its polarity. At stage 6, the posterior terminal follicle cells differentiate upon Epidermal Growth Factor Receptor (Egfr) activation, and then produce an as-yet unidentified feedback signal to the germline. A consequence of this feedback is that the posterior oocyte microtubule organizing centre (MTOC) breaks down and a new one forms at the anterior pole, thus reversing the polarity of the oocyte's microtubule network. Accompanying this process is a movement of the germinal vesicle away from the posterior pole to localize at the anterior corner of the oocyte, where it activates the Egfr once more to establish the polarity of the dorsal ventral axis (Lopez-Schier, 2003). During oogenesis, nurse cells also undergo nuclear changes, which involve a series of endoreplication cycles that increase their polyploid values (from 512 to 2,048). Nurse cells develop a complex microtubular apparatus organized in ring canals through which they transfer to the oocyte mRNA, proteins, organelles, and lipidic droplets, contents that are important for the correct development

of the future embryo. During early stages of oogenesis, this transfer is slow but continuous and increases strongly at stage 10B. From stage 10B to stage 12, nurse cells transfer all their cytoplasmic contents to the oocyte and finally undergo apoptosis (Cavaliere et al., 1998; Foley and Cooley, 1998). At stage 14 of oogenesis, after the construction of eggshell, the follicle cells die by apoptosis (Nezis et al., 2002).

1.4. Eggshell morphology

The *Drosophila* eggshell is an extracellular structure functional to the different roles it absolves, from egg fertilization to the hatching of the larva at the end of embryogenesis (Margaritis, 1985; Margaritis and Mazzini, 1998; Waring, 2000). This framework is laid down during late oogenesis between the oocyte and overlying follicle cells. The eggshell proteins, secreted by the follicle cells, assemble into a highly organized structure featuring both radial and regional complexity. This eggshell specialization depends on sequential and in some cases combined activities of the known major signaling pathways during the middle and late stages of oogenesis. Five morphologically distinct layers have been identified in the *Drosophila* eggshell: an oocyte proximal vitelline membrane (approximately 300 nm), a lipid wax layer, an inner chorion layer (40-50 nm), an endochorion (500-700 nm), and an exochorion (300-500 nm) (Fig. 4A). The vitelline membrane is the first layer to be made up by follicular epithelium and appears as a continuous granular layer without prominent substructures. Its deposition begins during stage 9, when the vitelline membrane proteins appear accumulated on the surface of the oocyte in small vesicles called vitelline bodies. At stage 10B, these vesicles fuse to form a continuous thick layer, which gradually thins down as oogenesis proceeds (Margaritis et al., 1980; Margaritis, 1985). Deposition of

the wax layer begins in late stage 10 with the accumulation of lipid-filled vesicles between follicle cells and vitelline membrane. Synthesis and secretion of lipid vesicles proceed through stage 12. As the lipid vesicles accumulate on the vitelline membrane surface, they take on a flat appearance. During stage 14, the vesicles are compressed into three to four planes of overlapping plaques, which create a water-impermeable layer between the vitelline membrane and chorion (reviewed in Waring, 2000). The inner chorion layer is also continuous and characterized by periodic structure. At the end of choriogenesis the inner chorion layer acquires its final thickness and unique crystalline substructure. Three-dimensional reconstructions reveal that the crystalline inner chorion layer consists of two types of subunits, which appear to be grouped into an octamer of four dimer pairs (Margaritis et al., 1984). Ultrastructural analyses of stage 14 egg chambers and isolated endochorions reveal the tripartite nature of this layer (Margaritis et al., 1980). A thin fenestrated floor is separated from a thick outer roof layer by vertical pillars creating cavities that facilitate gas exchange (Fig. 4A). The continuous outer roof network displays ridges and it defines the borders of the follicle cell imprints. The imprints in the main body of the eggshell are fairly uniform, with those on the dorsal side being more elongate than those found ventrally. Freeze-fractured views of endochorion reveal globular structures interconnected via fine fibrils (Margaritis and Mazzini, 1998). The exochorion consists of loose fibers that tend to be oriented parallel to the oocyte surface. It usually appears to consist of two layers, the innermost being less electron dense.

Like most insect eggs, several regional specializations are apparent on the surface of the *Drosophila* eggshell. Its anterior end is characterized by a nearly flat plate called operculum, a specialized region that has evolved to facilitate hatching of the larva

at the end of embryogenesis. The operculum is flanked by the micropyle at its anterior end and two long appendages at its posterior end (Fig. 4B). The micropylar apparatus is a protuberance through which sperm gains access to the oocyte membrane. By serving as gills, the respiratory appendages on either side of the dorsal midline allow eggs to carry out gas exchange when they are submerged under water. These appendages are long and largely cylindrical, but slightly paddle-shaped at the tip. Each appendage starts to be formed at stage 11 by a population of 65-70 columnar follicle cells, which migrate out over the stretched cells on either side of the dorsal midline. The follicle cells then spread out to form the flat paddle structure (Rittenhouse and Berg, 1995). In the posterior pole, a group of approximately 20-30 follicle cells leave imprints distinctly smaller than those in the main body. Here, two nested rings of distinct cell imprints form the aeropyle (Fig. 4B) (Margaritis et al., 1980; Dobens and Raftery, 2000) a specialized region thought to be also involved in gas exchange.

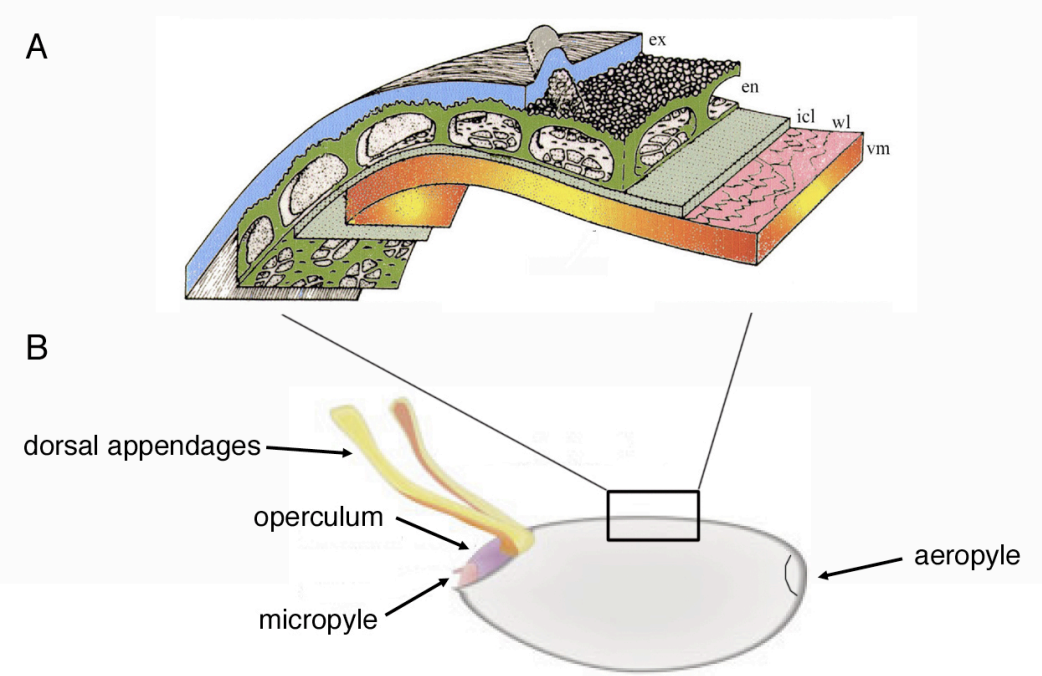

Figure 4. Eggshell morphology.
A: Schematic view of a multilayered eggshell as seen in the central main body region. The inner layers include the vitelline membrane (vm), the wax layer (wl), and the inner chorion layer (icl). The outer layers include the endochorion (en), where a thin fenestrated floor is separated from an outer roof by vertical pillar creating cavities as indicated, and the exochorion (ex). B: Schematic structure of *Drosophila* egg illustrating the specialized regions of the shell. The prominent structures indicated are the micropyle, the operculum, and the dorsal appendages. Aeropyle is also indicated.

1.5. Expression in time and space of eggshell genes: *VM32E*'s case

Precise timing of synthesis of different eggshell components is relevant for the ordered assembly of the five layers and it relies on a fine regulation of gene expression (Waring, 2000). The genes encoding major eggshell structural proteins are transcribed in follicle cells during stages 8-14 of oogenesis in a well-defined temporal order (King, 1970; Spradling, 1993; Waring, 2000). The vitelline membrane genes are mainly expressed during mid-oogenesis stages 8-10, while the chorion genes are transcribed from stage 11 onward. The chorion synthesis, which occurs in the last 5-6 hours of oogenesis, requires both rapid production of large amounts of protein as well as fine control over the timing of gene expression. These requirements are met in two ways: (1)

by amplification of the two chorion gene clusters and (2) by precise transcriptional control of the individual chorion genes (Cavaliere et al., 2008).

Developmental control of eggshell gene expression relies in some instances on transcription of closely linked genes. Four vitelline membrane structural components genes are located on the left arm of the second chromosome. Their names refer to the map location on the polytene chromosome: *VM32E*, *VM34C*, *VM26A.1*, and *VM26A.2* (Higgins et al., 1984; Mindrinos et al., 1985; Burke et al., 1987; Popodi et al., 1988; Gigliotti et al., 1989). While *VM32E* and *VM34C* are isolated, *VM26A.1* and *VM26A.2* appear to be clustered with other putative vitelline membrane genes (Popodi et al., 1988).

The timing of eggshell protein synthesis is not always related to the final position of the proteins in the eggshell. Indeed, after their secretion the eggshell components could undergo trafficking between layers. Therefore, classifying them either as vitelline membrane or chorion proteins is not always clear. The highly dynamic state shown by some eggshell components, reflected by their trafficking between layers, appears evident by analyzing the VM32E protein (Andrenacci et al., 2001). At the time of its synthesis (stage 10), VM32E protein is not detectable in anterior and posterior follicle cells. However, it is able to diffuse in the extracellular space around the oocyte, and by stage 11 it is evenly distributed in the vitelline membrane. Moreover, as assessed by immunoelectron microscopy, at late stages of oogenesis VM32E protein is partially released from the vitelline membrane and becomes included in the endochorion layer too. A detailed functional analysis of the different VM32E domains showed that the C-terminal domain is required for this partial relocalization of the VM32E protein.

Chorion Gene Amplification

To compensate for the limited time for maximal expression, chorion genes undergo selective amplification in order to meet production of massive amounts of chorion proteins (Parks and Spradling, 1987). The degree of amplification differs between the two chorion gene clusters. The X chromosome cluster is amplified 16-fold, while the third chromosome cluster undergoes 60 rounds of amplification (Delidakis et al., 1989; Orr-Weaver, 1991). Besides these clusters, two other developmental amplicons have been isolated. These are localized, respectively, at 30B and 62D and are ampliflied to a less extent. Although they do not contain chorion genes, these sites include genes that are expressed in the follicle cells during late oogenesis and could probably function in eggshell formation (Claycomb et al., 2004).

Transcriptional control of Eggshell Genes

The *Drosophila* egg has a characteristic asymmetric shape and contains functionally important regional features that are constructed by subgroups of follicle cells. The existence of regional specializations suggests that eggshell gene expression is regulated spatially as well as temporally during oogenesis. Indeed, the spatial expression pattern of the different chorion genes has shown that while the genes of the third chromosome cluster (*s15*, *s16*, *s18*, and *s19*) are expressed throughout the follicular epithelium, the expression of X-linked chorion genes (*s36* and *s38*) is initially detected in a small dorsal sub-population of stage 10B follicle cells. However, in later stages these genes are expressed in all follicle cells. In addition, some minor chorion genes are expressed in a more localized manner (Parks and Spradling, 1987). Interestingly, among the putative chorion genes recently identified, several show

preferential expression in follicle cells covering specific regions of the eggshell suggesting they encode components that could contribute to specific structural features of the eggshell (Fakhouri et al., 2006).

Since the vitelline membrane is made up of only a single eggshell layer distributed all around the egg membrane, the different vitelline membrane genes should have a similar expression pattern. The transcript of the *VM26A.2* gene, encoding the most abundant component of the vitelline membrane, is detected in all follicle cells surrounding the oocyte from stage 8. Conversely, the *VM32E* gene shows a peculiar spatial transcriptional profile and its expression is restricted at stage 10 of oogenesis (Gargiulo et al., 1991). Its transcript is detected in the main body follicle cells and is absent in the anterior and posterior follicle cells. Within the main body follicle cells, the expression of VM32E is temporally regulated. The expression starts at stage 10A and it appears to spread from the ventral to the dorsal follicle cell domain. This unique expression pattern may be linked to some special functions that the VM32E protein would carry out during vitelline membrane assembly and/or in endochorion formation.

1.6. Egfr pathway during oogenesis

During oogenesis, the Egfr pathway establishes both the anterior-posterior and dorsoventral axes of the egg chamber. Axis specification requires spatially restricted activation of the Egfr in the somatically-derived follicular epithelium of the egg chamber by its germline specific ligand Gurken (Grk), a transforming growth factor-alpha (TGF-α) signaling molecule (Neuman-Silberberg and Schüpbach, 1993, 1996; Schüpbach, 1987). During oogenesis, the egg chamber acquires a dorsoventral polarity when the asymmetrically localized Grk protein activates a gradient of Egfr activity

resulting in the induction of distinct follicle cell fates along the dorsoventral axis. High levels of Grk induce dorsal follicle cell fates (Ray and Schüpbach, 1996; Perrimon and Perkins, 1997; Dobens and Raftery, 2000), and activate both a positive and a negative feedback signaling leading to the definition of two separate populations of dorsal follicle cells that will guide the production of the two dorsal appendages (Wasserman and Freeman, 1998; Peri et al., 1999). The most ventral follicle cells, which have the lowest level of Egfr activity, express the *pipe* gene, which determines the ventral follicle cell fate of the future embryo (Sen et al., 1998). Therefore, a gradient of Egfr activity along the dorsoventral axis determines the full range of follicle cell fates.

Anterior posterior axis formation in the oocyte requires activation of Egfr pathway in the posterior follicle cells (PFC) where it also redirects them from the default anterior to the posterior cell fate (González-Reyes and St Johnston, 1998).

Despite the importance of Egfr signaling in axis formation, this receptor is also involved in the correct follicle cell fate specification since has been shown that mutation affecting Ras, known to transduce Egfr signal, disrupt follicle cell polarity (Poulton and Deng, 2006). *grk* and *egfr* mutations in the posterior follicle cells (PFCs) cause the affected cells to express behavioral and morphological characteristics associated with the anterior follicle cells fate (AFCs). Subsequently the affected cells tend to lose the columnar morphology typical of PFC (González-Reyes and St Johnston, 1995; González-Reyes and St Johnston, 1998) which is almost certainly linked to their apicabasal polarity (Poulton and Deng, 2006).

1.7. Follicular epithelium morphology

The follicular epithelium surrounding the germline cyst is a simple monolayer with a pronounced apicobasal polarity. The follicle cell membrane is partitioned into apical and basolateral domains that accumulate different sets of membrane proteins, which become separated by the formation of a series of cell junctions along the apicobasal axis of the lateral membrane (Müller, 2000; Wu et al., 2008; Horne-Badovinac and Bilder, 2005; Knust, 2000; Knust et al., 2002; Tepass et al., 2001). Disruption of different apical/basal polarity complexes has different consequences (Wu et al., 2008). Each junction contains proteins conserved in vertebrate's epithelia (Table 1). Vertebrate epithelial cells contain two types of apical junctions, the tight junction (TJ) and the adherens junction (AJ). In the epithelial cells of *Drosophila*, the most apical junction is the zonula adherens (ZA), followed by the septate junction (SJ) basally. Apical to the ZA is the sub-apical or marginal zone (SAZ) (Knust et al., 2002). Each apical junction contains specific proteins, conserved between vertebrate and *Drosophila*.

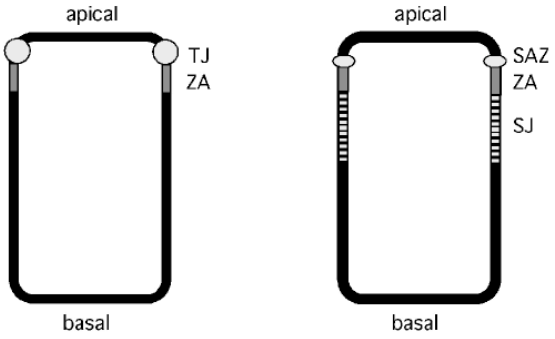

Vertebrate		*Drosophila*	
Site	Proteins[a]	Site	Proteins
Tight junction	claudin, occludin, JAM	Sub-apical zone	Crumbs (Crb)
	ZO-1, ZO-2, ZO-3		Stardust (Sdt)
	ASIP/Par-3[b]		Discs Lost (Dlt)
	aPKC[b]		Bazooka (Baz)/Par-3[b]
	PAR-6[b]		DmPar-6[b]
	Scribble		aPKC[b]
Adherens junction	E-cadherin	Zonula adherens	E-cadherin (Shotgun)
	α-catenin		α-catenin
	β-catenin		β-catenin (Armadillo)
Lateral membrane	ERBIN	Septate junction	Neurexin, FAS III
			Scribble
			Discs large (Dlg)

Table 1. Distribution of some proteins in epithelial cells of vertebrate and flies (from Knust et al., 2002). For a detailed description of the composition of tight junctions see Zahraoui et al. (2000) and Tsukita et al. (2001).

Each *Drosophila* epithelial follicle cell is characterized by five type of junctions (Szafranski and Goode, 2007). The apical junction connects follicle cells to the germ cells, the three conserved lateral junctions, the apicolateral, adherens and basolateral junctions, intereconnet follicle cells to each other, while a basal junction connects to the outer basement membrane (Fig. 5). These five domains contain different protein complexes and genetic studies have revealed that these protein complexes function in a sequential yet interdependent manner to regulate the establishment, elaboration, and

maintenance of cellular polarity (Tepass et al., 2001; Bilder et al., 2003; Tanentzapf and Tepass, 2003).

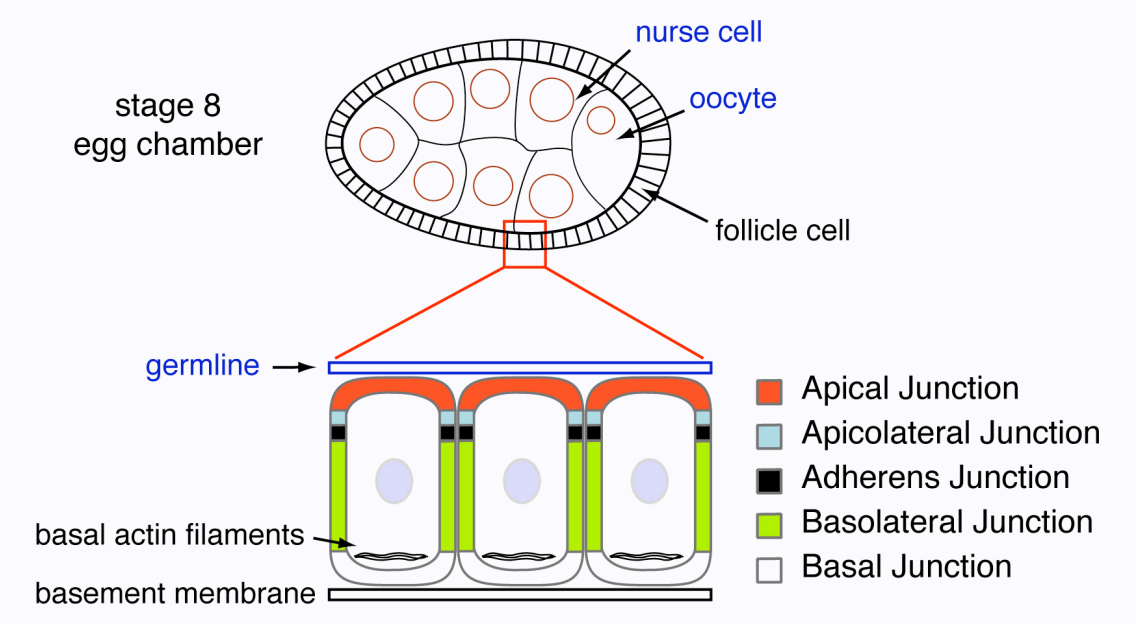

Figure 5. Apico-basal polarity in the follicle cell epithelium
The magnified view of three follicle cells shows the localization of certain cellular junctions in the different subdomains of the plasma membrane. The proximity of the apical surface to the germline and basal surface to a basement membrane as well as the position of the basal actin filament are shown.

Apical Junction

The apical membrane domains of the follicle cells are lining the germ cells and presumably adhere to the oocyte plasma membrane via DE-cadherin (Oda et al., 1997; Godt and Tepass, 1998; Gonzalez-Reyes and St Johnston, 1998) (Fig. 6). Later during oogenesis, eggshell material is synthesized from the follicle cells and secreted from their apical membrane domains (Pascucci et al., 1996).

Three genes *shotgun*, *egghead* (*egh*) and *brainiac* (*brn*), appear to be required for the interaction of the apical membrane of the follicle cells and the oocyte membrane.

Mutations in these genes lead to loss of epithelial polarity and multilayering of the follicle cell sheet (Goode et al., 1996; Rübsam et al., 1998). Both *egh* and *brn* encode for putative secreted or transmembrane proteins, suggesting that the germ line sends out a signal via Egh and Brn that is received by the follicle cells and is required for the maintenance of epithelial polarity in these cells. It has been proposed that Notch (N) is the receptor for this signal because mutations in N mutant follicle cells exhibit a similar multilayering phenotype as seen in *brn* and *egh* germ line clones (Goode et al., 1996; Ruohola et al., 1991).

The apical domain presents high levels of filamentous proteins such as α and β−Spectrin which are part of the cytoskeleton of the follicle cells. The cytoskeleton exhibits some characteristic features of polarized cells. The spectrin based cytocortex shows a specific polarized distribution of its components in the follicular epithelium (Fig. 6) (Lee et al., 1997; Zarnescu and Thomas, 1999): the apical domain is composed of β_{heavy} Spectrin and α-Spectrin, and the basolateral domain contains β/α Spectrin complexes (Lee et al., 1997). The filamentous protein α-Spectrin forms a network with actin cytoskeleton that regulates and stabilizes the membrane shape. By using mosaic analysis, Lee et al. (1997) showed that β-Spectrin is required for the proper localization of the α - and β_{heavy} -chains and mutations resulted in multilayering and loss of apical-basal polarity of the epithelium. Spectrin binds to Ankyrin, another submembranous cytoskeletal element (Dubreuil and Yu, 1994). Ankyrin is localized to the lateral cell membranes in the wild type follicle epithelium. In α-Spectrin mutant cells, Ankyrin is no longer detected at the membranes (Lee et al., 1997). In vertebrates the Spectrin/Ankyrin cytoskeleton has been implicated in anchorage of membrane proteins like the Na/K ATPase (Nelson et al., 1990). However, the distribution of Na/K ATPase

in α-Spectrin mutant follicle cells remains largely normal. It is also interesting to note that the Na/K ATPase, which exhibits a polarized distribution in many vertebrate epithelia is localized on both the apical and the basolateral membrane domains of the follicle cells (Bohrmann and Braun, 1999; Lee et al., 1997).

Apicolateral Junction

The apical compartment is composed of PAR-3/PAR-6/aPKC complex which is required to establish polarity in many different cell types, including the *C. elegans* zygote and epithelial and neuronal cells in *Drosophila* and mammals (Ohno, 2001). This complex in follicle cells is localized right above the adherens junctions (Horne-Badovinac and Bilder, 2005) and beside aPKC, is composed by Bazooka (Baz, homolog of PAR-3) e dmPAR-6 (homolog of Par6), cytosolic scaffolds with PDZ domains and other binding domains for proteins interaction. The aPKC proteins are a subgroup of the PKC family of serine-threonine protein kinases that comprise the *i/λ* and *z* isoforms in mammals, whereas only the aPKC*z* isoform exists in *Drosophila* (Suzuki et al., 2001; Rolls et al., 2003; Kovac et al., 2007). Mutations that affect these genes, cause pluristratification and epithelium discontinuity (Abdelilah-Seyfried et al., 2003; Tanentzapf et al., 2000), lose of monostratification organization, polarity and correct cell shape (Wodarz et al., 2000).

The subapical region (SAR), located right below the apical domain, can be visualized by Crumbs (Crb), a transmembrane protein required for the establishment of this domain, together with its cytoplasmic-binding partners, such as aPKC (Knust and Bossinger, 2002; Tepass et al., 1990; Wodarz et al., 1995). Interestingly aPKC during *Drosophila* embryogenesis is required for the phosphorylation of Crb. This

phosphorylation may be necessary for Crb to adopt a correct conformation and/or to interact with proteins required for Crb stabilization at the apical domain (Sotillos et al., 2004). More in general, it has been shown that aPKC kinase activity is essential and instructive for proper localization of apical and basolateral proteins therefore for establishing and/or maintaining cell polarity (Sotillos et al., 2004).

Adherens Junction

The lateral compartment is characterized by the adherens junction (AJ; Zonula adherens in vertebrate's eptihelia), a belt composed of protein complexes and actin filaments that encircle the cell just below its apical face. AJ are one of the crucial components for the establishment and maintenance of both the polarized shape of individual epithelial cells and the integrity of cell sheets. These functions can be attributed to the ability of DE-cadherin (encoded by the gene *shotgun*) to set up during early stages of oogenesis the initial polarity of the follicular epithelium (Dobens and Raftery, 2000; Godt and Tepass, 1998). Moreover DE-cadherin is able to interact with the cytoskeleton on one hand and with neighbouring cells via homophilic interactions on the other (Knust, 2000). The cytoplasmic tail of the Ca^{++}-dependent homophilic adhesion protein DE-cadherin is in fact linked to the actin filaments via α-Catenin (Pfeifer et al., 1993) and β-Catenin (Armadillo) (Yap et al, 1997; Tepass, 1997; Tepass, 1999) and they are components of AJ compartment. DE-cadherin turnover, which results in asymmetrical distribution of DE-cadherin, is necessary to ensure follicle cells movements and rearrangements during oogenesis (Schober and Perrimon, 2005). Homozygous mutant cell clones for *armadillo* exhibit a major loss in normal cell shape and cell contacts (Müller, 2000). This indicates that cadherin cell adhesion molecules

maintain cell shape and junctional communication between the follicle cells. Interestingly, cell clones that are homozygously mutant for null alleles of *shotgun* do not exhibit any significant abnormalities in the epithelial structure of the follicle cell epithelium (Godt and Tepass, 1998; Niewiadomska et al., 1999). In fact another cadherin, DN-cadherin supplements the adhesive function of DE-cadherin in the follicle cells (Tepass, 1999).

Basolateral Junction (BLJ)

The basolateral domain in *Drosophila* is represented by the Septate Junctions (SJ), functional barriers that enable transepithelial circulation. In this domain is localized the Scrib complex, that includes the oncosoppressor genes *scribble* (*scrib*), *lethal giant larvae* (*lgl*) and *discs large* (*dlg*). Genetic studies have revealed that these three tumor suppressors genes cooperatively regulate cell polarity, junction formation and cell growth in epithelial cells (Yamanaka and Ohno, 2008). During oogenesis, SJ build up from stage 6 when follicle cells stop proliferating, although the complete development takes place at stage 10 (Horne-Badovinac and Bilder, 2005). Discs Large (DLG) is involved in maintaining the structure of the follicular epithelium, by prohibiting cell growth and maintaining cell adhesion and cell polarity. The role of DLG in maintaining cell polarity, for example restricting Crumbs to the apical surface appears to be separable from its role in proliferation control (Woods et al., 1996). Moreover it has been shown that adherens junctions restrict DLG to the lateral membrane by a mechanism that is reinforced by Crb (Le Bivic, 2005; Lecuit, 2004).

Lethal giant larvae (Lgl), a WD40 domain-containing protein, is implicated in cellular asymmetry formation in a number of cell types (Vasioukhin, 2006; Wirtz-Peitz

and Knoblich, 2006). It is not clear through which interactions Lgl is brought to membranes. However, in *scrib* or *dlg* mutant embryos, Lgl plasma membrane association is also lost (Bilder et al., 2000). This finding suggests that a critical role of Scrib and DLG is to recruit Lgl to the membrane (Tepass, 2001). Loss of *lgl* in *Drosophila* results in loss of apicobasal polarity in epithelial cells and in the neoplastic transformation of the imaginal discs which lose their epithelial monolayer structure (Agrawal et al., 1995; Bilder et al., 2000; Ohshiro et al., 2000; Peng et al., 2000). It has been shown that mammalian Lgl forms complexes with Par6/atypical PKC regulating epithelial cell polarity (Plant et al., 2003; Yamanaka et al., 2003). Upon cell–cell contact-induced cell polarization, Lgl is phosphorylated by aPKC resulting in a dissociation of Lgl from Par6/aPKC followed by an accumulation of Lgl along the basolateral membrane, where it contributes to the formation of the basolateral membrane domain (Tanentzapf and Tepass, 2003; Hutterer et al., 2004) and to correct positioning of epithelial junctions (Borg, 2004). Also in neuroblasts it has been shown that Lgl is phosphorylated by aPKC in the apical region to direct localization of basal components involved in asymmetric cell divisions (Betschinger et al., 2003).

Basal Junction

The follicle cell's basal membrane is facing the basal lamina or basement membrane (BM). The BM is a highly specialized form of extracellular matrix (ECM) found on the basal side of every polarized epithelia, which is made up primarily of protein networks containing collagen and other glycoproteins, laminin and Collagen IV (Fessler and Fessler, 1989; Quondamatteo, 2002*)*. The laminin containing extracellular matrix appears to be organized in parallel bundles (Gutzeit et al., 1991). Interestingly,

the basal actin microfilament system of the follicle cells is also organized in parallel bundles, suggesting some kind of planar polarization of the follicle epithelium (Gutzeit, 1990). The attachment of the epithelium to its BM substrate is largely mediated by integrins, heterodimers of α and β subunits that bind components of ECM along the basal surfaces (Brown, 2000). It has been shown that integrin-mediated signaling during *Drosophila* oogenesis is required for proper alignment of the mitotic spindle and thus for the maintenance of the follicular-epithelium monolayer, through an interaction between the acto-myosin cytoskeleton and integrin activity (Fernández-Miñán et al., 2007; Fernández-Miñán et al., 2008). The *Drosophila* genome contains two integrin β subunits, βPS and βν (Yee and Hynes,1993; Brown, 2000). βPS, encoded by the *myospheroid* (*mys*) gene, is the only β chain present in the ovary (Fernández-Miñán et al., 2007). Dystroglican (DG) is an adhesion molecule known to function as an essential link between the extracellular matrix and the actin cytoskeleton through its role in the dystrophin-glycoprotein complex. In mammals, disruption of DG function in this complex is believed to contribute to several forms of muscular and neurodegenerative disorders (Brancaccio, 2005).

It has been suspected that modulation of BM could be an important step in tumor metastasis because the BM would be a barrier for tumor cells to leave their tissues of origin and invade different organs. The importance of BM is inferred from the facts that this structure surrounds organs and tissues and is evolutionarily conserved from invertebrates to mammals.

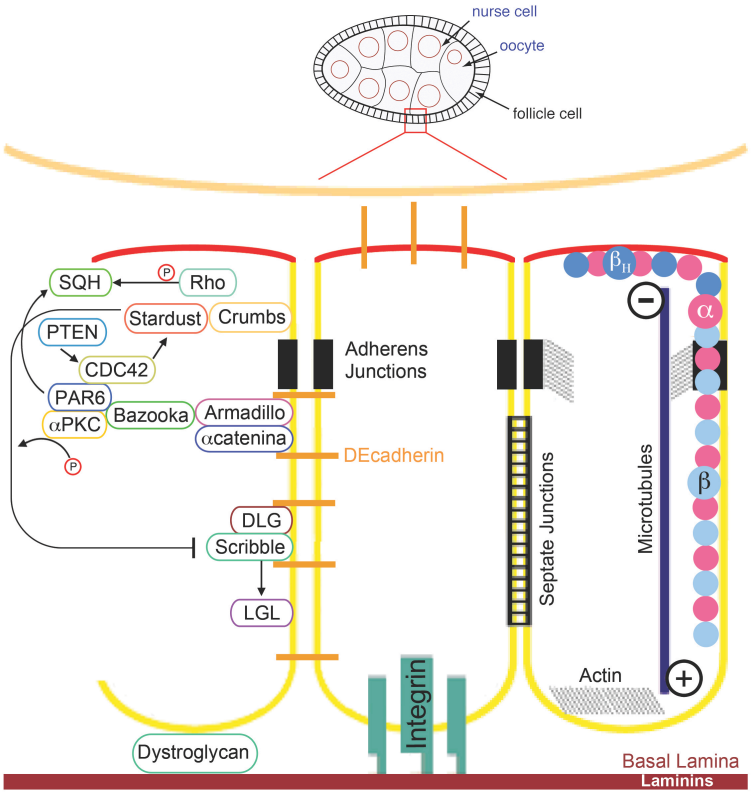

Figure 6. Detailed scheme of polarized follicle epithelium (modified from Muller, 2000).
The magnified view of three follicle cells shows the localization of the different polarity markers from the apical domain (red) and from the lateral-basal membrane domain (yellow).

1.8. Epithelial morphogenesis and microtubules network

Epithelial development can be subdivided roughly into three phases in which (I) the initial establishment of polarity is (II) followed by the consolidation and elaboration of surface domains and cytoplasmic asymmetries, and finally, (III) the terminal differentiation and specialization of surface domains. This mechanism is similar to the blastoderm ephitelium cellularization during embryogenesis as explained by Tepass et al. (2001) and shown in Figure 7.

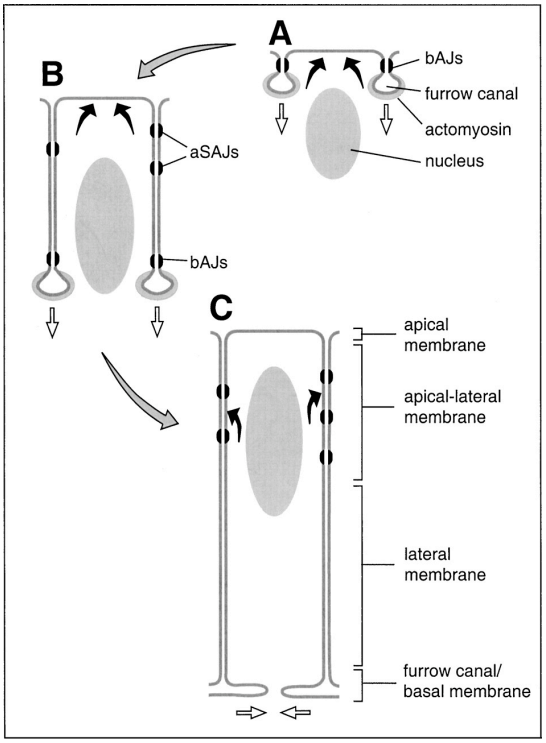

Figure7. Cellularization forms the blastoderm epithelium in *Drosophila.*
Three stages at early (A), mid- (B) and late- (C) cellularization are illustrated. The open arrows indicate the direction of plasma membrane movement and the black arrows point to the main membrane insertion sites. A. Invaginations of the egg membrane form the furrow canals. The basal adherens junctions (bAJs) remain closely linked with the furrow canals during cellularization. B. Apical spot adherens junctions (aSAJs) form at midcellularization, increase in number and are retained in the apical one third of the lateral membrane. These SAJs will form the ZA during gastrulation. C. Four membrane domains, indicated to the right, have formed at late-cellularization. The bAJs and the actomyosin ring resolve at this time and the furrow canals expand to form the basal membrane.

The follicular epithelium renews itself constantly as follicle cells originate from stem cells, and allows the analysis of the full range of phases in epithelial differentiation, including epithelial formation by mesenchymal-epithelial transition (MET).

Typically, the early cues that establish apicobasal polarity come in the form of basal cues through furrow and through cell-substrate adhesion, and lateral cues in the form of cadherin-based cell-cell adhesion. Before encapsulation, the FC precursors adhere to a basement membrane that surrounds the germarium and contact each other

laterally through adherens junctions. These contacts appear to be sufficient to establish a basal membrane domain; however, apical and lateral markers are intermixed, suggesting that contact with the germ cells is necessary to resolve the apical and lateral domains (Tanentzapf et al., 2000). These adhesive events then trigger the formation of protein complexes at the cell surface, which further refine the apical and basolateral membrane domains and lead to the localization of adherens junction and the apical complex. The aPKC complex localizes to the marginal zone just apical to and overlapping with the AJ and acts first in the hierarchy to specify the apical domain. The Scrib complex is found just basolateral to the AJ and functions as a basolateral determinant by repressing the apicalizing activity of the aPKC complex. Finally, the aPKC complex recruits the Crumbs group to the apical domain, to antagonize the activity of the Scrib complex, which is part of the septate junction (SJ). These membrane asymmetries are propagated to other cellular compartments such as Spectrin and Actin cytoskeleton (Baum et al., 2000; Mooseker, 1985). The microtubule cytoskeleton is also polarized to form an array of very stable microtubules (MTs) that run parallel to the apicobasal axis, with their minus ends at the apical membrane and their plus ends oriented toward the basal membrane (Bacallao et al., 1989; Bre et al., 1990; Clark et al., 1997). By using microtubule motor domain fusion proteins, Clark et al. (1997) clearly showed that the microtubule network is polarized (Fig. 6). Kinesin is the motor domain of the plus end-directed MT motor and accumulates at the basal side of the cell, whereas the minus end motor protein Nod localizes apically.

The distinct membrane domains are further reinforced by sorting in the secretory pathway that delivers different sets of proteins to the apical and basolateral domains. This subcellular trafficking of proteins takes place via the trans-Golgi network (TGN).

Delivery of transport vesicles from the TGN to different plasma membrane domains has a remarkably high fidelity. Such fidelity could be based on vesicles targeting along the cytoskeleton, and/or by specifying vesicle docking and fusion with the correct membrane domain (Rodriguez-Boulan et al., 2005). The vesicular-trafficking routes correspond to those in Figure 8.

Sorting signals promote the incorporation of apical proteins at the trans-Golgi network (TGN) or in common recycling endosomes (CREs) into clustered lipid rafts that recruit microtubule motors (such as kinesin) directly or through unknown adaptors; in some cases (rhodopsin) the motor (dynein) is recruited through direct interactions. The motors generate tubular elements that move along microtubules (inset). Basolateral proteins are incorporated into clathrin-coated or into uncoated tubules (which are pulled by unidentified microtubule motors that are presumably different from those used by apical proteins). Cdc42 stimulates the exit of apical proteins and inhibits the exit of basolateral proteins from the TGN through unknown downstream effectors and might have similar functions at CREs. Fission of apical transporters is mediated by the GTPase dynamin; protein kinase D (PKD) promotes vesicle release for the basolateral route (Fig. 8, see inset). Dynamins 1 and 2, the adaptor DAB2 and the GTPase ARNO regulate specific endocytic steps. Other regulators of protein trafficking include phosphatidylinositol 4-kinases, heterotrimeric G-proteins and Retromer. Microtubule and actin motors (myosins I, II, Vb and VI) probably participate at several stages of endocytic and biosynthetic trafficking. Hip1R, a linker between actin and clathrin, promotes the release of clathrin-coated vesicles that contain mannose-6-phosphate receptors from the TGN. The production of a vesicle from a donor compartment is coordinated with delivery to the acceptor compartment by various compartment-specific

Rab proteins. The exocyst, together with RalA and Rab8, coordinates basolateral exocytic routes, whereas Rab25 and Rab11 coordinate apical recycling.

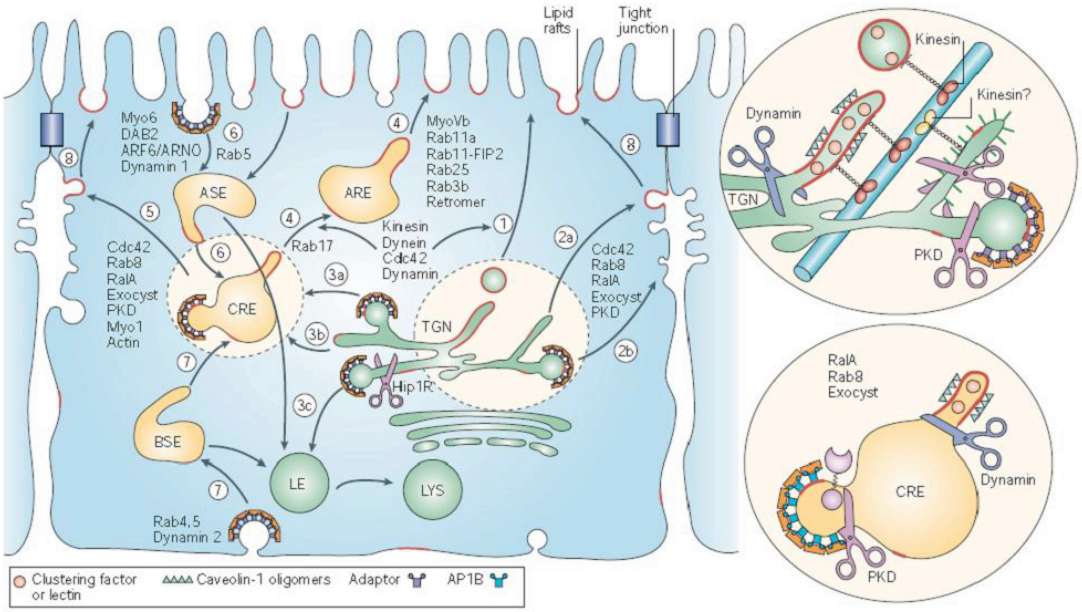

Figure 8. Representation of the vesicular-trafficking routes.
Apical exocytic routes (1 and 4): glycosylphosphatidylinositol (GPI) anchors, N-glycans and O-glycans sort apical proteins at the trans-Golgi network (TGN), common recycling endosomes (CREs) and apical recycling endosomes (AREs). This sorting might involve clustering small lipid rafts into larger functional lipid rafts, a process that might be promoted by a luminal lectin, caveolin oligomers and MAL (inset). Basolateral exocytic routes (2 and 5): basolateral signals interact with adaptors of the clathrin (adaptor protein-1 (AP1), AP3, GGA (Golgi-localized, gamma-ear-containing, Arf-binding protein)) or non-clathrin (AP4) type at the TGN or CREs. AP1B operates at the level of CREs (route 5; inset). AP4 might mediate basolateral sorting through microtubule motors. Newly synthesized lysosomal membrane proteins (LAMPs) seem to be transported to the lysosome via the basolateral membrane (route 2 followed by route 7 to basal sorting endosomes (BSEs), late endosomes (LEs) and lysosomes (LYS)). Endocytic routes (6 and 7): endocytosed apical (route 6) or basolateral (route 7) membrane proteins are internalized into apical sorting endosomes (ASEs) or BSEs by AP2, mix in CREs and are sorted into apical and basolateral exocytic routes by sorting signals that are similar to those used in the biosynthetic route (routes 4 and 5). Soluble proteins are sorted from membrane proteins in ASEs and BSEs, mixed in LEs and degraded in LYS. Biosynthetic route through endosomes (routes 3a–c): some newly synthesized basolateral proteins reach CREs directly from the TGN (routes 3a and 3b; via unknown adaptors) from where they are sorted to the basolateral membrane via AP1B (route 5). Mannose-6-phosphate receptors and their ligands (lysosomal hydrolases) move through clathrin-coated vesicles, possibly into LEs (route 3c) from where they are transported back to the TGN. Recycling and transcytosing apical membrane proteins transfer from CREs to AREs (route 4). Some GPI-anchored proteins seem to use a transcytotic route (route 8) in Madin–Darby canine kidney cells23 (from Rodriguez-Boulan et al., 2005).

1.9. The human oncosoppressor VHL and the VHL disease

The von Hippel-Lindau disease is a multiple tumor syndrome resulting from germline mutations in the *von Hippel-Lindau* tumor suppressor gene (*VHL*) and somatic inactivation of the other allele (Latif et al., 1993; Kaelin, 2002). The disease is characterized by development of highly vascularized benign and malignant tumors, including retinal and central nervous system hemangioblastoma, pheochromocytoma, and clear-cell renal cell carcinoma (RCC) (Kaelin, 2007). VHL disease affects approximately 1 in 35,000 individuals, and transmission of the disease seems to occur in an autosomal-dominant manner. Like most human hereditary cancer syndromes, is caused by the germ-line mutation of a tumour-suppressor gene, and conforms to the Knudson 2-hit model. Individuals with VHL disease have typically inherited a defective *VHL* allele from one of their parents. Pathology, such as the development of cysts or tumours, is linked to the somatic inactivation or loss of the remaining wild-type *VHL* allele. The human *VHL* (*h-VHL*) gene maps in the region 3p25 and encodes two polypeptides of 213 and 160 amino acids, resulting from in-frame alternative start codon usage (Latif et al., 1993; Iliopoulos et al., 1998). The 213 amino acid-long protein is formed by two major domains: the α-domain, which contains three α-helices, and the β-domain, which consists of seven β-sheets and a single α-helix (Stebbins et al., 1999; Min et al., 2002). The 213 amino acid-long protein migrates with an apparent molecular weight of 24 KDa. The second protein isoform migrates with an apparent molecular weight of 19 KDa.

Biochemical fractionation and immunohistochemical studies, coupled with the analysis of VHL–green fluorescent protein fusion proteins in living cells, indicate that

VHL shuttles back and forth between the cytosol and nucleus, with most of the protein located in the cytosol (Iliopoulos, 1995; Bonicalzi, 2001).

Genetic and clinical studies have identified a number of *h-VHL* mutations correlated with tumor development (Beroud et al., 1998). These mutations can be mapped to several distinct clusters on the *h-VHL* surface. For some, but not all, mutation clusters the detailed molecular consequences are known (Sikora and Godzik, 2004).

Recent studies have shown that the 213 protein isoform is phospohrilated by casein Kinase 2 on Ser 33, 38 and 43 (Lolkema et al., 2005). Mutations affecting these amminoacids, lead to altered assembly of fibronectin matrix. Hergovich et al (2006) demonstrated that h-VHL30 is phosphorylated on serine 68 and 72 by glycogen synthase kinase 3 (GSK3). Functional analysis of h-VHL species carrying nonphosphorylatable or phosphomimicking mutations at S68 and/or S72 reveals a central role for these phosphorylation events in the regulation of h-VHL's MT stabilization (but not binding) activity.

However the most studied h-VHL function is the E3 ubiquitin ligase activity in homeostatic responses to external variation of oxygen (Iwai et al. 1999; Kamura et al. 1999; Lisztwan et al., 1999). The ubiquitin ligase complex, in addition to the h-VHL, contains Elongin B, Elongin C, Cullin-2, and Rbx-1 (Lonergan et al. 1998; Iwai et al. 1999; Kamura et al., 1999). The best characterized h-VHL function thus far has been its involvement in hypoxia-induced angiogenesis. Supporting this functional role is the identification of one of its degradation targets: the alpha subunit of the hypoxia-inducible factor 1 (Hif-1α; Wang and Semenza, 1995; Maxwell et al., 1999). Hif-1 is a transcription activator that mediates the hypoxia-induced up-regulation of vascular

endothelial growth factor (VEGF), Transforming Growth Factor α (TGFα) and erythropoietin (EPO) (Maxwell et al., 1997), which are potent inducers of angiogenesis (Leung et al., 1989; Shweiki et al., 1992). HIF-1α, is regulated by the oxygen concentration (Semenza, 1999). In normal cells under hypoxic conditions HIF-1α expression is high, whereas under normoxic conditions HIF-1α is ubiquitinated and directed for a proteosome-dependent degradation (Ivan and Kaelin Jr., 2001). Ubiquitination of the HIF-1α protein is mediated by the E3 ubiquitin ligase complex, with the h-VHL protein specifically recognizing oxygen-modified HIF-1α and recruiting it to the E3 ubiquitin ligase complex (Maxwell et al. 1999; Ivan and Kaelin Jr. 2001). Tumorigenic mutations in the h-VHL protein disable the HIF-1α degradation pathway and allow the tumor cells to mimic the hypoxic conditions despite normal levels of oxygen leading to the activation of HIF target genes. h-VHL can therefore be considered an anti-angiogenic factor and this function can explain the over-vascularized phenotypes in the VHL tumors.

An important question is whether h-VHL has targets or functions that are unrelated to HIF. The existence of multiple functions would offer an explanation for the genotype–phenotype correlations that are observed in VHL disease (Kaelin, 2002). *h-VHL* has been shown to be implicated in other processes such as cell-cycle control, differentiation, extracellular matrix formation and turnover, microtubule stability and cellular morphology and cell motility. For example, *h-VHL* loss of function causes loss of cellular differentiation and Davidovitz et al., (2001) and Lieubeau-Teillet et al. (1998) demonstrated an epithelial-mesenchymal transition (EMT) in renal cell carcinoma (RCC) caused by loss of h-VHL. h-VHL-defective renal carcinoma cells display abnormalities in cytoskeletal architecture (actin, vinculin, and tubulin), cell-cell

adhesion, integrin expression, and extracellular matrix formation, all of which are related to EMT and can be corrected upon reintroduction of wild-type h-VHL (Fig. 9) (Kaelin, 2007).

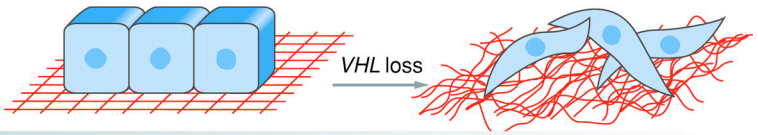

Cell morphology	Epithelial	Mesenchymal
Extracellular matrix	Organized	Disorganized
E-cadherin	Positive	Negative
Cytoskeleton	Stable	Unstable
Adhesion	Increased	Decreased
Motility	Decreased	Increased

Figure 9. Cellular phenotypes associated with h-VHL inactivation in renal carcinoma cells (from Kaelin, 2007).

These abnormalities appear to be at least partially HIF-independent, and genetic studies in *Caenorhabditis elegans* strongly suggest a role for h-VHL in extracellular matrix control independent of its role in HIF regulation (Bishop et al., 2004).

h-VHL is involved in determination and maintenance of cellular morphology. h-VHL in RCC cell lines is necessary for the normal organization of adherens and tight intercellular junctions, the maintenance of cell polarity, and control of paracellular permeability through HIF-independent events, supporting the concept that h-VHL has additional functions beside its role in the regulation of HIF (Calzada et al., 2006; Esteban et al., 2006; Evans et al., 2007; Krishnamachary et al., 2006).

Hergovich et al., (2003) demonstrated that h-VHL might associate to and stabilizes microtubules. Additionally has been shown that h-VHL is critically involved in regulating the orientation of microtubular growth at the cell periphery.

Immunoprecipitation experiments revealed that h-VHL interacts with βTub and controls ciliogenesis by orienting microtubule growth (Schermer et al., 2006).

h-VHL is involved in cell cycle control and Roe et al. (2006) demonstrated that h-VHL might bind p53 by stabilizing and enhance its transcriptional activity, cell cycle arrest and p54 mediated apoptosis.

h-VHL is required for proper assembly of an extracellular fibronectin matrix (Ohh et al., 1998). Esteban-Barragan et al. (2002) showed that h-VHL is an important regulator of integrins and is essential for the formation of beta1 fibrillar adhesions. These findings help to explain the abnormal extracellular matrix organization and increased motility of h-VHL defective renal cancer cells.

It has been demonstrated a novel HIF-independent function of h-VHL in cell motility control via regulation of fibroblast growth factor receptor 1 (FGFR1) endocytosis. In h-VHL null tumor cells or h-VHL knock-down cells, and in the endothelial cells, FGFR1 internalization is defective, leading to surface accumulation and abnormal activation of FGFR1. The enhanced FGFR1 activity directly correlates with increased cell migration. Additionally h-VHL exhibits a functional relationship with Rab5a and dynamin 2 in FGFR1 internalization, and seems that the endocytic function of h-VHL is mediated through the metastasis suppressor Nm23, a protein known to regulate dynamin-dependent endocytosis (Hsu et al., 2006; Champion et al., 2008).

h-VHL has been reported to bind to specific isoforms of protein kinase C (PKC) and might serve as an E3 for PKC-lambda (Okuda et al., 1999; Okuda et al., 2001; Pal et al., 1997).

1.10. The oncosoppressor d-VHL in *Drosophila melanogaster*

h-VHL is evolutionary conserved and homologs are found in several organisms, from invertebrates to vertebrates (Bruick and McKnight, 2001; Epstein et al., 2001; Sutovsky and Gazit, 2004). *Drosophila VHL* (*d-VHL*) is highly conserved as compared to the human counterpart and the fruit fly represents an excellent model system to study VHL function in vivo.

d-VHL is localized on right arm of second chromosome, in the cytological region 47E5-47E6 and cover a region of 2100 bp. Adryan et al. (2000) localized the gene in the cytological portion 47E1-47E3 through in situ hybridization. The coding sequence does not contain introns and encodes a 178 amminoacids long protein that migrates with an apparent molecular weight of 21 KDa.

The candidate 178-amino acid d-VHL protein can be aligned along its entire length with the smaller of the two h-VHLs (Figure 10; Adryan et al., 2000; Gnarra et al., 1994; Beroud et al., 1998; Stebbins et al., 1999). d-VHL has an overall 22% identity to h-VHL and is 50% similar when conserved amino acid changes were considered (Figure 10). In the two functionally significant protein interaction domains, human residues 113-121 and 157-172 that encompass the protein kinase C λ (PKCλ) and the elongin C binding sites, respectively (Okuda et al., 1999; Kibel et al., 1995), the conservation is significantly higher at 67 and 76%. The most evident difference between the two sequences is the amino-terminal portion which is missing in the d-VHL protein (Adryan et al., 2000). PKCλ has an overall 71% identity to the PKC *z* isoform which has in turn an overall 63% identity with Drosophila aPKC. The aPKC*z* is the only isoform that exists in *Drosophila* as mentioned above.

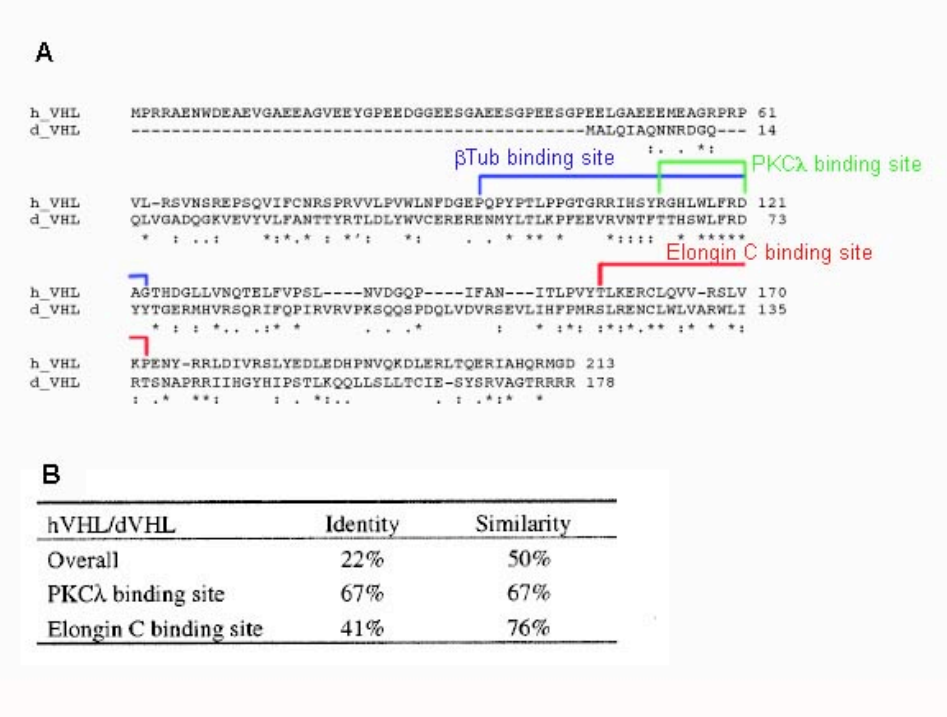

B

hVHL/dVHL	Identity	Similarity
Overall	22%	50%
PKCλ binding site	67%	67%
Elongin C binding site	41%	76%

Figure 10. Conservation of the VHL protein.
A. Amino acid sequence alignment of the VHL proteins from human (h-VHL) and *Drosophila* (d-VHL). Identical residues are marked by stars and similar residues are marked by (:) or (.), according to the degree of similarity. d-VHL has an overall 22% identity to h-VHL and is 50% similar when conserved amino acid changes were considered. The most evident difference between the two sequences is the amino-terminal portion which is missing in the d-VHL protein (Adryan et al., 2000). Residues highlighted by colored brackets are those identified as minimally required for specific protein interaction. Blu bracket is the βTubulin binding site (human residues 95-123); green bracket is the PKCλ binding site (human residues 113-121) (Okuda et al., 1999; Kibel et al., 1995); red bracket is the Elongin C binding site (human residues 157-172).
B. Extent of homology between Drosophila and human VHL proteins.

The gene is expressed in ovary, embryo, pupa, and adults, and at low level in larva as assayed through Northern blot analysis (Adryan et al., 2000; Aso et al., 2000). This data demonstrated that d-VHL is expressed in all the *Drosophila* developmental stages. Moreover in situ hybridization on embryos has shown that *d-VHL* is expressed in a tissue dependent manner in the tracheal epithelium from stage 15 of embryogenesis (Arquier et al., 2006). Giving that, d-VHL has been demonstrated to function during the development of the *Drosophila* vasculature, the tracheal system. Reduction of d-VHL activity can either disrupt or induce vascular growth, depending on the nature of the tracheal branches. Reduced d-VHL activity caused breakage of the main vasculature

accompanied by excessive looping of smaller branches, whereas over-expression caused a general lack of vasculature. Importantly, h-VHL can induce the same gain-of-function phenotypes. d-VHL is likely involved in halting cell migration at the end of vascular tube outgrowth. Loss of d-VHL activity can therefore lead to disruption of major vasculature (as in the mouse embryo), which requires precise cell movement and tube fusion, or ectopic outgrowth from existing secondary vascular branches (as in the adult tumors) (Adryan et al., 2000).

The hallmark of h-VHL activity is its ability to bind Elongin C. *Drosophila* Elongin C (d-Elongin C) has been cloned and it showed over 90% identity to the human counterpart (Aso and Conrad, 1997) and d-VHL can interact with d-Elongin C without the presence of other factors such as Elongin B. This complex has an ubiquitin ligase activity that can promote the poliubiquitination of HIF-α, suggesting that the hypoxia-induced mechanism is highly conserved from flies to human (Arquier et al., 2006).

In the *Drosophila melanogaster* genome have been found three homologs of human HIF-α: *trachealess* (*trh*), key regulator of tracheal system (Isaac and Andrew, 1996; Wilk et al., 1996); *single-minded* (*sim*), that encodes a transcription factor that regulates the development of the central nervous system midline cell lineage (Nambu et al., 1996); *similar* (*sima*), the most similar to human counterpart (Nambu et al., 1991; Bacon et al., 1998). The proteins encoded by these three genes are able to heterodimerize with *tango*, homolog of human HIF-β subunit (Oshiro and Saigo, 1997; Sonnenfield et al., 1997). The heterodimer activates the transcription of genes homolog to the mammalian counterpart: *branchless* (*bnl*), homolog to fibroblast growth factor (FGF); *breathless* (*btl*), homolog to fibroblast growth factor receptor (FGFR); *rhomboid* (*rho*), homolog to the activator of epidermal growth factor (EGF) pathway.

Through biochemical analyses Arquier et al., (2006) demonstrated that Sima is hydroxylated on a key proline (P850) by the prolyl hydroxilase dPHD. This hydroxylation is oxygen dependent and under normoxic conditions d-VHL binds hydroxilated Sima to mediate its proteasomal degradation. Hypoxia induces morphological changes of the main tracheal trunks, such as ectopic and excessive branchings, increase terminal branches, dorsal tube followed by a more tortuous and circonvoluted shape (Arquier et al., 2006).

Studies performed *in vivo* and in S2 cells culture (Dammai et al., 2003) have been addressed to understand the molecular role of d-VHL during the development of tracheal system. Human nm23 has been implicated in suppression of metastasis in various cancers, but the underlying mechanism of such activity has not been fully understood. Using *Drosophila* tracheal system as a genetic model, they examined the function of the Drosophila homolog of *nm23*, the *awd* gene, in cell migration. They show that loss of Drosophila *awd* results in dysregulated tracheal cell motility. This phenotype is similar to that observed in *d-VHL* mutants and can be suppressed by reducing the dosage of the chemotactic FGF receptor (FGFR) homolog, breathless (*btl*), indicating that *btl* and *awd* are functionally antagonists. In addition, mutants of *shi*/*dynamin* show similar tracheal phenotypes as in *awd*, suggesting defects in vesicle-mediated turnover of FGFR in the *awd* mutant and thus, they propose that *awd* regulates tracheal cell motility by modulating the FGFR levels, through a dynamin-mediated pathway. In this model *d-VHL* seems to be involved in the recruitment of Awd and in the formation of endosome. This hypothesis is further reinforced by the phenotypes observed in d-VHL mutants, which are similar to those observed in *awd* or *shi* mutants cells (Hsu et al., 2006; Champion et al., 2008).

2. AIM OF RESEARCH

Epithelial cells are the cells that line virtually every organ in human body and 85% of cancers derive from epithelial cells. These cells are tightly connected to each other through a variety of cell-cell junctions and they are polarized, with distinct apical and basolateral sides. During development epithelial cells sometimes dissolve their junctions with their neighbours and become mesenchymal. Mesenchymal cells have a less rigid shape and are more likely to be motile. Epithelial to mesenchymal transition (EMT), as well as the reverse process (MET), are extremely important for normal development. In addition, these transitions are important in wound healing, and tumor cells that develop from epithelial cells must transform into motile cells in order to metastasize.

Importantly, loss of apicobasal cell polarity and cell adhesion, cytoskeleton reorganization, microtubule dynamics, disruption of basement membrane are some of the processes required for epithelial–mesenchymal transition (EMT), and they represent critical steps in cellular motility and invasiveness (Thiery, 2002).

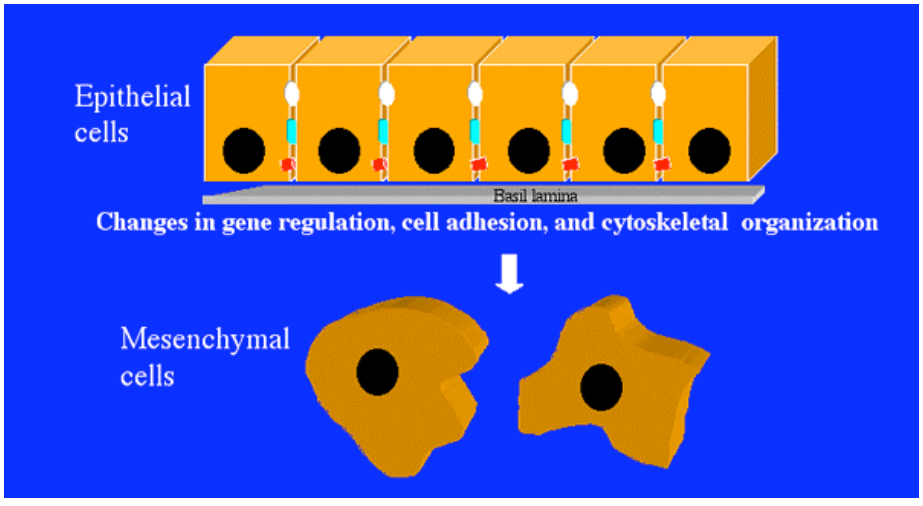

Figure 11. The diagram of the events during which epithelial cells are transformed into mesenchymal cells.

In *Drosophila* the follicle cells form the follicular epithelium that surrounds the egg chamber and this epithelium is a powerful model system in which to study mechanisms underlying biological processes relevant to epithelial morphogenesis such as cell proliferation, cell growth, cell polarity, cell motility and cell death. The follicular epithelium shares morphological and molecular features with vertebrate's epithelia, so represents an excellent model system for studying signaling pathways involved in the correct differentiation of the subpopulation that compose it. Moreover follicular epithelium forms through a mesenchymal–epithelial transition (Tanentzapf et al, 2000) and indeed represents a powerful model for studying the EMT transition. Moreover, it is already well established that cellular mechanisms activated during border cell migration closely resemble those observed in human EMT (Jang et al., 2007; Naora and Montell, 2005).

During my PhD I have been involved in several projects regarding the morphogenesis of the follicular epithelium. I have analyzed signaling pathways involved in the progression of the oogenetic processes that lead to the production of a mature egg. In particular, I focused the analysis on the expression of genes involved in the determination of follicular cell subpopulations and eggshell structures that derives from them. Eggshell formation is a complex process that requires time-coordinated synthesis, cleavage, and transport of various proteins and finally cross-linking mediated by particular functional domains. It has been suggested that the eggshell can act as a storage site for spatial cues involved in embryonic pattern formation. Its structural components are synthesized in the somatic follicle cells in a precise temporally and spatially regulated manner. One of the main interest in Prof. Giuseppe Gargiulo's lab is to focus on the pathways that correlate follicular epithelium patterning and eggshell

gene expression and the regulatory elements controlling transcription of eggshell genes. The exquisite temporal and spatial regulation of some eggshell structural genes suggests a crucial role of their encoded proteins in the complex process of eggshell formation.

Epithelial morphogenesis is important for organogenesis and pivotal for carcinogenesis, but mechanisms that control it are poorly understood. The *Drosophila* follicular epithelium is a genetically tractable model to understand these mechanisms *in vivo*. Cell–cell communication is important, but the same signals are used repeatedly to control distinct events. Understanding intrinsic mechanisms that alter responses to developmental signals will be important to understand regulation of cell shape and organization.

Moreover, during my PhD I used the follicular epithelium as a model system to analyze *d-VHL* function during oogenesis in order to gain insight into the role of h-VHL for the pathogenesis of VHL disease. h-VHL is implicated in a variety of processes and there is now a greater appreciation of HIF-independent h-VHL functions that are relevant to tumour development, including maintenance and organization of the primary cilium, regulation of extracellular matrix formation and turnover, regulation of EMT, and modulation of cell death in certain cell types following growth factor withdrawal or in response to other forms of stress (Kaelin, 2008). However, the function of *h-VHL* gene during development has not been fully understood. Adryan et al (2000) studied the *d-VHL* function during *Drosophila* embryogenesis and they showed that beside the highly conservation of *d-VHL* compared to the human counterpart, it has a role in the development of the *Drosophila* vasculature, the tracheal system. More in general, *h-VHL* has been implicated in maintaining the differentiated phenotype in renal cells (Maxwell, 2005). Furthermore, *in vitro* experiments with *h-VHL* defective cells have

shown that the addition of h-VHL can induce a mesenchymal to epithelial transition. This evidence suggests that h-VHL has a central role in maintaining a differentiated phenotype in the cell (Kaelin, 2007). Therefore, to examine whether *d-VHL* has a role in epithelial morphogenesis and maintenance, I performed genetic and molecular analyses by using *in vivo* and *in vitro* approaches. For the *in vivo* studies I analyzed the follicle cells phenotype produced by loss of d-VHL during the entire oogenesis. Through immunoprecipitation I identify the d-VHL interactors during oogenesis. In order to understand functional relation between d-VHL and microtubules I performed experiments on S2 cells and ex vivo analysis on egg chambers.

Most of my thesis work has been carried out in Prof. Giuseppe Gargiulo's lab, Dipartimento di Biologia Evoluzionistica Sperimentale (Bologna, Italy). I spent 8 months in the lab of Prof. Tien Hsu, *Department of Pathology and Lab Medicine*, *Medical University of South Carolina* (*Charleston, SC, USA*) which is studying since several years the function of *Drosophila* homolog of the human tumor suppressor gene *h-VHL*.

3. MATERIALS AND METHODS

3.1. Fly food

The *Drosophila melanogaster* strains used were grown on a corn meal based food supplemented with glucose, yeast, agar and water. The food is prepared by melting 10 gr of agar and 50 gr of Glucose in 1600 ml water (tap water). Then 150 gr of corn meal are added and food is cooked on medium for 20 minutes mixing well. Afterward 50 gr of yeast are added and food is cooked for 10 minutes more, again on medium and mixing well. While food is cooling, 4 gr of Nipagine (an antimocotic) are dissolved in 16 ml of EtOH 98% and then added. The food is left to dry for at least 5 hours.

3.2. Fly Strains

The following stocks were used:

- y^{1}, w^{67c23} as a wild-type stock
- y^{1}, w^{67c23}; *P{FRTw^{hs}}G13, P{ubi-GFP}/CyO; P{T155-Gal4}, P{UAS-Flp}/TM6* (Duffy et al., 1998)
- y^{1}, w^{67c23}; *P{FRTw^{hs}}G13, P{dVHL$^{1.1}$}/CyO* was generated in Tien Hsu's lab
- y^{1}, w^{67c23}; *P{FRTw^{hs}}G13, P{Df(2R)enA}/SM6a* was generated in Tien Hsu's lab starting from Bloomington stock 7542.
- *FRT(42D),aPKC(k06403)/CyO* and *hsFLP;FRT(42D),Ubi-GFP (S65T)* were kindly provided by WM Deng, University of West Florida (Tian and Deng, 2008)
- *pUASP:aPKC-GFP/CyO* was kindly provided by C. D. Doe (Lee et al., 2006)
- *hs-d-VHL^{SB}-T4* : pCaspeR-hs-snapback d-VHL on third generated in Tien Hsu's lab (in the text I will refer at this as *hs-d-VHLRNAi*)
- *Cy2-Gal4* (Queenan et al., 1997); genotype *w*; Cy2-Gal4; P{w1mC1/4tubP-GAL80ts}7* was kindly provided by T.Schupbach, Princeton University

- *w^{1118}*, P*{ hsFLP}; CyO/Adv^{1}* (Golic, 1991; Bloomington #6)
- *w^{1118}; P{ry[+t7.2]=neoFRT}42D P{w[+mC]=Ubi-GFP(S65T)nls}2R/CyO* (Xu and Rubin, 1993; Bloomingoton # 5626)
- *FRT42D, egfr FRT42D, egfr ^{CO}/CyO* (Clifford and Schupbach, 1989) was kindly provided by T.Schupbach, Princeton University

Stocks were raised at 25°C and crosses were carried out at the same temperature unless otherwise stated.

3.3. Clonal Analyses

Follicle cell clones mutant for *d-VHL* were generated using site-directed mitotic recombination by using the Flp/FRT system (Golic, 1991; Xu and Rubin, 1993) and were induced by driving the Flp enzyme under the control of the *T155Gal4* promoter (Duffy et al. 1998). The *enhancer trap* line *T155-Gal4* is ubiquitous active in the follicle cells over the oogenesis and the Flp induces recombination at FRT target elements. Freshly eclosed females of the genotype *w^{67c23}; P{FRTw^{hs}}G13, P{Df(2R)enA}/ P{FRTw^{hs}}G13, P{ubi-GFP}; P{T155-Gal4}, P{UAS-Flp}/+* and *w^{67c23}; P{FRTw^{hs}}G13, P{$dVHL^{1.1}$}/ P{FRTw^{hs}}G13, P{ubi-GFP}; P{T155-Gal4}, P{UAS-Flp}/+* were transferred with *yw^{67c23}* males to fresh, yeasted food daily at 29°C for 3 days and then dissected.

Follicle cell clones mutant for *aPKC* were generated by the Flp/FRT technique by crossing the appropriate fly strains. Freshly eclosed females of the genotype *hsFLP; FRT(42D),aPKC(k06403)/ FRT(42D),Ubi-GFP (S65T)* were collected and heat shocked four times for 1 hr at 37°C. After the fourth heat shock, flies were transferred with *yw^{67c23}* males to fresh, yeasted food daily at 25°C for 3 days and then dissected.

Follicle cell clones mutant for *egfr* were generated by the same Flp/FRT technique by crossing the appropriate fly strains and site-directed mitotic recombination was catalyzed by the heat shock-inducible FLP yeast recombinase. Freshly eclosed females of the genotype *hsFLP;FRT42D,UbiGFP/FRT42D,egfr*^{CO} were collected and heat shocked three times for 1 hr at 37°C. After the third heat shock, flies were transferred with *yw*^{67c23} males to fresh, yeasted food daily at 25°C for 3 days and then dissected.

3.4. Gal4 Driven Expression in Follicle Cells

Females *w*; Cy2-Gal4/pUASP:aPKC-GFP; hs-d-VHLRNAi* and *w*; Cy2-Gal4/pUASP:aPKC-GFP* were obtained by crossing the parental strains. The crosses were performed at 18°C. Females *w*; Cy2-Gal4/pUASP:aPKC-GFP; hs-d-VHLRNAi* and the females used as a control carrying the *hs-d-VHLRNAi* transgene alone, were transferred with *yw*^{67c23} males to yeasted vials at 18°C and heat shocked four times for 1 hr at 37°C. After the fourth heat shock the flies were transferred to fresh, yeasted food at 29°C for 12 hours and then dissected.

3.5. Immunofluorescence Microscopy on egg chambers

Ovaries were dissected at room temperature in phosphate buffer saline (PBS 1X) pH 7.5, fixed in 4% paraformaldehyde in PBS1X pH 7.5 freshly prepared for 20 minutes at room temperature and the ovaries were then kept at room temperature to ensure that the microtubules did not depolymerize. After three washes 5 minutes each in PBS+0,1% Triton X-100 (PBT), egg chambers were dissected with needles and were permeabilized 1 hour at room temperature on a rotating wheel in PBS+1% Triton X-

100, incubated for 15 minutes in PBT+3%BSA at room temperature and then incubated with primary antibodies diluted in PBT+3%BSA overnight at 4°C on a rotating wheel. Next day egg chambers were washed three times 15 minutes each in PBT and incubated 15 minutes in PBT+3%BSA. Egg chambers were then incubated for 2 hours at room temperature on a rotating wheel with secondary antibodies diluted in PBT+3%BSA. After several washes in PBT, egg chambers were mounted in Fluoromount G (Electron Microscopy Sciences) and subsequently were analyzed with conventional epifluorescence on a Nikon Eclipse 90i microscope and with TCS SL Leica confocal system.

For propidium iodide nuclear staining the ovaries after incubation with secondary antibody were washed three times in PBT and treated with RNase A (400 g/ml in PBS, Sigma) for 2 hr. After three washes 10 minutes each in PBT, the ovaries were labeled for 15 min with propidium iodide (5 g/ml in PBT, Molecular Probes). Afterwards, the egg chambers were washed five times in PBT and mounted as indicated above.

TO-PRO 3 Iodide nuclear staining was carried out after immunodetection by incubating for 2 hr the egg chambers with TO-PRO 3 (Molecular Probes) at 0,01 mM in PBT 1X pH 7,5 and, after several washes with PBT, the egg chambers were mounted as indicated above.

Alexa Fluor 633-Phalloidin staining was carried out by incubating the egg chambers for 1 hour at room temperature with 633-Phalloidin diluted 1:100 (Molecular Probes) and after several washes with PBT, the egg chambers were mounted as indicated above.

3.6. Antibodies

Primary antibodies used for the immulocalization experiments are:

- polyclonal rabbit anti-Cleaved Caspase-3 (Cell Signaling Technology) was used at 1:50 dilution
- polyclonal rabbit anti-phospho-histone H3 (PH3, Upstate Biotechnology) was used at 1:200 dilution
- polyclonal rabbit anti-aPKCζ (C20, sc-216, Santa Cruz Biotechnology) was used at 1:200 dilution
- monoclonal mouse anti-Crumbs (Cq4, Developmental Studies Hybridoma Bank, DSHB) was used 1:5 and ovaries were fixed in methanol for 10 minutes instead of standard procedure with 4% paraformaldehyde
- polyclonal rabbit anti-d-VHL was raised against the full length of d-VHL protein and was generated in Tien Hsu's Department. It was used 1:10000 dilution for western blot and 1:1000 dilution for S2 cells immunostaining
- monoclonal mouse anti-βTubulin (E7, DSHB) was used at 1:25 dilution and 1:250 for western blot
- polyclonal rabbit anti-Lgl (Grifoni et al., 2004) was used at 1:500 dilution and was kindly provided by D. Grifoni (University of Bologna)
- polyclonal rabbit anti-Dystroglycan (Poulton and Deng, 2006) was used at 1:1000 dilution and was kindly provided by WM. Deng
- polyclonal rabbit anti-Bazooka (a gift from A.Wodarz) was used at 1:2000 dilution and 1:5000 dilution for western blot
- monoclonal mouse anti-α-Spectrin (3A9, DSHB) was used at 1:10 dilution
- monoclonal mouse anti-Armadillo (N2 7A1, DSHB) was used at 1:10 dilution

- monoclonal anti-Discs large (DLG, 4F2, DSHB) was used at 1:50 dilution
- monoclonal mouse Anti-βActin (clone AC-74, Sigma) used 1:2000 for western blot
- polyclonal rabbit anti-Par 6 (Petronczki and Knoblich, 2001) was used 1:1500 for western blot and was kindly provided by JA. Knoblich
- monoclonal mouse anti-Integrin βPS (CF6G11, DSHB) was used at 1:5 dilution
- monoclonal mouse anti-GFP (Santa Cruz, sc -9996) at a 1:1000 dilution
- polyclonal rabbit anti-VM32E (anti-CVM32E, Andrenacci et al., 2001) is directed against a peptide of 15 amminoacids corresponding to residues 102-106 at the C terminal and was used 1:100 diluted.

Secondary antibodies: rabbit antibodies were detected with Cy3-conjugated anti-rabbit secondary antibody (1:1000, Sigma), Cy3-conjugated anti-rabbit secondary antibody (1:2000, Jackson), Alexa-546 conjugated anti rabbit secondary antibody (1:200, Molecular Probes), Alexa-633 conjugated anti rabbit secondary antibody (1:200, Molecular Probes).

Mouse antibodies were detected with Cy3-conjugated anti-mouse secondary antibody (1:100, Sigma), Cy3-conjugated anti-mouse secondary antibody (1:200, Jackson), Alexa-546 conjugated anti rabbit secondary antibody (1:200, Molecular Probes).

3.7. *Ex Vivo* Culturing of *Drosophila* Egg Chambers

The protocol for this procedure was adapted from Prasad et al. (2007). Ovaries were dissected at room temperature in phosphate buffer saline (PBS 1X) pH 7.5 and all of the following steps are done at room temperature unless stated otherwise. Ovaries were transferred into 24 well dishes with 1 ml per well of 25°C-oxygenated Schneider's

complete medium cocktail (SCMC) (Schneider's Medium, 15% fetal bovine serum, 0.6X penicillin/streptomycin with a final pH of 6.95 to 7.00, before use add insulin 0.2mg/ml).

The drug treatments are then added to the labeled wells and gently rocked for 1 minute. The first treatment is DMSO only as a control. The second is paclitaxel at a final concentration of 3.2 μM or 6.4 μM. The third is nocodazole at a final concentration of 2.0 μM. Both drugs are dissolved in DMSO. The 24-well plate with the ovaries is then wrapped in aluminum foil and incubated undisturbed at 25°C for five hours.

After the five hour incubation, the ovaries are gently collected from the 24-well plate into individual tubes and washed twice with room temperature 1X PBS to remove any drug. The ovaries are then fixed in 4% paraformaldehyde in PBS1X pH 7.5 freshly prepared for 20 minutes at room temperature and then processed following the standard immunostaining procedures described in section 3.5..

3.8. Twin spots counting

The number of cells in mutant and wild-type twin spots of stage 10 egg chambers were counted. The spots contained at least two cells. I collected and examined with conventional epifluorescence on a Nikon Eclipse 90i microscope 25 different images of clones. I calculated the ratio of the cell number within the *d-VHL*$^{1.1}$ mutant clones per cell number within the sister wild-type clones and obtained a mean value of 0,96 (± 0,16 standard deviation).

3.9. Protein Immunoprecipitation

Ovaries from 50-150 females are collected in 1X PBS and rinsed twice with 1X PBS. Then 180 ml protein extraction buffer (50 mM HEPES (pH7.6), 100 mM KCL, 1 mM EGTA, 1mM $MgCl_2$, 1% Triton-X, and 10% glycerol) and 20 ml of 10X protein inhibitor cocktail were added. The ovaries were grinded up manually on ice for two minutes using an Eppendorf tissue grinder, then sonicated on ice four times with two-second intervals and spinned down at 6,000g for 20 minutes at 4°C. The supernatant was stored at -20°C in 50 μl aliquots and a small quantity was used to perform a protein quantification assay. 500 μg of protein was used for each Immunoprecipitation in a total volume of 500 μl of protein extraction buffer. At the same time, the proper amount of protein A/G agarose beads was added (Pierce catalog number 20421) (50 μl per Immunoprecipitation) to an Eppendorf and spinned briefly at 2,000g for two minutes. Half of the total volume of the supernatant was removed and replaced with protein extraction buffer. This process of briefly spinning the beads, removing half of the supernatant and replacing it with protein extraction buffer was repeated five times to equilibrate the A/G agarose beads. The eggs were pre-absorbed by adding 50 μl of the equilibrated A/G agarose beads and tumbled for 2-3 hours at 4°C. After a spinning at 2,000g for 2 minutes at 4°C the supernatant was placed into a new labeled Eppendorf tube, and the pre-absorbed beads discarded. Then the antibody of interest were added (anti-βTub, anti-GFP, anti-aPKC) to one Eppendorf (2-4 μg of antibody) to the supernatant and tumbled overnight at 4°C. Control IgG experiment (Rabbit IgG from Sigma, 10 mg/ml) was added to complement the antibody of interest. After incubation, 50 μl of the equilibrated A/G agarose beads were added to each sample and tumbled for 1-2 hours at 4°C. The samples were spinned down at 2,000g for two minutes and the

supernatant placed in a new Eppendorf. The last step was repeated one more time. After the final wash, 60 μl of 2X Sample buffer (SDS, Tris pH 6.8, 100% glycerol, β-mercaptoethanol) were added to the beads and boiled for 10 minutes before load the samples for regular Western Blot.

3.10. Protein extraction from ovaries

Ovaries from 50-150 females are collected in 1X PBS and rinsed twice with 1X PBS were quickly collected in cold 2X Sample buffer. The ovaries were grinded up manually on ice for two minutes using an Eppendorf tissue grinder, then sonicated on ice four times with two-second intervals and spinned down at 6,000g for 20 minutes at 4°C. The supernatant was stored at -20°C in 50 μl aliquots and a small quantity was used to perform a protein quantification assay.

3.11. Western Blot

The protein samples are placed in a boiling water bath for five to ten minutes and then loaded into the wells of 12% Acrilamide gel with a protein ladder. The proteins are then ran in the Western electrode box at 100 volts for one to two hours until the samples have reached the bottom of the cassette without running off.

For the transfer, I prepare the 0.45 μM PVDF membrane by quickly washing it with 100% Methanol followed by two quick rinses with dH_20. The membrane is then equilibrated in transfer buffer for 30 minutes before beginning the transfer. The transfer is run at 25 volts for approximately three hours.

Once the transfer is complete, the PVDF membrane is removed from the transfer apparatus and blocked in 5% milk in 1X TBST (Tris, NaCl, 0,1% Tween 20) for one

hour at room temperature. The blocking milk is removed and replaced with 5% milk with the primary antibody overnight at 4°C. The membrane is then rinsed with 1X TBST for two quick washes and an additional wash for 15 minutes at room temperature. The washes are removed, replaced with the secondary antibody conjugated to HRP in 10 ml 1X TBST, and incubated at room temperature for one hour. The membrane is then rinsed four times in 1X TBST for 10 minutes each wash and incubated with 1.6 ml of chemiluminescent substrate (Pierce catalog number 34080). The membrane is then wrapped in a plastic cover and developed in the dark room.

After developing, the membrane can be stripped and re-probed for a second antibody by adding 15 ml of stripping buffer (Pierce catalog number 21059) and incubating at 37°C for 10 to 15 minutes. The membrane is then washed twice for 15 minutes each with 1X TBST and then is ready to be re-probed with primary antibody and incubated overnight at 4°C or stored in plastic wrap at -20°C.

3.12. Cells Culture

Schneider S2 cells were maintained in Schneider's *Drosophila* medium (Sigma) supplementes with 10% heat-inactivated FBS (Invitrogen), 1X Penicillin-Streptomycin-Glutamine (Invitrogen) and 2.5 μg/ml of Fungizone (Invitrogen).

For microscopy, cells were plated on coverslips previously coated with 0,01 mg/ml Poly-L-lisine (Sigma, P4832) and 0,5 mg/ml Concanavalin A (Sigma, C5275) (Rogers et al., 2002).

3.13. Plasmids and transfection of S2 cells

The following plasmids were used: pCaspeR-hs (DGRC) empty as a control.

pCaspeR-hs *d-VHL* full length was generated by subcloning the full length *d-VHL* cDNA into EcoR I and XbaI sites of pCaspeR-hs vector. pCaspeR-hs *d-VHLRNAi* construct was generated by cloning two VHL ORFs head to head to make the duplex and then subcloning it into pCaspeR-hs vector.

S2 cells were plated and growth until 80% confluence, then left overnight in Schneider's Media with serum but not antibiotic and fungicide. The next day cells were transfected by using Lipofectamine 2000 (Roche) according to the manufactured protocol. Briefly for 12 well plate, the plasmid DNA (2μg for each 12 well plate) and Lipofectamine were diluted separately in Schneider's Media, mixed gently and incubated 5 minutes at RT. Then DNA and Lipofectamine (200 μl total volume) were combined, mixed gently and incubated for 20 min at RT. The media from cells was removed and 800 μl per well of Schneider's Media without serum was added. Then the 200 μl of mix (DNA+Lipofectamine) was added into 800 μl media cells, gently mixed by rolling the plate back and forward and incubated overnight at 25°C. The next day the mix was removed and fresh complete Schneider's media (without Fungicide) was added. Cells were allowed to recover at 25°C for 72-96 hr and then placed for 2 days at 29°C to induce Hsp70 promoter in pCaspeR-hs and subsequently processed for protein extraction or immunofluorescence.

3.14. Immunofluorescence Microscopy on S2 cells

Cells were fixed for 15 minutes in 3,7% formaldehyde (freshly prepared) at RT without rolling. After three washes in PBS 1X at RT without rolling, cells were permeabilized for 20 min in PBT (PBS1X + 0,1% Triton) at RT without rolling. Then cells were incubated in blocking solution (PBT + 1% BSA) for 30 minutes without

rolling at RT. Then Primary antibody diluted in PBT + 1% BSA was added and incubated for 2 hr at RT. After three washes in PBS 1X, secondary antibodies were added diluted in PBT + 1% BSA and incubate for 2 hr at RT. After three washes in PBS 1X cells on coverslips were directly mounted in Fluoromount G and were mounted in Fluoromount G (Electron Microscopy Sciences) and subsequently were analyzed with conventional epifluorescence on a Nikon Eclipse 90i microscope and with TCS SL Leica confocal system.

3.15. S2 cells Protein Extracts

Cells were rinsed once with 1X PBS and quickly collected in cold 2X Sample buffer. The cells were then sonicated on ice four times with two-second intervals and spinned down at 6,000g for 20 minutes at 4°C. The supernatant was stored at -20°C in 50 ml aliquots and a small quantity was used to perform a protein quantification assay.

Western blot was performed as previously described in section 3.11. by loading 75 μg of protein extract.

3.16. RT-PCR on S2 cells

Total RNA was extracted using TRI Reagent and concentration and purity was determined by measuring optical density at 260 and 280 nm using a spectrophotometer. Briefly, 5 μg of total RNA was reverse transcribed with random hexamers using a Transcriptor First Strand cDNA Synthesis kit (Roche) according to the manufacturer's protocol. Real-time RT-PCR was performed using IQTM SYBR Green Supermix (Bio-Rad) and MyiQ™ Single-Color Real-Time PCR Detection System (Bio-Rad). The amount of template used in the PCR reactions was cDNA corresponding to 200 ng

reverse-transcribed total RNA. The amplification mixture (10 µl) contained 0.125 µg of cDNA, 0.25 µM of each primer (F primer: TGAATTTTATCTATACTTGTTGTTAGC; R primer: TGCAAACAGCACGTACACCT, according to the *d-VHL* cDNA sequence), and 5 µl of iQSybr Green Supermix (Bio-Rad). DNA polymerase was first activated at 95 °C for 3 min, denatured at 95 °C for 30 s, and annealed/extended at 61 °C for 30 s, for 40 cycles according to the manufacturer's protocol. Expression of the housekeeping gene rp49 served as an internal positive control in each assay performed. The relative change in the levels of genes of interest was determined by the 2–{Delta}{Delta}CT method. To compare the different samples in an experiment, RNA expression levels in samples were compared to expression of the control in each experiment. After measurement of the relative fluorescence intensity for each sample, the amount of each mRNA transcript was expressed as a threshold cycle (ct) value.

4. RESULTS

4.1. During oogenesis *d-VHL* is required to maintain follicular epithelium integrity

To examine whether *d-VHL* has a role in epithelial morphogenesis, I analyzed the follicle cell phenotype produced by loss of *d-VHL* during oogenesis through clonal analysis. To this purpose I generated follicle cell clones by using loss-of-function *d-VHL* mutations. The two mutant lines used in my analysis were *d-VHL Df(2R)enA* and *d-VHL*$^{1.1}$, both generated in Prof. Tien Hsu's lab. The first one is a chromosomal deletion (Parks et al., 2004) homozygous lethal, that covers the region 47D6-48F8 on second chromosome (211952 bp deleted), including the genomic *d-VHL* sequences 47E5-47E6. The deletion results in the complete loss of *d-VHL* function. The *d-VHL*$^{1.1}$ mutant was generated by replacing the wild-type copy, via homologous recombination, with a deletion that removes the 81 codons encompassing the first two in-frame AUGs, resulting in a protein null mutation.

Homozygous *d-VHL* clones, genetically marked by the absence of GFP, were obtained through somatic recombination using the Flp/FRT system (Golic, 1991; Xu and Rubin, 1993) and were induced by driving the Flp enzyme under the control of the *T155Gal4* promoter. The *enhancer trap* line *T155-Gal4* is ubiquitously active in the follicle cells over the oogenesis (Duffy et al., 1998; Liu and Montell, 1999; Yu et al., 2006; Hrdlicka et al., 2002). To induce mutant clones, adult females were kept at 29ºC for 3 days and then dissected. The analyzed egg chambers showed mosaic follicular epithelium, containing three cellular populations: homozygous clones carrying two copies of *d-VHL Df(2R)enA* or *d-VHL*$^{1.1}$; homozygous clones presenting two copies of UbiGFP and heterozygous clones carrying one copy of UbiGFP and one copy of *d-VHL Df(2R)enA* or *d-VHL*$^{1.1}$ in the cells where mitotic recombination did not take place. It

should be noted that the follicular mutant clones are most likely generated early during oogenesis because follicular mitotic cycle ends at stage 6 (Liu and Montell, 1999).

To analyze follicle cell morphology, egg chambers from *w; d-VHL*$^{1.1}$*,FRT*^{G13}*/FRT*^{G13}*UbiGFP; T155Flp/+* females, were stained with the nuclear marker propidium iodide. Figure 12 shows the confocal analysis of stage a 10A egg chamber containing a mutant clone observed in surface (Fig. 12 A-C) and in cross section (Fig. 12 D-F). The follicle cells homozygous for the *d-VHL*$^{1.1}$ mutation, marked by the absence of GFP (green, Fig. 12 B,E), show a strong propidium iodide staining compared to the neighbour wild-type cells (red, Fig. 12 A,D). By counting the number of cells in mutant and wild-type twin spots of stage 10 egg chambers it appears that follicle cell proliferation is not affected by the loss of *d-VHL*. I calculated the ratio of the cell number within the *d-VHL*$^{1.1}$ mutant clones per cell number within the sister wild-type clones (number of clones examined = 25) and obtained a mean value of 0,961 (± 0,16 standard deviation). Importantly, the ratio between the cell number in mutant and sister clones did not change as a function of the clone size (Fig. 12 G,H; G is plotted as a function of increasing sister clone size, H is the mutant:sister ratio of G as a function of increasing sister clone size). Furthermore, the mosaic ovaries were stained with an antibody against phospho-histone H3 (PH3) that is specific for the phosphorylated form of histone H3 present only in mitotic nuclei (anti-PH3; Hendzel et al., 1997). In mosaic *d-VHL*$^{1.1}$ egg chambers as in wild-type ovaries no PH3-positive cells were detected beyond stage 6 (data not shown), indicating that loss of *d-VHL* function in follicular clones does not induce detectable extension of the proliferative program of the follicle cell population. The propidium iodide staining shows no chromatin condensation in *d-VHL*$^{1.1}$ clones and anti-Cleaved Caspase-3 antibody

(Peterson et al., 2003) did not show immunoreactivity on *d-VHL*$^{1.1}$ clones (data not shown), suggesting that loss of *d-VHL* function does not cause apoptosis in the follicle cell clones. Therefore the strong propidium iodide nuclear staining observed in *d-VHL*$^{1.1}$ clones might suggest a possible deregulation of follicle cells endocycles. By stage 7, the epithelial follicle cells cease proliferation and enter endocycles, a change in cell cycle triggered by Notch signaling (Shcherbata et al., 2004; Horna-Badovinac and Bilder, 2005). Thus, loss of *d-VHL* function causes a cell-autonomous effect on follicle cell and considering that VHL is also involved in cell cycle control (Pause et al., 1998), deregulation of endocycles could be linked to the cell cycle control function ruled out by *d-VHL*.

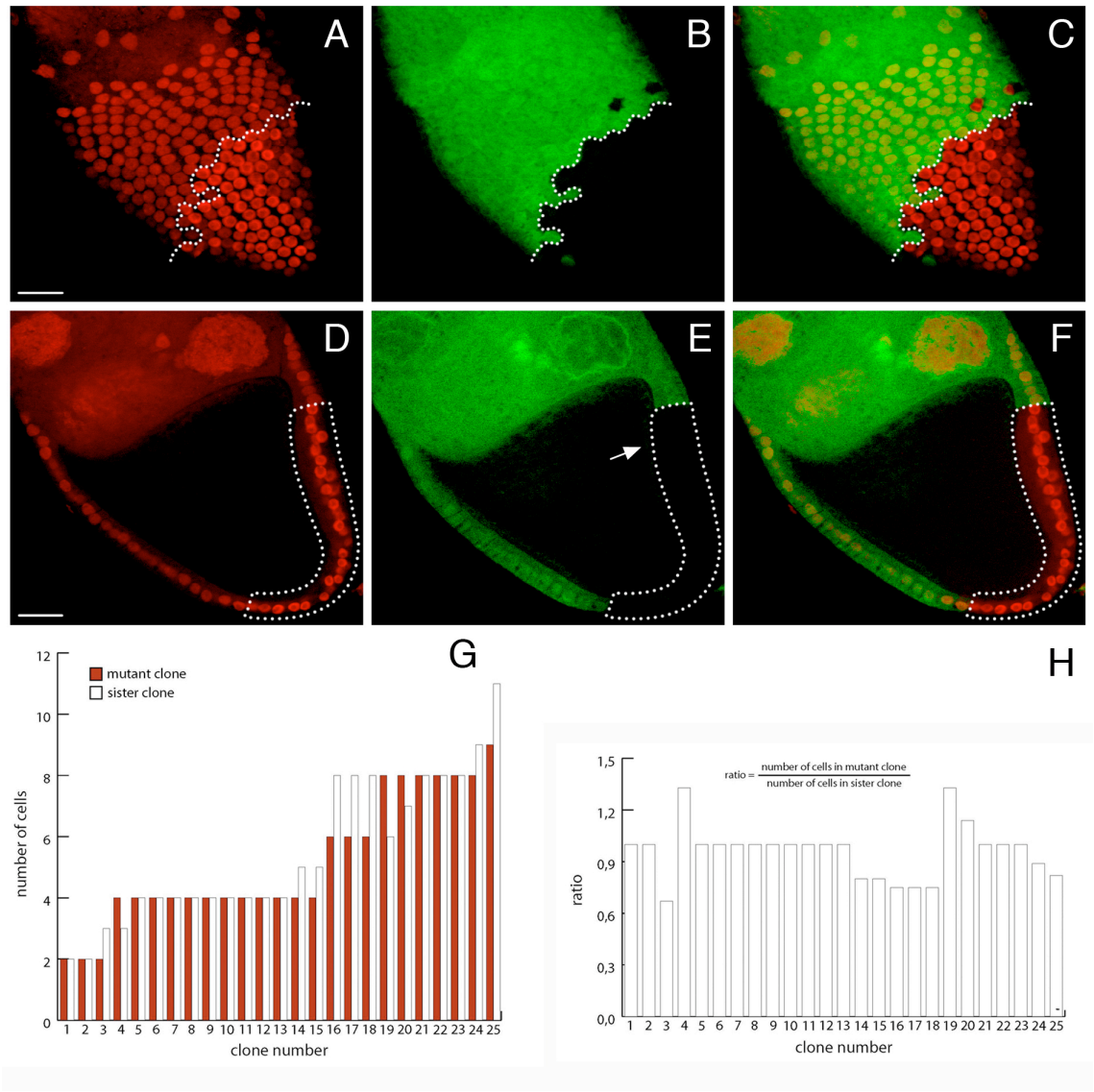

Figure 12. d-VHL is required to maintain follicular epithelium integrity.
Confocal surface-section (A-C) and cross-section (D-F) of a stage 10A egg chamber from females *w; dVHL*$^{1.1}$*, FRT*^{G13}*/FRT*^{G13}*UbiGFP; T155Flp/+* stained with propidium iodide (A and D; red). Dotted line in A-C and dotted area in D-F set the mitotic clone marked by the absence of GFP (B and E; green). C merged image of A and B. F merged image of D and E. Arrow in E points the thickening of mutant epithelium. Anterior is up in all panels. Bars, 20 µm.
G. Quantification of the number of cells in d-VHL mutant clones (red bars) compared with the sister clones (white bars). H. Ratio of the size of mutant clone per the size of sister clone in G plotted as a function of sister clone size. Number of clones examined is 25 and the mean value is 0,961 (± 0,16 standard deviation).

The follicle cells mutant clones displayed abnormal epithelial characteristics, such as the pronounced stacking of the mutant cells shown in the cross section in Figure 12 D-F. Moreover in this clone the epithelium is thicker (arrow in Fig. 12 E) if compared to the wild-type cells and is evident how mutant cells fail to form a coherent single-layered epithelium. I then analyzed the phenotypic effects on epithelium morphology caused by the loss of *d-VHL* in 100 clones. Smaller clones display a much lower frequency of defects which are usually milder, so for this analysis I considered clones larger than 2 cells. In 38% of analyzed clones I observed a pronounced stacking of cells; in 42% of clones I observed a shrinking of the epithelium. In the rest of clones analyzed I observed an evident thickening of the epithelium. The penetrance of these defects tends to increase with the size of the clone and the stage of oogenesis, but even single mutant cells show defects, such as the shrinking of the epithelium.

Phenotypes	**Percentage**
Cells stacking	38 %
Thin epithelium	42 %
Thick epithelium	20 %

Perturbation of d-VHL function in follicle cells causes indeed altered cell distribution without affecting cell proliferation or cell death and results in morphological defects in the epithelium.

Results similar to those described above, have been obtained by analyzing follicle cell clones of egg chambers from *w; d-VHL Df(2R)enA,*

FRT^{G13}/FRT^{G13}UbiGFP; T155Flp/+ females. Therefore, the *d-VHL$^{1.1}$* mutation behaves as a null mutation that causes the absence of a functional protein.

In the text will be presented results relative to the analysis carried out by using the *d-VHL$^{1.1}$* mutant line.

4.2. Loss of *d-VHL* in follicle cell clones affects intercellular adhesion and cell polarity

I analyzed the epithelial junction proteins pattern in the *d-VHL* loss of function follicle cell clones through immunostainings on egg chambers from *w; d-VHL $^{1.1}$,FRT^{G13}/FRT^{G13}UbiGFP; T155Flp/+* females. I took into account components from each epithelial follicle cells domains: the apical junction that connects to the germ cells, the three conserved lateral junctions, the apicolateral, adherens and basolateral junctions which intereconnet follicle cells to each other, and the basal junction that connects to the outer basement membrane (Figure 5; Szafranski and Goode, 2007).

Apical Junction

The filamentous protein α-Spectrin forms a network with actin cytoskeleton that regulates and stabilizes the membrane shape in the apical domain and also in the basolateral domain as described in section 1.7.. Interestingly in the homozygous *d-VHL$^{1.1}$* clones, genetically marked by the absence of GFP, after stage 6 of oogenesis α-Spectrin is strongly enhanced. This is clearly shown in follicle cell clones from a stage 9 egg chamber observed in cross section (Fig. 13 A-F) and in two large follicle cell clones from a stage 10B egg chamber observed in surface section (Fig. 13 G-L). In Figure 13 E α-Spectrin is strongly enhanced in the apical (arrows in Fig. 13 E) and lateral side of

mutant follicle cells. Moreover, in the higher magnification of the clone observed in surface section is possible to appreciate more signal as dots interspersed in the *d-VHL* mutant cells cytoplasm (stars in Fig. 13 K). This could be due to the loss of correct follicle cell shape in the *d-VHL* loss of function cells. As a consequence, the correct localization of the filamentous protein α-Spectrin along the cellular membrane is compromised. This data could raise the possibility that in *d-VHL* loss of function cells the protein trafficking system along the cytoskeleton network is compromised then protein delivery and recycle results affected.

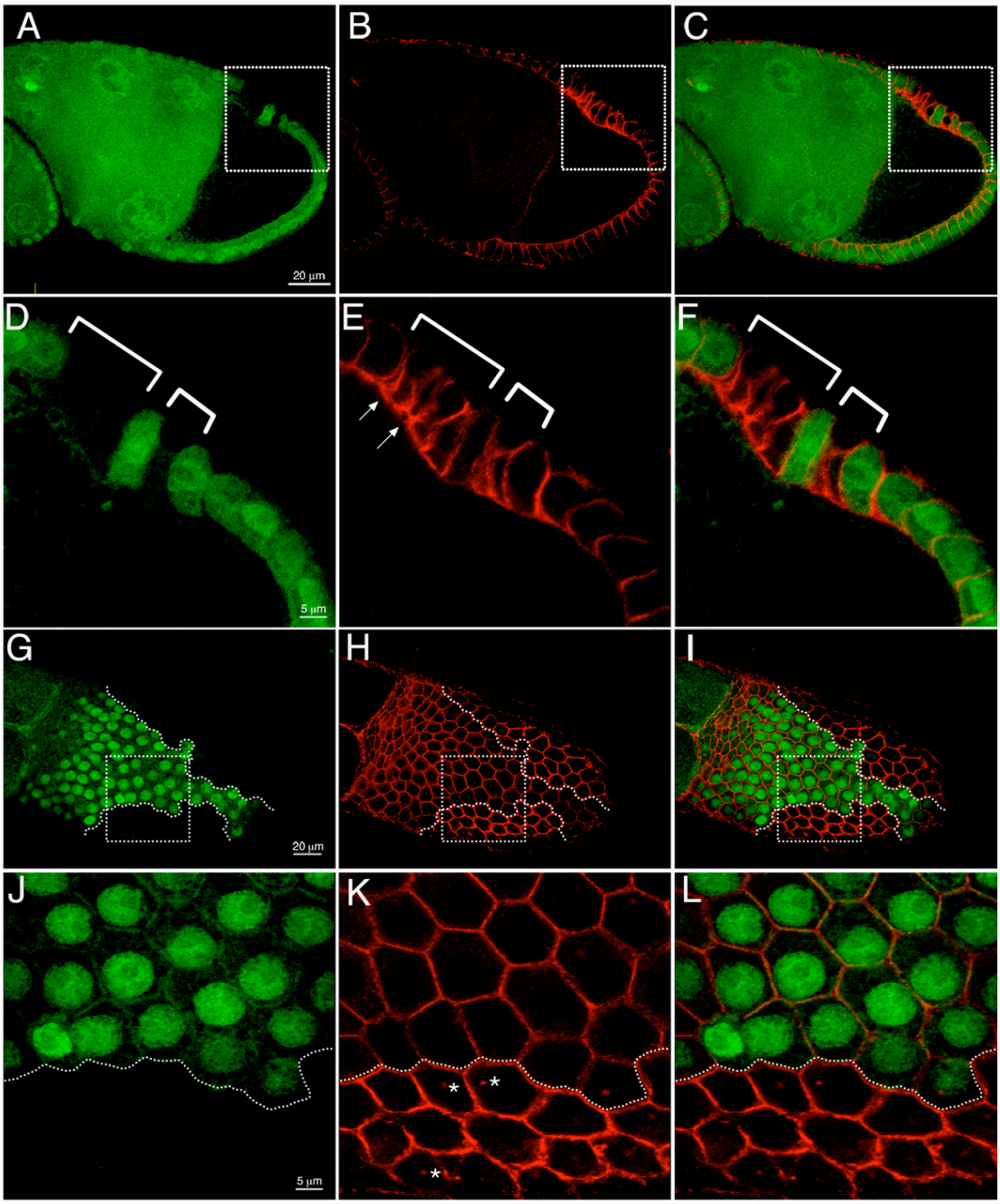

Figure 13. d-VHL loss of function analysis in the Apical Junction.
Confocal cross-sections of a stage 9 egg chamber (A-F) and surface section of a stage 10B egg chamber (G-L) from females *w; dVHL$^{1.1}$,FRT^{G13}/FRT^{G13}UbiGFP; T155Flp/+*. ⟨-Spectrin (B, E, H, K; red) is abundantly enriched in the apical (arrows in E) and lateral domains of mutant follicular cells. D-F: higher magnification views of boxed region in A-C. Brackets in D-F point the mitotic clones marked by the absence of GFP (A and D; green). J-L: higher magnification view of boxed region in G-I. Dotted lines in G-L point the mitotic clones marked by the absence of GFP (G and J; green) where is clearly visible more ⟨-Spectrin signal from the apical surface view. Stars in K point the α-Spectrin dots displaced inside the mutant cells cytoplasm. Merged images of GFP and ⟨-Spectrin signals is shown in C, F, I, L.
Anterior is on the left in all panels.

Apicolateral Junction

Drosophila aPKC is a component of the PAR-3/PAR-6/aPKC complex, which is part of apicolateral junction domain and is required to establish polarity in many different cell types.

In homozygous *d-VHL*$^{1.1}$ clones, aPKC protein is not correctly localized to the apical side of follicle cells (Fig. 14 A-C), but is instead delocalized in the follicle cells cytoplasm (stage 9, Fig. 14 B) and concentrated all around the cell nuclei (arrowhead in Fig. 14 B). At stage 10A in homozygous *d-VHL*$^{1.1}$ clones I observed a strong reduction of aPKC signal (Fig. 14 E). I next analyzed the distribution of Bazooka (Baz) and I found that Baz is also altered in homozygous *d-VHL*$^{1.1}$ clones (Fig. 14 G-L). During early stages Baz (stage 4, Fig. 14 H) is less accumulated on the apical domain of follicle cells and is instead more spread along the lateral membrane (arrowhead in Fig. 14 H). During mid-oogenesis (stage 10A, Fig. 14 J-L) Baz appears delocalized and spreads around the nuclei instead of being localized on the apical surface (arrowheads in Fig. 14 K). When the epithelium is dramatically compromised Baz is almost completely lost (arrow in Fig. 14 K).

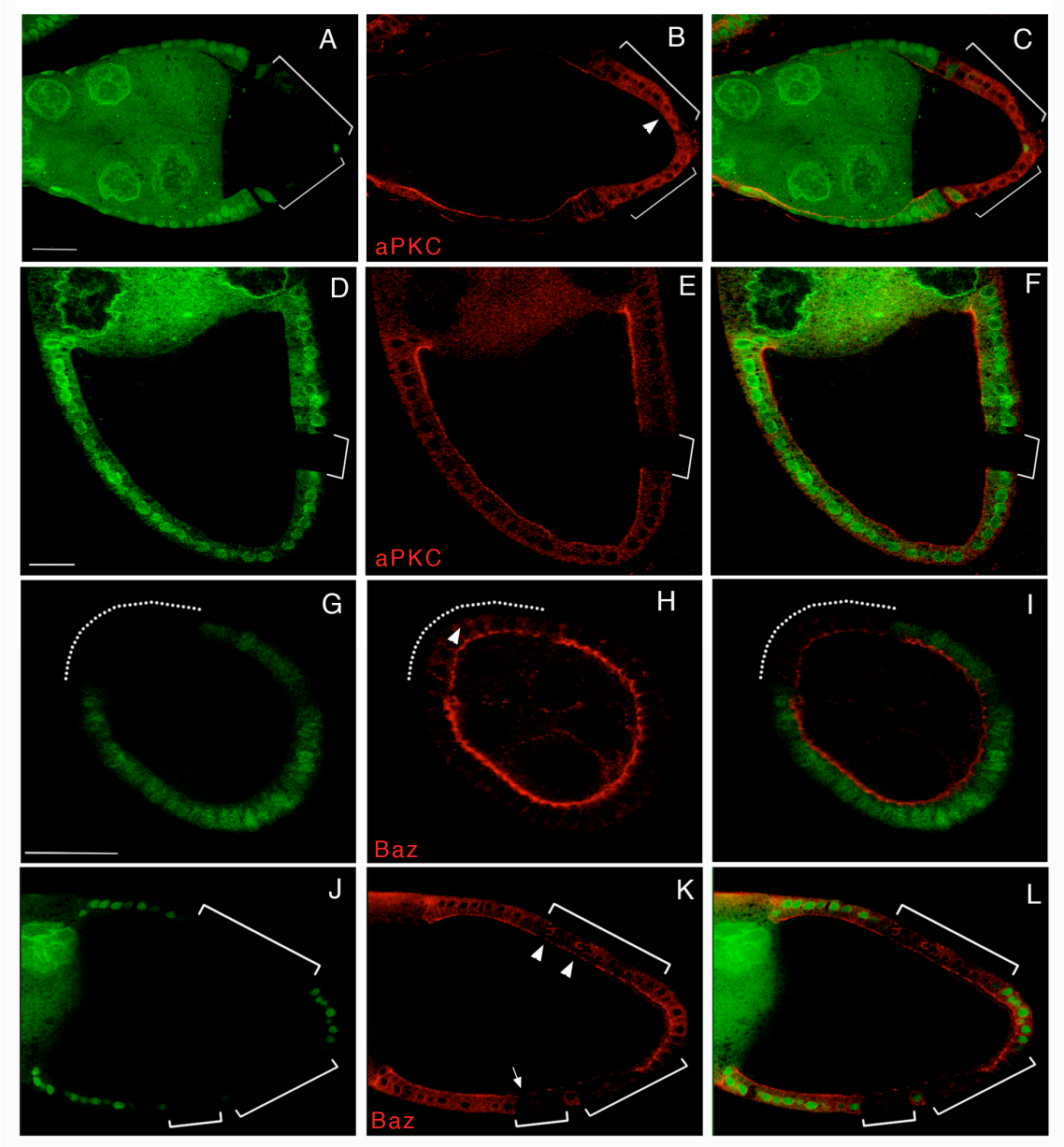

Figure 14. d-VHL loss of function analysis in the Apicolateral Junction.
Confocal cross-sections of a stage 9 egg chamber (A-C) and 10A egg chamber (D-F) from females *w; dVHL$^{1.1}$,FRT^{G13}/FRT^{G13}UbiGFP; T155Flp/+*. aPKC (B, E; red) is strongly altered in mitotic clones marked by the absence of GFP (A and D; green). Brackets in A-C point the mitotic clones where aPKC is delocalized in the follicle cell cytoplasm instead of being accumulated on the apical side. Arrowhead in B points the aPKC accumulation around the mutant nuclei. Brackets in D-F point the clone where aPKC staining is undetectable. Merged images of GFP and aPKC signals is shown in C and F.

Confocal cross-sections of a stage 4 egg chamber (G-I) and 10A egg chamber (J-L) from females *w; dVHL$^{1.1}$,FRT^{G13}/FRT^{G13}UbiGFP; T155Flp/+*. Baz (H, K; red) is strongly altered in mitotic clones marked by the absence of GFP (G and J; green). Dotted lines in G-I shows that Baz is less accumulated on the apical side and arrowhead in H shows that Baz is more spread on the lateral domain. Brackets in J-L point the mitotic clones where Baz is strongly altered. Arrow in K points the mutant cell where Baz in undetectable. Arrowheads in K point the Baz accumulation around the mutant nuclei. Merged images of GFP and Baz signals are shown in I and L. Bars 20 μm.

These data clearly show that homozygous *d-VHL* loss of function cells lose their polarity and this could be due to a possible deregulation in the subcellular trafficking transport of these polarity markers from Golgi apparatus to the apical domain of follicle cells (Nelson and Yeaman, 2001). Moreover several studies demonstrated the direct interaction between h-VHL and aPKC (Iturrioz et al., 2006 ; Okuda et al., 2001; Okuda et al., 1999) raising the possibility that h-VHL might be an anchor for signalling proteins such as aPKC required for regulating growth and differentiation (Okuda et al., 1999).

The subapical region (SAR), located right below the apical domain, can be visualized by Crumbs (Crb), a transmembrane protein required for the establishment of this domain, together with its cytoplasmic-binding partners, such as aPKC (Knust and Bossinger, 2002; Tepass et al., 1990; Wodarz et al., 1995). In homozygous *d-VHL*$^{1.1}$ clones at early stages (stage 6, Fig. 15 A-D) and during mid-oogenesis (stage 10A, Fig. 15 E-H) Crb is strongly altered. The protein level is lower compared to the wild-type cells and in some case Crb is undetectable on the apical compartment (Fig. 15 G) or is delocalized as dots in the mutant cells cytoplasm (star in Fig. 15 G).

Adherens Junction (AJ)

In homozygous *d-VHL*$^{1.1}$ clones, DE-cadherin appears slightly compromised (data not shown), whereas Armadillo (Arm) distribution is altered after stage 6 of oogenesis. As shown in Figure 15 I-N, loss of *d-VHL* causes a pronounced thickening of the epithelium and Arm appears more abundant at the AJ compartment and spreads along the lateral side (stage 9, Fig. 15 M). Moreover Arm signal is found as dots displaced inside the mutant cells cytoplasm (star in Fig. 15 M). This data suggests a

possible deregulation in the mechanism of proteins recycling, since the correctlocalization of Arm is lost only after stage 6, when the AJ are already set up but they need to rearrange to allow the migration of follicle cells (Dobens and Raftery, 2000).

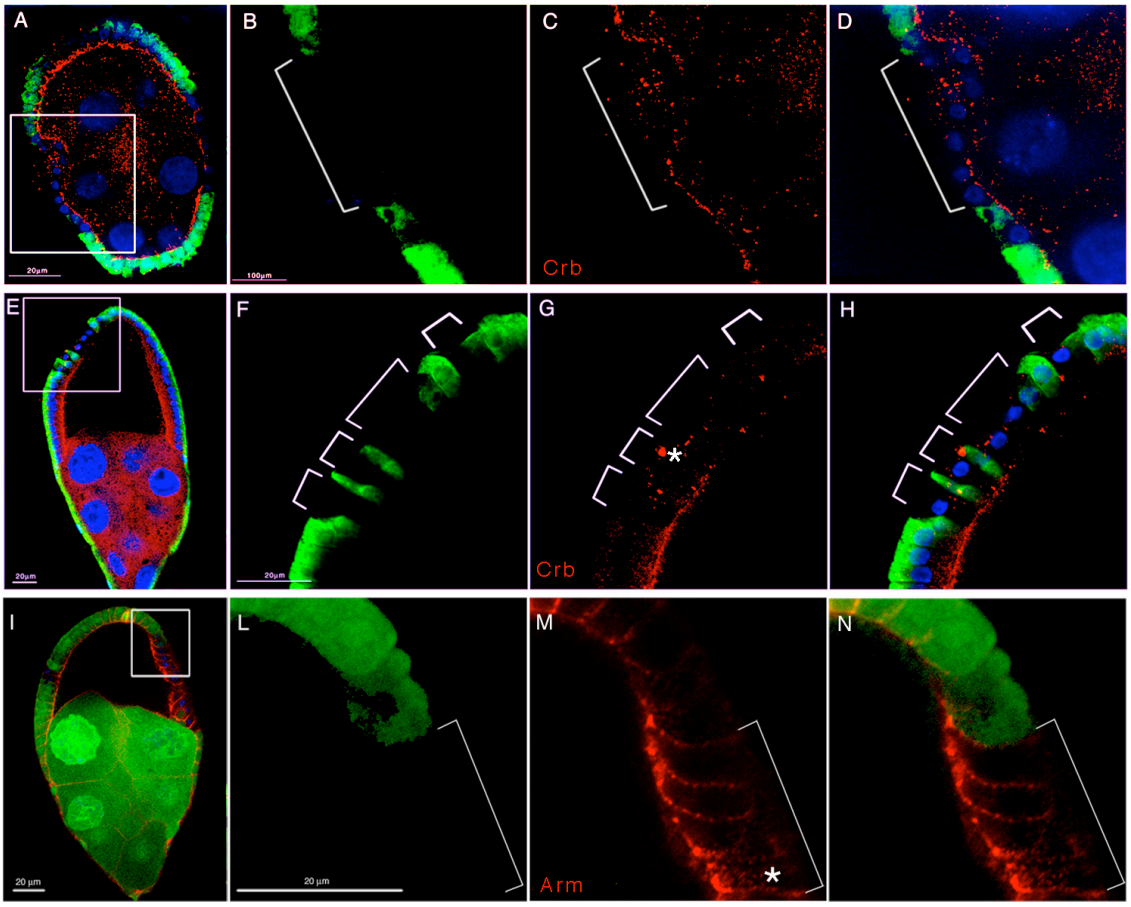

Figure 15. d-VHL loss of function analysis in the SAR and AJ.
Confocal cross-sections of a stage 6 egg chamber (A-D) and 10A egg chamber (E-H) from females *w; dVHL$^{1.1}$,FRT^{G13}/FRT^{G13}UbiGFP; T155Flp/+* showing that Crb (C and G; red) is strongly affected in mitotic clones marked by the absence of GFP (B and F; green). A,E. Merged images of GFP (green), Crb (red), Topro (blu). B-D: higher magnification view of boxed region in A. F-H: higher magnification view of boxed region in E. Brackets in B-D and F-H point the mitotic clones where Crb is clearly less accumulated or undetectable. Star in G points the delocalization of Crb as dots in the mutant cells cytoplasm. Merged images of GFP and Crb signals are shown in D and H.
Confocal cross-sections of a stage 9 egg chamber (I-N) from females *w; dVHL$^{1.1}$,FRT^{G13}/FRT^{G13}UbiGFP; T155Flp/+* showing that Arm (M; red) is strongly affected in mitotic clones marked by the absence of GFP (L; green). I. Merged image of GFP (green), Crb (red), Topro (blu). L-N: higher magnification view of boxed region in I. Brackets in L-N point the mitotic clone where Arm is clearly abundantly enriched at the AJ compartment and spread along the lateral side of mutant follicle cells. Star in M points the Arm signal as displaced dots inside the mutant cells. Merged image of GFP and Arm signals is shown in N.
Anterior is up in all panels.

Basolateral Junction (BLJ)

I next took in to account the epithelial junction proteins pattern along the basolateral side of follicle cells. The basolateral domain in *Drosophila* is represented by the Septate Junctions (SJ), functional barriers that enable transepithelial circulation. In the homozygous *d-VHL* loss of function clones DLG pattern is strongly affected (stage 10B, Fig. 16 A-I) since is evident a significant reduction of DLG staining on the most basal side (arrows in Fig. 16 E) and a spreading of the protein along the apical surface (arrowheads in Fig. 16 E). By observing *d-VHL* loss of function clones in a surface view from the basal side, DLG is not detectable (stage 10B, Fig. 16 H). It has been shown that AJ restrict DLG to the lateral membrane by a mechanism that is reinforced by Crb (Le Bivic A, 2005; Lecuit, 2004), so it is conceivable that when Arm and Crb are mislocalized, DLG is not correctly restricted to the basolateral side and diffuses along the apical side.

In the homozygous *d-VHL*$^{1.1}$ clones, Lgl pattern is dramatically affected as shown in a stage 10B egg chamber (Fig. 16 J-L) where no signal was detected along the lateral side of the mutant cells, if compared with the neighbours wild-type cells in which Lgl is correctly distributed along the lateral domain (Fig. 16 K).

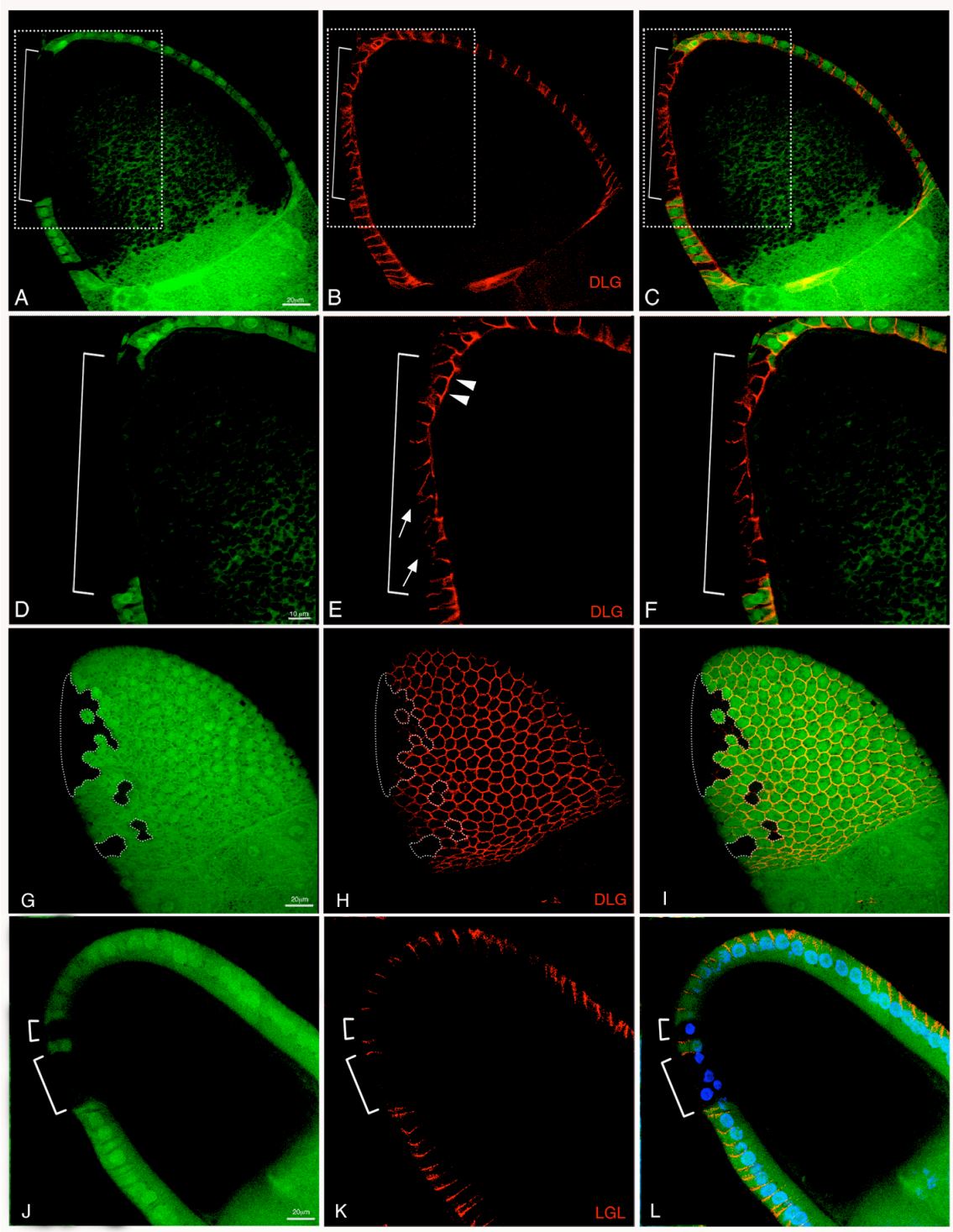

Figure 16. d-VHL loss of function analysis in the BLJ.
Confocal cross-section (A-F) and surface section (G-I) of a stage 10B egg chamber from females *w; dVHL$^{1.1}$,FRT^{G13}/FRT^{G13}UbiGFP; T155Flp/+.* DLG (B, E, H; red) is strongly altered in mitotic clones marked by the absence of GFP (A, D, G; green). D-F: higher magnification view of dotted region in A-C. Brackets in D-F point the mitotic clone in which DLG is undetectable in the basal side (arrows in E) and it spreads on the apical side (arrowheads in E). Dotted area in G-I point the mitotic clones showing that DLG is undetectable on the follicle cells basal side. Merged images of GFP and DLG signals are shown in C, F, I.
Confocal cross-sections (J-L) of a stage 10B egg chamber from females *w;*

dVHL$^{1.1}$,FRT^{G13}/FRT^{G13}UbiGFP; T155Flp/. Lgl (K; red) is undetectable in mitotic clones marked by the absence of GFP (J; green) and by the white brackets. Merged image of GFP, Lgl and Topro (blu) signals is shown in L.
Anterior is down in all panels.

Basal Junction

I then analyzed protein expression pattern of proteins involved in the attachment to the basement membrane (BM) or basal lamina. In homozygous *d-VHL$^{1.1}$* clones βPS integrin level is dramatically reduced (Fig. 17 A-D), as observed by a surface section of a clone in stage 9 egg chamber (Fig. 17 C). By analyzing this clone in cross section (Fig. 17 E-H), it is evident that mutant follicle cells showing the multilayered phenotype lose βPS from basal and lateral side and only delocalized signal on the apical side of *d-VHL$^{1.1}$* cells is still visible (arrowheads in Fig. 17 G). The neighbour wild-type cells show the correct βPS localization in the basal side of follicle cells (Bateman et al., 2001; Brown et al., 2002) and in the lateral and apical domains as observed by Fernández-Miñán et al. (2007).

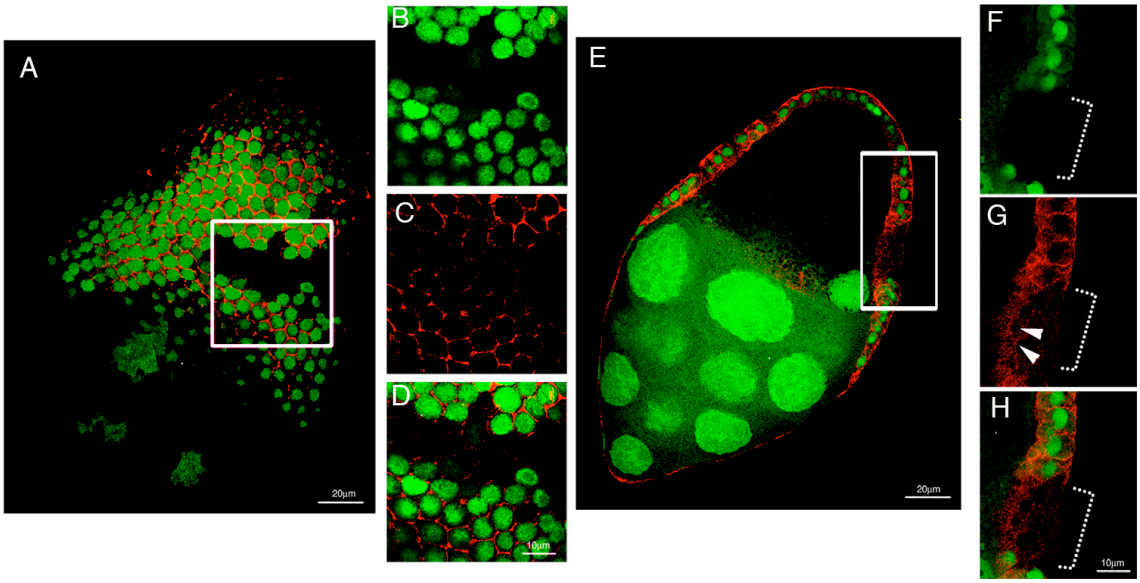

Figure 17. d-VHL loss of function analysis in the Basal Junction.
Confocal surface section (A-D) and cross-section (E-H) of a stage 9 egg chamber from females *w; dVHL$^{1.1}$,FRT^{G13}/FRT^{G13}UbiGFP; T155Flp/+.* A,E. Merged images of GFP (green) and βPS (red) signals. B-D: higher magnification view of boxed region in A. F-H: higher magnification view of boxed region in E. βPS (C and G; red) is strongly altered in mitotic clones marked by the absence of GFP (B and F; green). Dotted brackets in F-H point the mitotic clone showing that βPS integrin staining is undetectable on the basal and lateral side. Arrowheads in G point the βPS signal still visible on the most apical side of mutant cells. Merged images of GFP and βPS signals are shown in D and H.
Anterior is down in all panels.

4.3. Loss of *d-VHL* in follicle cell clones affects actin cytoskeleton

The membrane asymmetries of follicle cells involve also the cytoskeleton components. The cortical Spectrin cytoskeleton becomes polarized into an apical domain that is composed of β_{heavy} spectrin and α-spectrin, and a basolateral domain that contains β/α spectrin complexes. Actin also becomes enriched in the apical cortex of these cells, as in other epithelia (Baum et al., 2000; Mooseker, 1985). In *d-VHL* $^{1.1}$ clones, F-actin distribution is extremely altered, as shown in a large stage 10B clone (Fig. 18). By looking at the cross section, actin cytoskeleton is completely lost in the most basal side of mutant follicle cells (Fig. 18 C). The mutant epithelium loses its proper monolayer structure (Fig. 18 B) and actin signal is reduced in the apical cortical domain (Fig. 18 C-E).

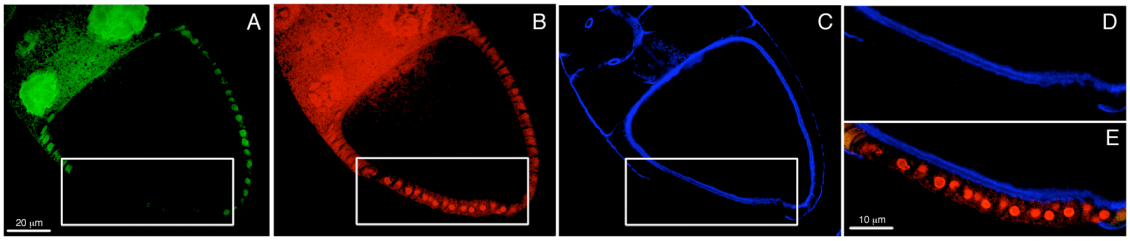

Figure 18. Actin cytoskeleton network in d-VHL loss of function cells.
Confocal cross-section of a stage 10B egg chamber from females *w; dVHL$^{1.1}$,FRT^{G13}/FRT^{G13}UbiGFP; T155Flp/+* stained with 633-phalloidin (C and D; blu), and propidium iodide staining (B; red). Actin signal is undetectable on the basal side and is reduced in the apical cortical domain of mitotic clone marked by the absence of GFP (A; green). D, E. Higher magnification view of boxed region in A-C where is clearly visible that mutant epithelium loses its proper monolayer structure. Anterior is up in all panels.

4.4. Loss of *d-VHL* affects microtubules architecture during oogenesis

The microtubule cytoskeleton is involved in long-range transport of vesicular carriers and in the morphogenesis of columnar-shaped, polarized epithelial cells. During polarization, microtubules are organized into a vertical network that orients along the apicobasal axis, with their minus ends oriented toward the apical side and plus ends toward the basal membrane (Bacallao et al., 1989; Bre et al., 1990; Clark et al., 1997). Biogenesis of the different domains in which epithelial polarized cell are commonly divided and maintenance of the cell shape depend on protein sorting and delivery. These mechanisms involve vesicle budding from the TGN and endosomes, transport of vesicles along the actin and microtubule cytoskeleton, and their fusion with the appropriate membrane domain (Musch, 2004; Rodriguez-Boulan et al., 2005). Disruption of the microtubule cytoskeleton and its motor proteins reduces the efficency of apical and basolateral protein delivery to their respective membrane domains. In previous studies the human VHL protein was described to stabilize microtubules (MTs) (Hergovich et al., 2003). This finding is significant because it ascribes a novel function for h-VHL and suggests a mechanism for its tumor suppressor activity. Moreover, it has been shown that h-VHL protects microtubules from destabilization by nocodazole

treatment and influences microtubule dynamics at the cell periphery (Lolkema et al., 2004). In order to understand the underlying cause of the phenotypes observed in *d-VHL* mutant follicle cells, I analyzed the distribution of microtubule network through immunostaining by using the anti-βTubulin (βTub) antibody.

In *d-VHL* homozygous mutant clones βTub is altered at early stages (Fig. 19 A-F). In a stage 7 egg chamber, d-VHL loss of function cells accumulate less βTub on the most apical side (Fig. 19 E). At stage 10A I observed a complete loss of βTub staining as shown in figure 19 G-L. This result suggests that the MTs in mutant cells are extremely unstable and depolymerize after stage 7.

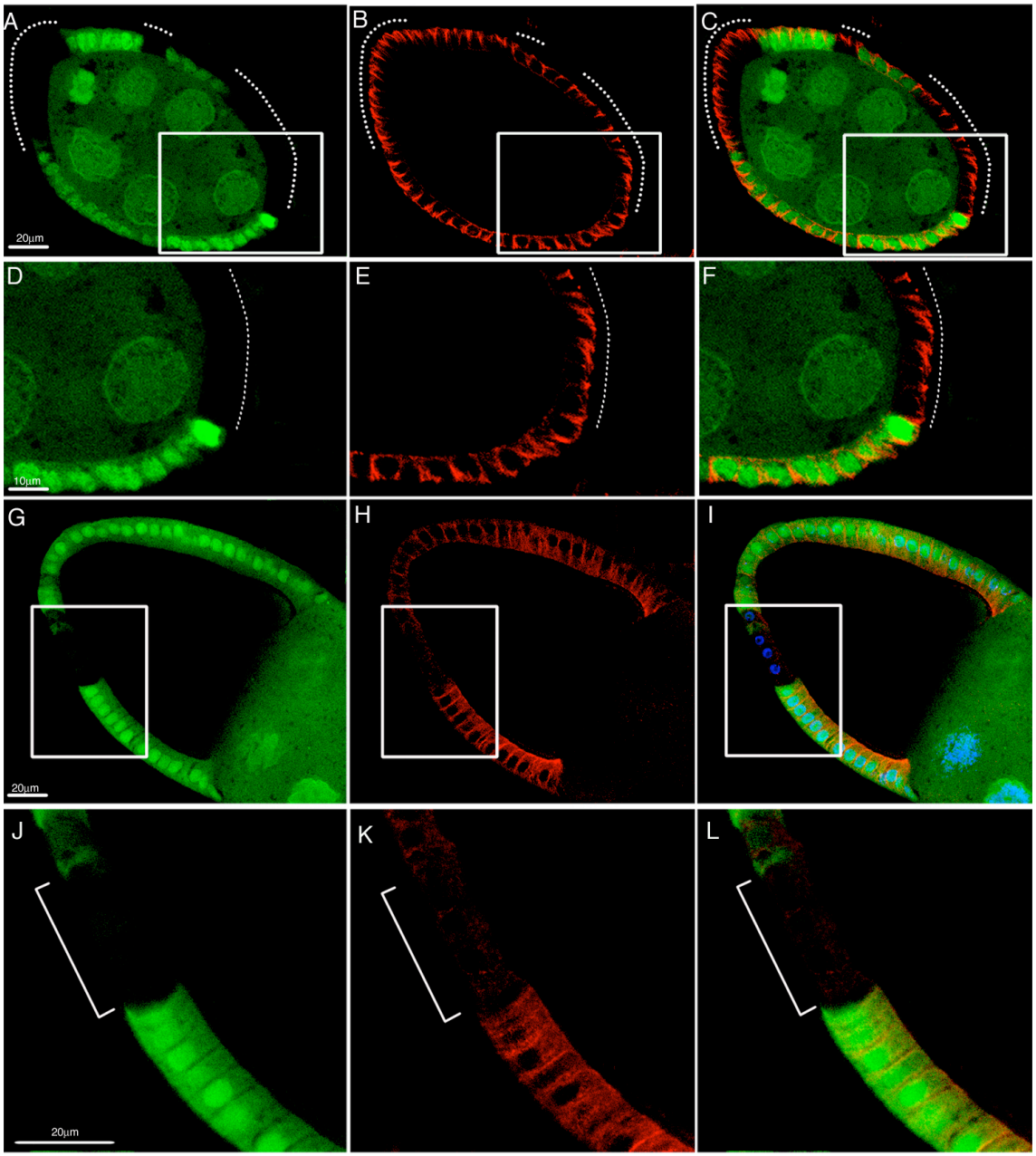

Figure 19. Analysis of microtubule architecture in d-VHL loss of function clones.
Confocal cross-sections of a stage 7 (A-F) and 10A (G-L) egg chambers from females *w; dVHL$^{1.1}$,FRT^{G13}/FRT^{G13}UbiGFP; T155Flp/+*. βTub (B, E, H, K; red) is strongly affected in mitotic clones marked by the absence of GFP (A, D, G, J; green). D-F: higher magnification view of boxed region in A-C. Dotted lines in A-C and D-F point the mitotic clones in which βTub is less detectable in the most apical side of follicle cells. J-L: higher magnification view of boxed region in G-I. Brackets in J-L point the mitotic clone in which βTub staining is strongly reduced suggesting that MTs depolymerize. Merged images of GFP (green) and βTub (red) signals are shown in C, F, L. Merged image of GFP (green), βTub (red) and Topro (blu) signals is shown in I. Anterior is down in all panels.

4.5. aPKC and microtubules are involved in maintaining follicular epithelium integrity by interacting with d-VHL

In wild-type egg chambers at stage 10A aPKC is localized and partially overlaps with microtubules on the apical side, as shown by the colocalization of aPKC and βTub in a stage 10A wild-type egg chamber (Fig. 20 A-F).

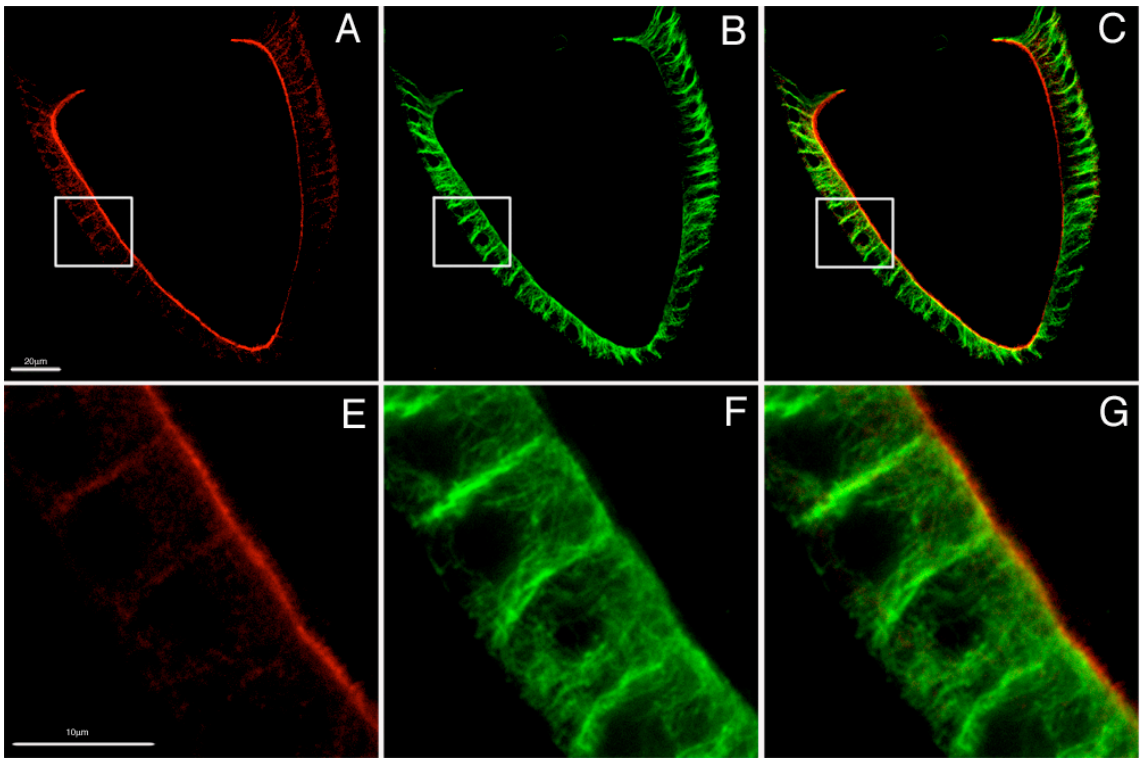

Figure 20. aPKC and βTub colocalization in wild-type egg chamber.
Confocal cross-section of a stage 10A egg chamber from *yw* females stained with anti-aPKC (A and D; red) and βTub (B and E, green). D-F: higher magnification view of boxed region in A-C showing that aPKC is localized in the apical domain where partially overlaps with microtubules. Merged images of aPKC (red) and βTub (green) signals are shown in C and F.

This suggests that an intact microtubule network is necessary for the correct delivery of aPKC. Therefore, in order to understand if the observed polarity defects in *d-VHL*$^{1.1}$ clones are caused by microtubules instability, I examined the effect of microtubules depolymerization on localization of aPKC. Wild-type egg chambers were dissected at early stages of oogenesis and were cultured in the presence of nocodazole

under conditions previously shown to abolish microtubules polymerization (Brito et al., 2008). After five hours incubation in the presence of depolymerizing agent or paclitaxel or DMSO, egg chambers were fixed and standard immunostaining with anti-aPKC and anti-βTub antibodies was performed. The nocodazole treatment affects the apical localization of aPKC. At stage 9 in correspondence of depolymerized MTs, aPKC is almost completely lost (Fig. 21 B) or found accumulated around the follicle cells nuclei (arrow in Fig. 21 B) as in *d-VHL*$^{1.1}$ clones. At later stages where MTs are undetectables through βTub staining (Fig. 21 D), aPKC is lost (stage 10A, Fig. 21 E) and these cells are piled up as cells in *d-VHL*$^{1.1}$ clones. Accordingly egg chambers treated with paclitaxel, which stabilizes microtubules (late stage 9, Fig. 21 G-I), show a normal aPKC apical signal (Fig. 21 H) as in the DMSO treated control egg chambers (stage 9, Fig. 21 J-L).

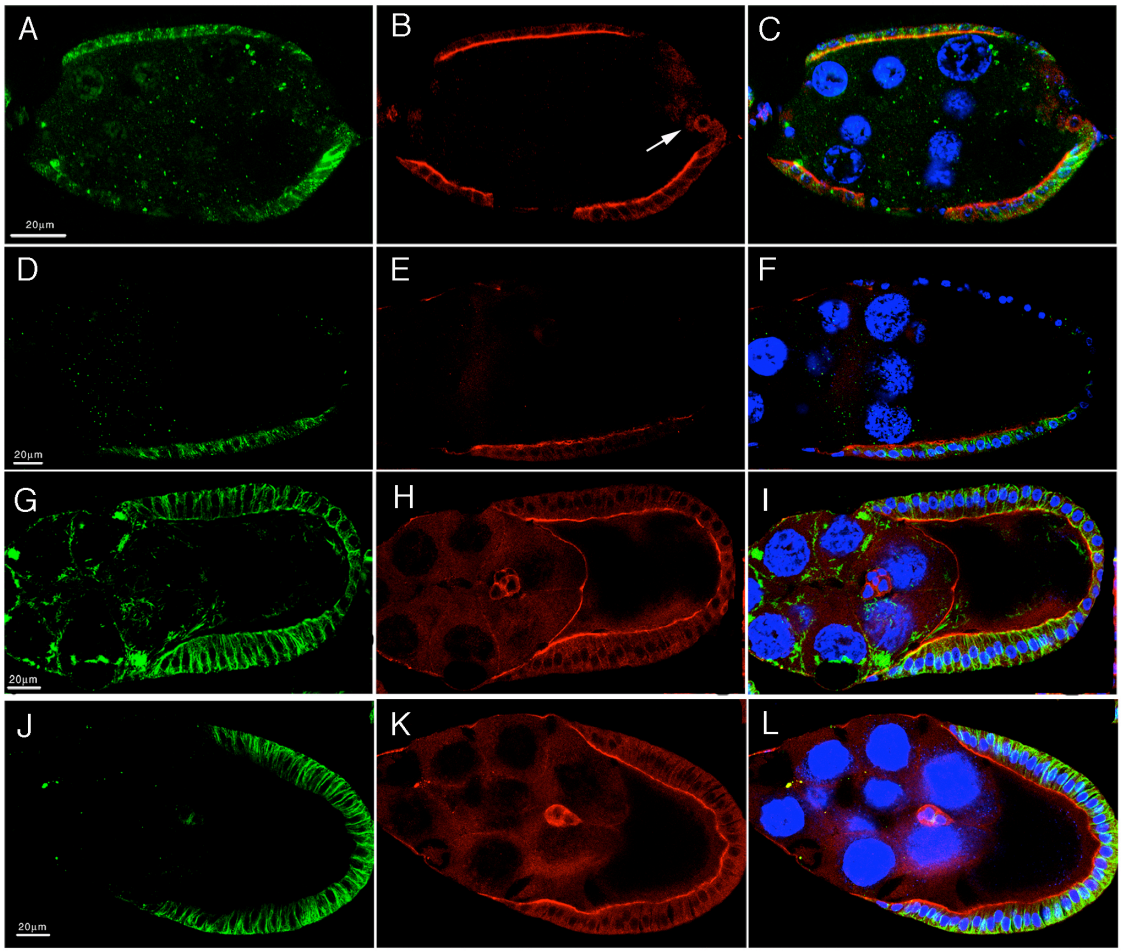

Figure 21. Ex vivo analysis of wild type egg chambers after drugs treatments.
Confocal cross-section of stages 9 (A-C and J-L), late stage 9 (G-I) and stage 10A (D-F) egg chambers from *yw* females treated with nocodazole (A-F), paclitaxel (G-I) and DMSO (J-L). These egg chambers have been stained with βTub (A, D, G, J; green) and aPKC (B, E, H, K; red). Merged images of βTub (green), aPKC (red) and Topro (blu) signals are shown in C, F, I, L. Nocodazole treated stage 9 egg chamber showing that MTs are dramatically altered (A) and aPKC is strongly affected and accumulated around the follicle cells nuclei (arrow in B). D-F. Nocodazole treated stage 10A egg chamber showing that MTs are almost completely undetectables (D) and aPKC is lost (E) in correspondence of depolymerized MTs. In paclitaxel treated late stage 9 egg chamber MTs are more abundant (G) accordingly to polymerizing effect of paclitaxel on microtubules and aPKC is correctly localized to the apical surface (H). J-L. MTs cytoskeleton (J) and aPKC distribution (K) are normal in DMSO stage 9 treated egg chamber (J-L). Anterior in on the left in all panels.

I next analyzed MTs distribution in aPKC mutant clones by using a strong loss of function (LOF) allele (k06403) kindly provided by WM. Deng (Tian and Deng, 2008). Homozygous aPKC LOF clones, genetically marked by the absence of GFP, were obtained through somatic recombination using the Flp/FRT system (Golic, 1991;

Xu and Rubin, 1993) and were induced by driving Flp under the control of a heat shock promoter (Xu and Harrison, 1994) (Fig. 22 A-H). I stained these egg chambers with βTub (red, Fig. 22 B-F) and with aPKC (blu, Fig. 22 C-G) in order to asses the efficency of the LOF allele. At early stages in aPKC LOF clones MTs organization is altered (stage 6, Fig. 22 B) and the epithelium appears thinner compared to the wild-type cells (Fig. 22 D). However at later stages, βTub completely disappeared and the epithelium appears dramatically thinner compared to the neighbour wild type cells (stage 9, Fig. 22 H). It has been recently shown that aPKC controls microtubule organization by regulating the balance of microtubule and actin interactions in order to control AJ symmetry (Harris and Peifer, 2007). Because h-VHL also interacts with Par3-Par6-aPKC complex, which is a key regulator of microtubule–cortex interactions and of coordinated growth of cortical microtubules (Etienne-Manneville and Hall, 2003), it is conceivable that h-VHL and Par6 complex are in a common pathway to regulate microtubule orientation (Schermer et al., 2006).

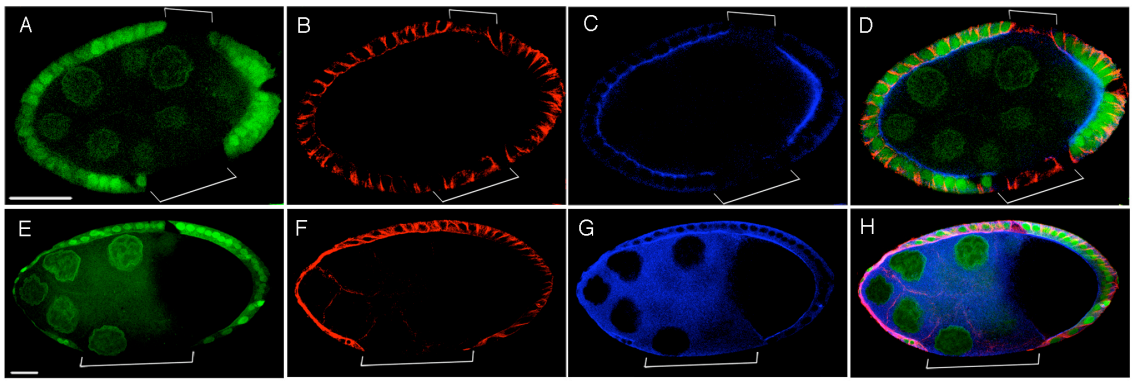

Figure 22. aPKC loss of function clones affect MTs architecture.
Confocal cross-sections of a stage 6 egg chamber (A-D) and cross-sections (E-H) of a stage 9 egg chamber from females *hsFLP; FRT(42D),aPKC(k06403)/ FRT(42D),Ubi-GFP (S65T).* βTub (B and F; red) is altered in mitotic clones marked by the absence of GFP (A and E; green). Brackets in A-D point the mitotic clones showing that ®Tub distribution is altered and that the epithelium appears thinner compared to the neighbour wild-type cells. Bracket in E-H points a clone showing that βTub completely disappeared and the epithelium appears dramatically thinner compared to the neighbour wild-type cells. Merged images of GFP (green), βTub (red) and aPKC (blu) signals are shown in D and H.
Anterior is on the left in all panels. Bars 20 μm.

Using the co-IP technique, I detected d-VHL in the protein complex pulled down by the monoclonal antibody against βTub in wild-type ovarian lysate and against GFP in the aPKC-GFP ovarian lysate (Fig. 23a). This data suggests that d-VHL interacts with both aPKC and βTub during oogenesis. As a control Par6 can be detected in western blots of aPKC and βTub immunoprecipitations (Fig. 23a). Conversely βTub cannot be detected in western blots of aPKC immunoprecipitation, whereas Baz interacts with aPKC in wild-type ovaries extracts (Fig. 23b). These results might suggest that d-VHL acts as an intermediate link between microtubule network and the polarity marker aPKC probably through Par6, therefore controlling microtubule organization and functioning.

The altered epithelium phenotype caused by loss of d-VHL can be partially rescue by overexpressing aPKC. I used the *hs-d-VHLRNAinterference* line in order to knock down *d-VHL* and then I induced overexpression of aPKC. In the *d-VHLRNAi* egg chambers follicle cells fail to form a coherent single-layered epithelium (data not shown) and the mutant cells pile up such as in the d-VHL loss of function clones. *UASaPKC-GFP; hs-d-VHLRNAi* flies were crossed with flies from *Cy2 Gal4* line, which expresses the *Gal4* transgene in all the follicle cells covering the oocyte from stage 8 (Queenan et al., 1997). I targeted the d-VHL interference by inducing heat shock promoter activity at 37ºC and after 12 hours at 29°C from the fourth heat shock treatment, ovaries from females carrying *hs-d-VHLRNAi* and *UASaPKC-GFP* or *hs-d-VHLRNAi* transgene alone were dissected and analyzed. Piling up phenotype was considered from stage 4 till 9 and only GFP expressing cells were considered in the UASaPKC rescued flies. In 50% of stage 4 and 5 *hs-d-VHLRNAi* egg chambers analyzed (n=30) follicular epithelium lost the coherent single-layered shape after heat

shock treatments and aPKC is variably reduced or absent (data not shown). Same percentage was obtained for the UASaPKC rescued flies (n=30), since Cy2Gal4 driver is expressed in the follicular epithelium after stage 8. 60% of stage 9 egg chambers analyzed (n=36) from *hs-d-VHLRNAi* females display multilayered phenotype (Fig. 23c). Conversely, 43% of egg chambers from UASaPKC rescued flies (n=36) display the mutated phenotype. These data suggest that a partial rescue of d-VHL loss of function phenotype can be achieved by overexpressing aPKC. The low percentage of rescue could be due to the driver used for this analysis which is expressed only after stage 6 of oogenesis or because loss of d-VHL is mainly affecting MT network and only consequentially aPKC distribution.

I next performed an *ex vivo* analysis by incubating the egg chambers carrying loss of function follicle cell clones in the presence of paclitaxel or DMSO as control (higher magnifications of stages 9 in Fig. 23d). After five hours incubation, egg chambers were fixed and standard immunostaining with anti-aPKC and anti-βTub antibodies was performed. Homozygous *d-VHL*$^{1.1}$ clones from egg chambers treated with DMSO showed that MTs are strongly compromised (red in Fig. 23d B) and aPKC is almost completely lost from the apical side (blu in Fig. 23d C). In homozygous *d-VHL*$^{1.1}$ clones from egg chambers treated with paclitaxel, MTs can recover and restore their correct distribution (Fig. 23d F). Interestingly, also aPKC can partially re-establish the correct localization on the apical side of mutant follicle cells (Fig. 23d G). This data might suggest that loss of d-VHL is mainly affecting MT network since restoring the MTs distribution by using the polymerizing agent paclitaxel, leads to an almost complete rescue of aPKC correct localization at the apical domain of mutant follicle cells. However I cannot exclude a mutual interaction among d-VHL, aPKC and βTub in

the maintenance of follicular epithelium architecture.

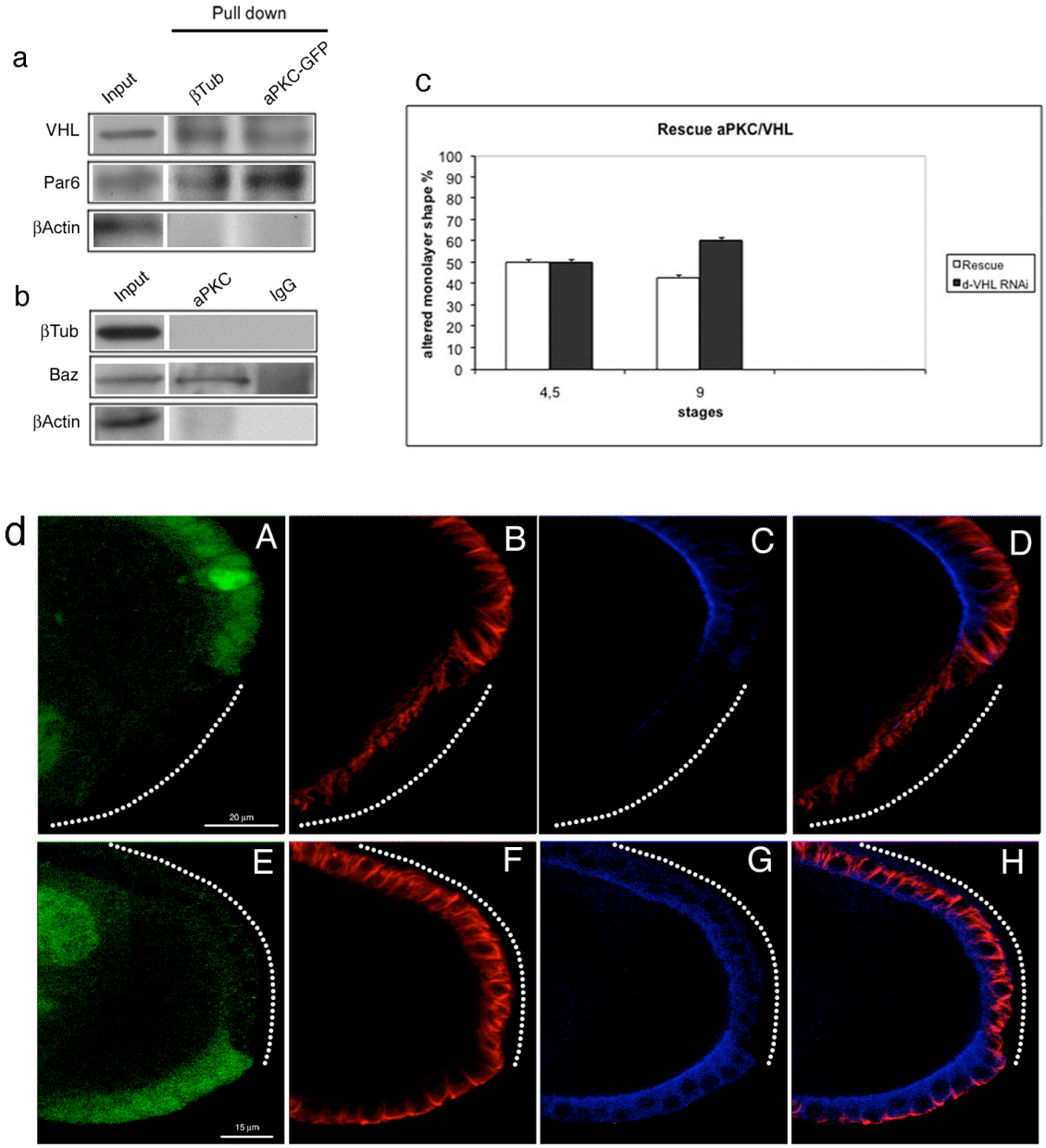

Figure 23. Direct interaction among d-VHL, aPKC and βTub.

a. Pull down of βTub from wild-type ovarian whole cell lysate and GFP from UASaPKC-GFP ovarian whole cell lysate probed on SDS page with anti-d-VHL and anti-Par6. d-VHL interacts with both aPKC and βTub in ovarian cell lysates. As a control Par6 can be detected in western blots of aPKC and βTub immunoprecipitations. **b**. Pull down of aPKC and rabbit IgG as a control from wild-type ovarian whole cell lysate probed on SDS page with anti-βTub and anti-Baz. aPKC interacts with Baz and not with βTub suggesting that d-VHL acts as an intermediate link between microtubule network and the polarity marker aPKC probably through Par6. βActin was used as a negative control.

c. Graphic representation of d-VHL mutant phenotype and aPKC rescue activity. Egg chambers from females *UASaPKC-GFP; hs-d-VHLRNAi* and *hs-d-VHLRNAi* were dissected and analyzed. I counted the % of egg chambers showing the follicle cells piling up phenotype in control and rescued flies. Piling up phenotype was considered from stage 4 till 9 and only GFP expressing

cells were considered in the UASaPKC rescued flies. 50% of stage 4 and 5 egg chambers analyzed (n=30) from both control (black bar) and rescued flies (white bar) showed the piling up phenotype. 60% of stage 9 egg chambers analyzed (n=36) from *hs-d-VHLRNAi* females display multilayered phenotype whereas 43% of egg chambers from rescued flies (n=36) display the piling up phenotype.
d. High magnification of confocal cross-sections of stages 9 egg chambers from females *w; dVHL$^{1.1}$,FRT^{G13}/FRT^{G13}UbiGFP; T155Flp/+* treated with DMSO (A-D) and paclitaxel 6,4 μM (E-H). In DMSO treated egg chamber, βTub (B; red) and aPKC (C; blu) are strongly affected in the mitotic clone. In paclitaxel treated egg chamber βTub (F; red) and aPKC (G; blu) almost completely recover the correct distribution in the mitotic clone. Dotted lines in all panels point the mitotic clones marked by the absence of GFP (A, E; green). Merged images of βTub (red) and aPKC (blu) signals are shown in D and H. Anterior is on the left on all panels.

4.6. d-VHL regulates microtubules stability in S2 cells

In order to analyze the possible d-VHL function as a microtubule-binding protein with associated microtubule stabilizing function, I performed *in vitro* experiments by using *Drosophila* S2 cells (Schneider, 1972). S2 cells were transfected with pCaspeR-hs vectors containing *d-VHL* full length sequence in order to have higher dosage of d-VHL and *d-VHLRNAi* construct in order to silence it. Through RT-PCR I determined the best heat shock treatment conditions in order to have a 90% of *d-VHL* silencing (Fig. 24b). S2 cells transfected with *d-VHLRNAi* transgene show a reduction in d-VHL protein level compared to control cells transfected with the empty vector. As shown through immunostaining (Fig. 24a A,D,G; red) and western blots of total cell lysates from transfected cells (Fig. 24c), d-VHL level is slightly higher in *d-VHL* overexpressing cells (Fig. 24a D) but strongly decreased in *d-VHLRNAi* transfected cells (Fig. 24a G) compared to control cells (Fig. 24a A). Immunostaining performed with anti-d-VHL in control cells (Fig. 24a A) resulted in a predominantly nuclear signal and punctate cytoplasmic signal (Fig. 24a A). It is possible that a small fraction of d-VHL might be associated with the Golgi network. Moreover in control cells and d-VHL overexpressing cells a strong membrane signal is also observed suggesting a possible interaction with MTs network (Fig. 24a A,D). I tested whether d-VHL colocalizes with

MTs, and the two-color confocal microscopy with anti-d-VHL (red) and anti-βTub (green) revealed that the d-VHL labels MTs. As shown in the merge images of control and d-VHL overxpressing cells (Fig. 24a C, F), d-VHL partially overlaps with MTs (yellow signal in Fig. 25a C and F). Moreover the d-VHL cytoplasmic signal dots label microtubules network scaffold inside the cells (Fig. 24a C, F). Control and d-VHL overexpressing cells show no difference in microtubule levels and distribution (Fig. 24a B, E) as assessed also through western blot (Fig. 24c). Moreover βTub levels do not appear altered also in *d-VHLRNAi* transfected cells (Fig. 24c). In order to analyze possible changes in microtubule architecture, I analyzed *d-VHLRNAi* transfected cells stained with anti-d-VHL, which appears dramatically reduced (Fig. 24a G) compared to control cells, and stained with βTub (Fig. 24a H). The microtubule network in *d-VHLRNAi* S2 cells appears disorganized and MTs are less accumulated on membrane domain (Fig. 24a H). This data suggests that MTs in absence of d-VHL are not properly organized.

I next checked aPKC and Par6 protein levels in those cells through western blots on the 3 different total protein lysates. Par6 levels in *d-VHLRNAi* trasfected cells appears lower than control cells whereas aPKC results dramatically reduced suggesting that aPKC is sensitive to the amount of d-VHL protein (Fig. 24c).

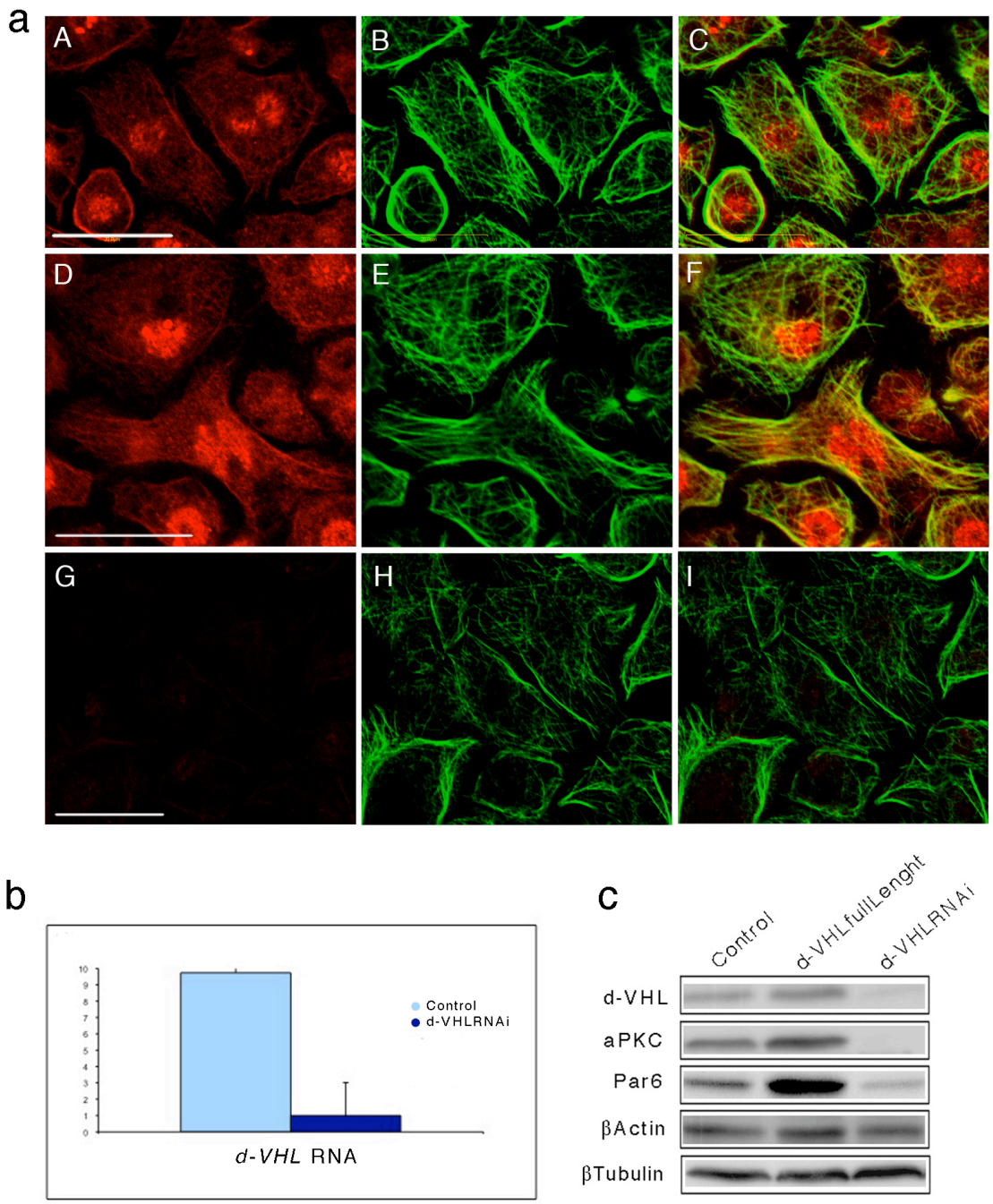

Figure 24. d-VHL and microtubules stability in S2 cells.

a. Confocal image of S2 cells transfected with pCaspeR-hs empty vector, heat shocked for two days at 29°C and stained with anti-d-VHL (A, red) and βTub (B, green). Merged image of d-VHL (red) and βTub (green) signals is shown in C. d-VHL (A, red) is predominantly localized to the nucleus and as a punctate signal in the cytoplasm (stars in A). As shown in the merged image d-VHL partially overlaps with MTs (yellow signal in C) and partially labels the MTs network in their entire length.

Confocal image of S2 cells transfected with pCaspeR-hs *d-VHL* full lenght vector, heat shocked for two days at 29°C and stained with anti-d-VHL (D, red) and βTub (E, green). Merged image of d-VHL and βTub is shown in F. d-VHL signal is higher than in control cells and the cellular

localization is similar to that shown in A. d-VHL signal is nuclear and punctate in the cytoplasm. G-I Confocal image of S2 cells transfected with pCaspeR-hs *d-VHLRNAi* vector, heat shocked for two days at 29°C and stained with anti-d-VHL (G; red) and βTub (H; green). Merged image of d-VHL and βTub is shown in I. d-VHL is dramatically reduced (G) compared to control cells and MTs appear disorganized and less accumulated on membrane domain (H). **b**. RT-PCR on total RNA extracted from S2 cells transfected with pCaspeR-hs empty as a control (cyan bar) and with pCaspeR-hs *d-VHLRNAi* (blu bar). In order to have a 90% of RNA silencing cells were kept at 29°C for two days. **c**. Western blot analysis on whole cell lysates from S2 cells transfected with pCaspeR-hs empty vector (control), pCaspeR-hs *d-VHL* full lenght and pCaspeR-hs *d-VHLRNAi*. The lysates were loaded on 12% SDS page and probed with different antibodies. See text for details.

These results suggest a mechanism similar to those observed in follicle cell clones through immunostainings on *d-VHL*$^{1.1}$ mutant cells and through immunoprecipitation assay. d-VHL might be important for regulating microtubule organization and stability, reinforcing the view that microtubule binding and stabilization are properties of the h-VHL tumour suppressor.

Future studies will be addressed to analyze during oogenesis the possible MTs orientation defects after depletion of d-VHL by using Kinesin and Nod respectively as a positive and negative microtubules binding markers.

4.7. d-VHL and EGFR

Recently it has been demonstrated that h-VHL promotes the oncogenic Epidermal Growth Factor Receptor (Egfr) signalling via Akt-1 and MEK-1 (Lee et al., 2008). Clear-cell renal cell carcinoma (RCC) is the most prevalent form of kidney cancer and is frequently associated with loss of *h-VHL* gene function, resulting in the aberrant transcriptional activation of genes that contribute to tumor growth and metastasis, including transforming growth factor-α (TGF-α), a ligand of the Egfr tyrosine kinase. Hsu et al. (2006) have demonstrated that in *h-VHL* null tumor cells or *h-VHL* knock-down cells, Fibroblast Growth Factor Receptor 1 (FGFR1) internalization is defective, leading to surface accumulation and abnormal activation of FGFR1. The

enhanced FGFR1 activity directly correlates with increased cell migration (Hsu et al., 2006). They also demonstrated that *d-VHL* down-regulates the motility of tubular epithelial cells (tracheal cells) during *Drosophila* embryogenesis by terminating cell migration in the developing tracheal system, ultimately resulting in cessation of tubular outgrowth (Adryan et al., 2000).

The epithelial phenotypic effects observed in d-VHL loss of function follicle cell clones, are similar to those observed in the follicle cell clones lacking Egfr function. By studying the effect of a null allele of *egfr* (*egfr*^{CO}; Clifford and Schüpbach, 1989) on *VM32E* gene expression, I observed that loss of Egfr in follicle cells causes a shrinking of the epithelium similar to the effect caused by loss of d-VHL (Fig. 25 A-C).

The vitelline membrane component VM32E, has been studied for several years in the Gargiulo's lab and one of the project I've been involed during my PhD program regards the analysis of the Egfr signalling pathway in the regulation of *VM32E* gene expression (Bernardi et al., 2007).

VM32E is one of the four *Drosophila* vitelline membrane protein genes that have been characterized so far: *VM26A.1*, *VM34C*, *VM26A.2*, and *VM32E* (Higgins et al. 1984; Mindrinos et al. 1985; Burke et al. 1987; Popodi et al. 1988; Gigliotti et al. 1989). Previous work on VM32E protein expression has identified several unique features of this protein compared with the other members of the same gene family (Cavaliere et al., 2008). The *VM32E* gene obeys to a complex temporal and spatial regulation that may reflect some special functions played by its protein in eggshell formation (Gargiulo et al., 1991; Cavaliere et al., 1997; Andrenacci et al., 2000). It has been demonstrated that the Dpp signalling pathway negatively controls *VM32E* gene expression in the centripetal follicle cells (Bernardi et al., 2006). I next showed that in the main body

follicle cells, the degree of *VM32E* gene expression depends on the level of Egfr activity (Bernardi et al., 2007). Therefore, it appears that the two main signalling pathways controlling follicle cells differentiation are also involved in the transcriptional regulation of this eggshell structural gene. I demonstrated through clonal analysis that loss of Egfr activity upregulates VM32E expression. Homozygous $egfr^{CO}$ clones, genetically marked by the absence of green fluorescent protein (GFP), were obtained through somatic recombination using the Flp/FRT system (Golic, 1991; Xu and Rubin, 1993) and were induced by driving Flp under the control of a heat-shock promoter (Xu and Harrison, 1994). As shown in a $egfr^{CO}$ clone observed in cross section from a stage 10B egg chamber(Fig. 25 A-C), VM32E expression is strongly enhanced in the follicle cells lacking the Egfr function and its total amount is significantly higher than in the adjacent GFP-positive cells (Fig. 25 B). Moreover the epithelium in the follicle cells lacking Egfr function appears thinner and is comparable to the phenotypic effect observed in the d-VHL loss of function clones. I next observed the VM32E distribution in the $d\text{-}VHL^{1.1}$ clones and as shown in figure 25 E the protein appears more abundant in the mutant cells compared to the wild type cells such as in $egfr^{CO}$ clones. Giving this result, it is conceivable that loss of d-VHL in follicle cells causes a defect in the Egfr activity. From my previous data, loss of d-VHL seems to affects microtubules stability, raising the possibility that endocytosis mechanisms necessary for receptor internalization and functionality (Jekely and Rørth, 2003) are compromised. Therefore, the presumed downregulation of Egfr activity could be due to defects in endocytosis and recycling mechanism through microtubules network.

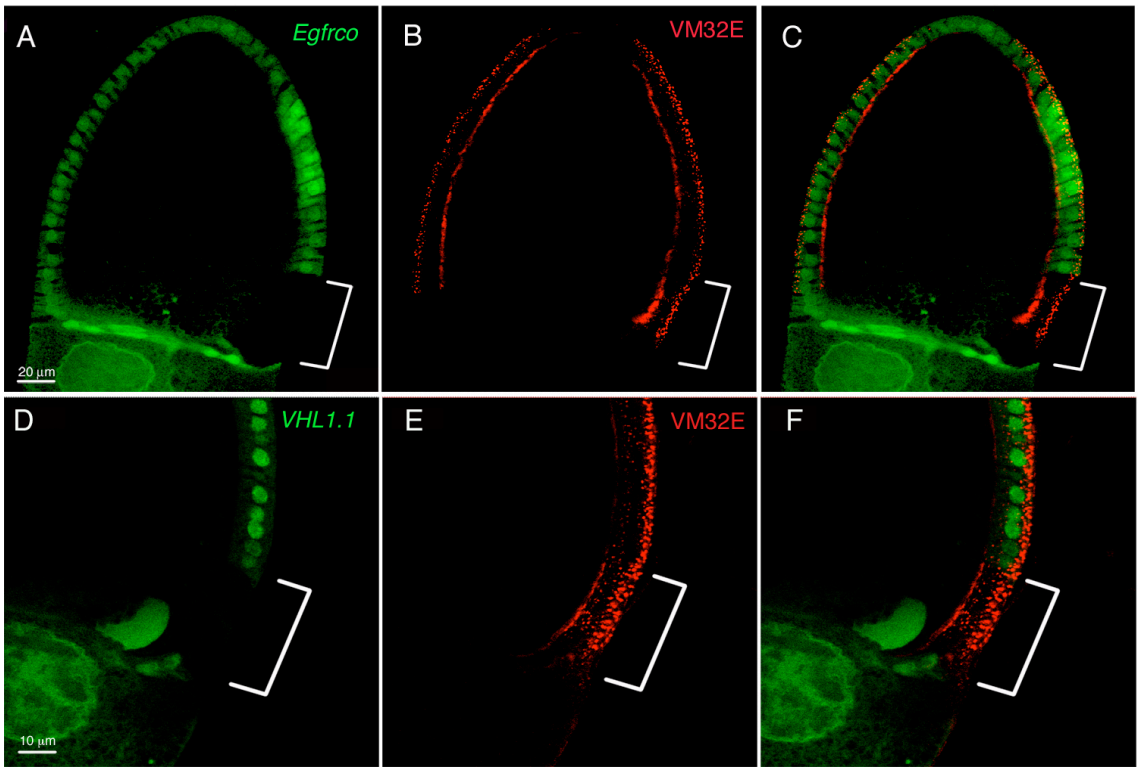

Figure 25. d-VHL and Egfr activity through VM32E expression profile analysis.
Confocal cross-section of a stage 10B egg chamber from females *hsFLP;FRT42D,UbiGFP/FRT42D,egfr*^{CO} (A-C) and from females *dVHL*$^{1.1}$*,FRT*^{G13}*/FRT*^{G13}*UbiGFP; T155Flp/+* (D-F). Merged images of VM32E (red) and GFP (green) signals are shown in C and F. VM32E signal (B and F; red) is enhanced in mitotic clones marked by the absence of GFP (A and E; green). Brackets in A-C point the *egfr*^{co} mitotic clone showing that VM32E expression is strongly enhanced in the follicle cells lacking the Egfr function and its total amount is significantly higher than in the adjacent GFP-positive cells. Moreover the epithelium in the follicle cells lacking Egfr function appears thinner (C) and is comparable to the phenotypic effect observed in the d-VHL loss of function clones. In the d-VHL$^{1.1}$ clone VM32E level is enhanced compared to the neighbor wild-type cells (E). Anterior is down in all panels.

Dystroglycan up-regulation links EGFR activity and d-VHL

Dystroglycan (DG) is an adhesion molecule known to function as an essential link between the extracellular matrix and the actin cytoskeleton through its role in the dystrophin-glycoprotein complex. In mammals, disruption of DG function in this complex is believed to contribute to several forms of muscular and neurodegenerative disorders (Brancaccio, 2005). During oogenesis, antibody staining for DG shows

relatively even expression on apical, basal, and lateral follicle cell surfaces, until about stage 6/7 when the protein is down-regulated in the posterior follicle cells (PFCs), and main body cells, leading to an anterior-posterior gradient of DG by stage 8/9. After stage 8, the minimal level of DG in the main body and PFCs is restricted to the basal surface (Poulton and Deng, 2006). The down-regulation of DG in the PFCs at stage 6/7 coincides with Egfr-induced differentiation of these subpopulation of follicle cells. Deng demonstrated that loss of Egfr function (Poulton and Deng, 2006) in the posterior follicle cells caused a cell autonomous up regulation of DG. In the *d-VHL* loss of function clones, I observed an upregulation of DG (Fig. 26 B, E), as observed by Poulton and Deng in $egfr^{CO}$ clones, consistent with the fact that loss of d-VHL causes a defect in the Egfr activity. Figure 26 shows a stage 10A egg chamber with a large $d\text{-}VHL^{1.1}$ posterior clone observed in surface view from the basal side. Increased DG level is evident in the mutant follicle cells (Fig. 26 B, E).

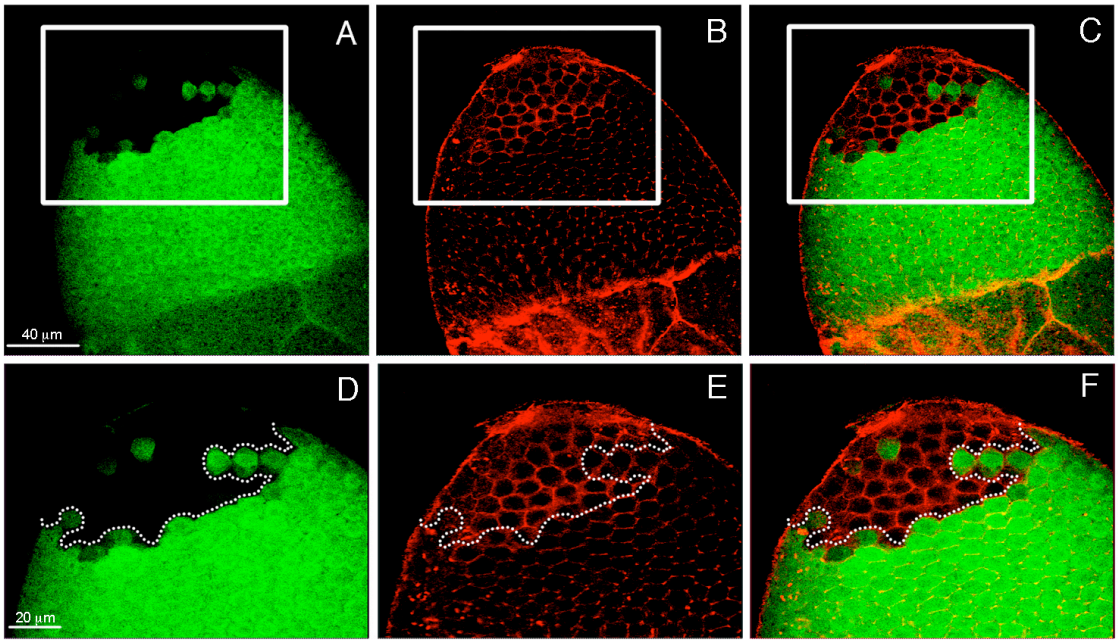

Figure 26. Dystroglycan up-regulation links EGFR activity and d-VHL.
Confocal surface-section of a stage 10A egg chamber from females *dVHL$^{1.1}$,FRT^{G13}/FRT^{G13}UbiGFP; T155Flp/+* (A-F) observed from the basal side. DG signal (B and F; red) is strongly enhanced in mitotic clones marked by the absence of GFP (A and E; green). D-F: higher magnification view of boxed region in A-C. Dotted area in D-F points the posterior mitotic clone showing up-regulation of DG suggesting that Egfr activity is probably altered by the absence of d-VHL. Merged images of DG (red) and GFP (green) signals are shown in C and F.
Anterior is down in all panels.

5. CONCLUSIONS

The analysis carried out on d-VHL function during follicular epithelium development has allowed to establish a significant role of d-VHL in the maintenance of the follicular epithelium integrity. A proposed model of d-VHL mechanism is shown in Figure 27.

In this model d-VHL binds to and stabilizes microtubules. Loss of d-VHL depolymerizes microtubules during oogenesis, leading to a possible deregulation in the subcellular trafficking transport of polarity markers from Golgi apparatus to the different domains in which follicle cells are divided (Nelson and Yeaman, 2001; Szafranski and Goode, 2007). This subcellular trafficking of proteins takes place via the trans-Golgi network (TGN). Delivery of transport vesicles from the TGN to different plasma membrane domains has a remarkably high fidelity. Such fidelity could be based on vesicles targeting along the cytoskeleton, and/or by specifying vesicle docking and fusion with the correct membrane domain as represented in Figure 8 (Rodriguez-Boulan et al., 2005). Moreover d-VHL binds to Par6 and aPKC acting as an intermediate link between microtubule network and the polarity marker aPKC, therefore controlling microtubule organization and functioning. aPKC in turn seems to control microtubules organization by regulating the balance of microtubules and actin interactions in order to control AJ symmetry (Harris and Peifer, 2007). When MTs are depolymerized by loss of d-VHL, aPKC and the other components of aPKC complex such as Baz, cannot reach the apical membrane domain. At stage 9 aPKC is found accumulated around the mutant cells nuclei and at stage 10 the delivery is totally compromised. aPKC is then probably degraded and the signal is undetectable on the apical domain. Recovery of MTs in paclitaxel treated mutant egg chambers, can restore the aPKC correct localization on the apical side of follicle cells, supporting the notion that MTs defects are probably the

cause of the observed polarity defects.

aPKC is required for the phosphorylation of Crb and this phosphorylation may be necessary for Crb to adopt a correct conformation and/or to interact with proteins required for Crb stabilization at the apical domain (Sotillos et al., 2004). Therefore, when aPKC complex is not correctly localized to the apical membrane, the phosphorylation of Crb is compromised, then the protein failed to be located on the subapical region. AJ component Armadillo is abundantly enriched at the AJ domain after depletion of d-VHL. This suggests a possible deregulation in the mechanism of proteins recycling through MTs network, since the correct localization is lost at stage 9, when the AJ are already established but they need to rearrange in order to allow the migration of follicle cells. During development, AJ regulation has been shown to be important for tissue morphogenesis in *Drosophila* and in several other model systems such as mouse and *Xenopus* embryos (Levine et al., 1994; Uemura et al., 1996). These morphogenic events involve the continual disruption and reformation of adhesive contacts that usually result in major changes in cell state or differentiation (Akhtar and Hotchin, 2001). As a consequence of loss of correct polarity, basolateral side results compromised. DLG is involved in maintaining the structure of the follicular epithelium, by prohibiting cell growth and maintaining cell adhesion and cell polarity. This role appears to be separable from its role in proliferation control (Woods et al., 1996). DLG in d-VHL mutant cells is significantly reduced on the most basal side and it spreads along the apical surface. It has been shown that component of apical and AJ junctions restrict DLG to the lateral membrane by a mechanism that is reinforced by Crb (Le Bivic A, 2005; Lecuit, 2004). So when Arm and Crb are mislocalized, DLG is not correctly restricted to the basolateral side and diffuse along the apical side. DLG

delocalization compromises Lgl localization since DLG seems to be required to recruit Lgl to the lateral membrane (Tepass et al., 2001). Loss of *lgl* in *Drosophila* results in loss of apicobasal polarity in epithelial cells and in the neoplastic transformation of the imaginal discs which lose their epithelial monolayer structure (Agrawal et al., 1995; Bilder et al., 2000; Ohshiro et al., 2000; Peng et al., 2000). Moreover, mammalian Lgl forms complexes with Par6/aPKC regulating epithelial cell polarity (Plant et al., 2003; Yamanaka et al., 2003). Upon cell–cell contact-induced cell polarization, Lgl is phosphorylated by aPKC resulting in a dissociation of Lgl from Par6/aPKC followed by an accumulation of Lgl along the basolateral membrane, where it contributes to the formation of the basolateral membrane domain (Tanentzapf and Tepass, 2003; Hutterer et al., 2004) and to correct positioning of epithelial junctions (Borg, 2004). Also in neuroblasts it has been shown that Lgl is phosphorylated by aPKC in the apical region to direct localization of basal components involved in asymmetric cell divisions (Betschinger et al., 2003). Therefore it is plausible that loss of aPKC in the d-VHL loss of function clones prevents Lgl phosphorylation and its correct localization.

The attachment to the basement membrane (BM) or Basal Lamina mediated by integrins results compromised since loss of d-VHL leads to a dramatic reduction in βPS integrin level. As a consequence of basal junction modification, actin cytoskeleton, which is organized in parallel bundles, is dramatically compromised and no actin staining is detected on the most basal domain of mutant follicle cells. Moreover F-actin bundles bind to AJ through Arm/αCatenin. Therefore the defects observed in AJ organization could lead to changes in actin distribution also in the most apical side where the actin cortical belt results in fact compromised.

The filamentous protein α-Spectrin that forms a network with actin cytoskeleton that regulates and stabilizes the membrane shape, is abundantly enriched in the apical and lateral domain of mutant follicle cells. This suggests that vesicle delivery and recycling through microtubule network system is compromised leading to an accumulation of this membrane protein.

Perturbation of d-VHL function in follicle cells clones causes indeed altered cell shape and distribution without affecting cell proliferation, as assessed through twin spots counting and anti-PH3 staining, or cell death, as demonstrated through anti-Cleaved Caspase-3 staining.

Since the major defects on d-VHL loss of function clones are observed after stage 7 of oogenesis, it is plausible that d-VHL is involved in the maintenance of the follicular epithelium integrity. During oogenesis the follicular epithelium needs to rearrange and move in order to follow the growing oocyte and differentiate. If the mechanisms requested to maintain follicle cell shape during developmental processes such as oogenesis are compromised, cells can lose their polarity and their correct cell junctions and become mesenchymal.

d-VHL is indeed important to stabilize microtubules network and might contribute to the their proper orientation, as assessed also by Hergovich et al. (2006). In their model h-VHL seems to control the orientation of microtubules. Schermer et al. (2006) showed that microtubules growth is oriented toward the periphery of the cells expressing h-VHL. In h-VHL-deficent cells, however, the orientation of microtubules growth is disturbed, resulting in disordered directions of microtubule assembly (Kuehn et al., 2007). In follicular epithelium, the microtubule cytoskeleton is polarized to form an array of very stable microtubules (MTs) that run parallel to the apicobasal axis, with

their minus ends at the apical membrane and their plus ends oriented toward the basal membrane (Bacallao et al., 1989; Bré et al., 1990; Clark et al., 1997). *Drosophila* Kinesin is the motor domain of the plus end-directed MT motor and accumulates at the basal side of the cell, whereas the minus end motor protein Nod localizes apically. Recently Lolkema et al. (2007) report the identification of Kinesin-2 as novel and endogenous h-VHL binding partner, mediating binding to MTs. Since h-VHL and Kinesin-2 have overlapping functions regarding primary cilia regulation, these data may provide novel mechanistic insight into MT-dependent regulation of primary cilia by h-VHL. The microtubule motors, such as Kinesin, are recruited on MTs and they bind directly or through unknown adaptors to endocytosis vesicles that sort from TGN. Endocytosis vesicles are then directed to the different follicle cells domains. Therefore the motors generate tubular elements that move along microtubules. In my proposed model d-VHL might bind to Kinesin and regulate the correct orientation and functionality of MTs. Future studies will be addressed to analyze during oogenesis the possible MTs orientation defects after depletion of d-VHL by observing Kinesin distribution.

h-VHL might also regulate cell cycle control and, consequently, loss of h-VHL might activate cell proliferation signals. In d-VHL loss of function clones increased propidium iodide signal suggests a possible deregulation of follicle cells endocycles. Recently it has been demonstrated that h-VHL promotes the oncogenic Epidermal Growth Factor Receptor (Egfr) signalling via Akt-1 and MEK-1 (Lee et al., 2008). Clear-cell renal cell carcinoma (RCC) is the most prevalent form of kidney cancer and is frequently associated with loss of *h-VHL* gene function, resulting in the aberrant transcriptional activation of genes that contribute to tumor growth and metastasis,

including transforming growth factor-α (TGF-α), a ligand of the Egfr. By analyzing the precise timing of synthesis of the *VM32E* eggshell component which relies on a fine regulation of gene expression, it is possible to assume an involvement of Egfr in d-VHL mechanism. Through clonal analysis I showed that loss of d-VHL causes an increase in VM32E protein levels comparable to the increment observed in Egfr loss of function clones (Bernardi et al., 2007). Moreover loss of Egfr activity affects the epithelium morphology, and this alteration in follicle cell shape is similar to the phenotypic effect caused by the loss of d-VHL. Also DG overaccumulation in d-VHL mutant clones suggests loss of Egfr activity since DG is negatively regulated by Egfr (Poulton and Deng, 2006). DG overexpression can also impair follicle-cell polarity (Deng et al., 2003), by disrupting accumulation of the apically localized Bazooka/Par3 proteins. Moreover mutations in Egfr signalling lead to defects in apicobasal polarity such as weakened accumulation of β_h-Spectrin on the apical surface, and a loss of lateral DLG localization observed in Ras loss of function clones (Poulton and Deng, 2006). Moreover Poulton et al. (2006) showed a mislocalization of Kin:βGal in Ras loss of function clones and in DG overexpressing clones. Kinesin is required for the localization of *osk* RNA, *staufen*, and various other posterior determinants (Clark et al., 1994). Mislocalization of Kin:βGal suggests that the microtubule reorganization initiated by Egfr signalling (Theurkauf et al., 1992; Clark et al., 1994; Clark et al., 1997) has not occurred properly in egg chambers bearing to polarity defects. The presence of ectopic DG in the posterior follicle cells after stage 6 can inhibit proper localization of posterior determinants in the oocyte, which is likely a result of mislocalization of the microtubule plus ends. Giving that, d-VHL loss of function could lead to the loss of Egfr activity, defects in microtubule reorganization and consequently to a failure in the

downregulation of DG. However several different explanations of this process can be considered, such as the direct involvement of Egfr in the correct establishment of cell polarity.

Hsu et al. (2006) have demonstrated that in *h-VHL* null tumor cells or *h-VHL* knock-down cells, FGFR1 internalization is defective, leading to surface accumulation and abnormal activation of FGFR1. The hypothesis I proposed in my model is that Egfr in d-VHL loss of function follicle cell clones, accumulates on follicle cell surface and loses its activity as a consequence of MTs depolymerization and defects in endocytosis mechanisms. The accumulation is then leading to inactivation of the receptor. The data acquired have allowed to correlate Egfr activity and d-VHL mechanism in follicle cells and future studies will be addressed to better understand this interaction.

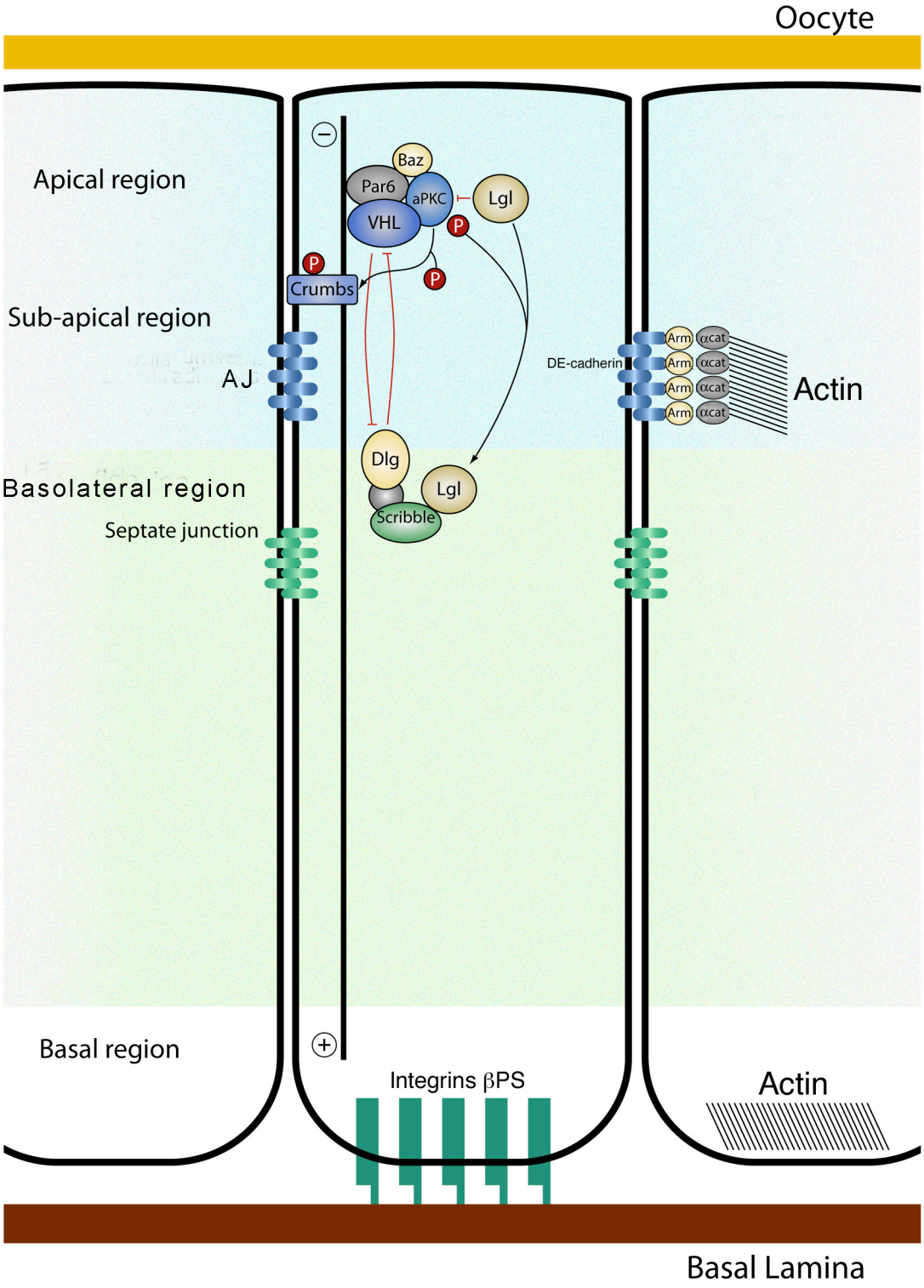

Figure 27.Proposed model of d-VHL mechanism for the maintenance of follicular epithelium integrity.

6. BIBLIOGRAPHY

Abdelilah-Seyfried S., Cox D.N., Jan Y.N., 2003 Bazooka is a permissive factor for the invasive behavior of discs large tumor cells in Drosophila ovarian follicular epithelia. *Development*, 130(9):1927-35;

Adryan B., Decker H.J., Papas T.S., Hsu T., 2000 Tracheal development and the von Hippel-Lindau tumor suppressor homolog in Drosophila. *Oncogene*, 19(24):2803-11;

Agrawal N., Kango M., Mishra A., Sinha P., 1995 Neoplastic transformation and aberrant cell-cell interactions in genetic mosaics of lethal(2)giant larvae (lgl), a tumor suppressor gene of Drosophila. *Dev Biol.*, 172(1):218-29;

Akhtar N., Hotchin NA., 2001 RAC1 regulates adherens junctions through endocytosis of E-cadherin. *Mol Biol Cell*., 12(4):847-62;

Andrenacci D., Cernilogar FM., Taddei C., Rotoli D., Cavaliere V., Graziani F., Gargiulo G., 2001 Specific domains drive VM32E protein distribution and integration in Drosophila eggshell layers. *J Cell Sci*, 114: 2819-2829;

Arquier N., Vigne P., Duplan E., Hsu T., Therond P.P., Frelin C., D'Angelo G., 2006 Analysis of the hypoxia-sensing pathway in Drosophila melanogaster. *Biochem. J.*, 393(Pt 2):471-80;

Aso T., Yamazaki K., Aigaki T., Kitajima S., 2000 Drosophila von Hippel-Lindau tumor suppressor complex possesses E3 ubiquitin ligase activity. *Biochem. Biophys. Res. Commun*., 276(1):355-61;

Aso T., Conrad MN., 1997 Molecular cloning of DNAs encoding the regulatory subunits of elongin from Saccharomyces cerevisiae and Drosophila melanogaster. *Biochem Biophys Res Commun*., 241(2):334-40;

Bacallao R., Antony C., Dotti C., Karsenti E., Stelzer EH., Simons K., 1989 The subcellular organization of Madin-Darby canine kidney cells during the formation of 3a

polarized epithelium. *J Cell Biol.*, 109(6 Pt 1):2817-32;

Bacon N.C., Wappner P., O'Rourke J.F., Bartlett S.M., Shilo B., Pugh C.W., Ratcliffe P.J., 1998 Regulation of the Drosophila bHLH-PAS protein Sima by hypoxia: functional evidence for homology with mammalian HIF-1 alpha. *Biochem. Biophys. Res. Commun.*, 249(3):811-6;

Bateman J., Reddy R.S., Saito H., Van Vactor D., 2001 The receptor tyrosine phosphatase Dlar and integrins organize actin filaments in the Drosophila follicular epithelium. *Curr. Biol.*, 11(17):1317-27;

Baum B., Li W., Perrimon N., 2000 A cyclase-associated protein regulates actin and cell polarity during Drosophila oogenesis and in yeast. *Curr Biol.*, 10(16):964-73;

Beccari S., Teixeira L., Rørth P., 2002 The JAK/STAT pathway is required for border cell migration during Drosophila oogenesis. *Mech Dev.*, 111(1-2):115-23;

Bernardi F., Cavaliere V., Andrenacci D., Gargiulo G., 2006 Dpp signaling down-regulates the expression of VM32E eggshell gene during Drosophila oogenesis. *Dev Dyn.*, 235(3):768-75;

Bernardi F., Duchi S., Cavaliere V., Donati A., Andrenacci D., Gargiulo G., 2007 Egfr signaling modulates VM32E gene expression during Drosophila oogenesis. *Dev Genes Evol.*, 217(7):529-40;

Béroud C., Joly D., Gallou C., Staroz F., Orfanelli M.T., Junien C., 1998 Software and database for the analysis of mutations in the VHL gene. *Nucleic Acids Res.*, 26(1):256-8;

Betschinger J., Mechtler K., Knoblich JA., 2003 The Par complex directs asymmetric cell division by phosphorylating the cytoskeletal protein Lgl. Nature, 422(6929):326-30;

Bilder D. and Perrimon N., 2000 Localization of apical epithelial determinants by the basolateral PDZ protein Scribble. *Nature*, 403(6770):676-80;

Bilder D., Schober M., Perrimon N., 2003 Integrated activity of PDZ protein complexes regulates epithelial polarity. *Nat. Cell. Biol.*, 5(1):53-8;

Bishop T., Lau K.W., Epstein A.C., Kim S.K., Jiang M., O'Rourke D., Pugh C.W., Gleadle J.M., Taylor M.S., Hodgkin J., Ratcliffe P.J., 2004 Genetic analysis of pathways regulated by the von Hippel-Lindau tumor suppressor in Caenorhabditis elegans. *PLoS Biol*., 2(10):e289;

Bohrmann J., Braun B., 1999 Na,K-ATPase and V-ATPase in ovarian follicles of Drosophila melanogaster. *Biol Cell.*, 91(2):85-98;

Bonicalzi M.E., Groulx I., de Paulsen N., Lee S., 2001 Role of exon 2-encoded beta - domain of the von Hippel-Lindau tumor suppressor protein. *J. Biol. Chem*., 276(2):1407-16;

Borg JP., 2004 hScrib: a potential novel tumor suppressor. *Pathol Biol (Paris),* 52(6):328-31;

Bossinger O., Klebes A., Segbert C., Theres C., Knust E., 2001 Zonula adherens formation in Caenorhabditis elegans requires dlg-1, the homologue of the Drosophila gene discs large. *Dev Biol.,* 230(1):29-42;

Brancaccio A., 2005 Alpha-dystroglycan, the usual suspect? *Neuromuscul Disord,* 15(12):825-8;

Bré MH., Pepperkok R., Hill AM., Levilliers N., Ansorge W., Stelzer EH., Karsenti E., 1990 Regulation of microtubule dynamics and nucleation during polarization in MDCK II cells. *J Cell Biol*., 111(6 Pt 2):3013-21;

Brito DA., Yang Z., Rieder CL., 2008 Microtubules do not promote mitotic slippage when the spindle assembly checkpoint cannot be satisfied. *J Cell Biol.*, 182(4):623-9;

Brown NH., 2000 Cell-cell adhesion via the ECM: integrin genetics in fly and worm. *Matrix Biol.,* 19(3):191-201;

Brown NH., Gregory SL., Rickoll WL., Fessler LI., Prout M., White RA., Fristrom JW., 2002 Talin is essential for integrin function in Drosophila. *Dev Cell*., 3(4):569-79;

Bruick R.K., McKnight S.L., 2001 A conserved family of prolyl-4-hydroxylases that modify HIF. *Science*, 294(5545):1337-40;

Burke T., Waring G. L., Popodi E. and Minoo P., 1987 Characterization and sequence of follicle cell genes selectively expressed during vitelline membrane formation in *Drosophila*. *Dev. Biol.*, 124:441-450;

Calzada M.J., Esteban M.A., Feijoo-Cuaresma M., Castellanos M.C., Naranjo-Suárez S., Temes E., Méndez F., Yánez-Mo M., Ohh M., Landázuri M.O., 2006 von Hippel-Lindau tumor suppressor protein regulates the assembly of intercellular junctions in renal cancer cells through hypoxia-inducible factor-independent mechanisms. *Cancer Res*., 66(3):1553-60;

Cavaliere V., Spanò S., Andrenacci D., Cortesi L., Gargiulo G., 1997 Regulatory elements in the promoter of the vitelline membrane gene VM32E of Drosophila melanogaster direct gene expression in distinct domains of the follicular epithelium. *Mol Gen Genet*., 254(3):231-7;

Cavaliere V., Taddei C. and Gargiulo G., 1998 Apoptosis of nurse cells at the late stages of oogenesis of *Drosophila melanogaster*. *Dev. Genes Evol.*, 208:106-112;

Cavaliere V., Bernardi F., Romani P., Duchi S., Gargiulo G., 2008 Building up the Drosophila eggshell: First of all the eggshell genes must be transcribed. *Developmental Dynamics* 237:2061-2072;

Champion K.J., Guinea M., Dammai V., Hsu T., 2008 Endothelial function of von Hippel-Lindau tumor suppressor gene: control of fibroblast growth factor receptor signaling. *Cancer Res*., 68(12):4649-57;

Clark I., Giniger E., Ruohola-Baker H., Jan LY., Jan YN., 1994 Transient posterior localization of a kinesin fusion protein reflects anteroposterior polarity of the Drosophila oocyte. *Curr Biol.*, 4(4):289-300;

Clark IE., Jan LY., Jan YN., 1997 Reciprocal localization of Nod and kinesin fusion proteins indicates microtubule polarity in the Drosophila oocyte, epithelium, neuron and muscle. *Development,* 124(2):461-70;

Claycomb JM., Benasutti M., Bosco G., Fenger DD., Orr-Weaver TL., 2004 Gene amplification as a developmental strategy: isolation of two developmental amplicons in Drosophila. Dev Cell, 6: 145-155;

Clifford RJ., Schüpbach T., 1989 Coordinately and differentially mutable activities of torpedo, the Drosophila melanogaster homolog of the vertebrate EGF receptor gene. *Genetics,* 123(4):771-87;

Dammai V., Adryan B., Lavenburg K.R., Hsu T., 2003 Drosophila awd, the homolog of human nm23, regulates FGF receptor levels and functions synergistically with shi/dynamin during tracheal development. *Genes Dev*., 17(22):2812-24;

Davidowitz E.J., Schoenfeld A.R., Burk R.D., 2001 VHL induces renal cell differentiation and growth arrest through integration of cell-cell and cell-extracellular matrix signaling. *Mol. Cell Biol*., 21(3):865-74;

Delidakis C., Kafatos FC., 1989 Amplification enhancers and replication origins in the autosomal chorion gene cluster of *Drosophila*. *EMBO J*, 8: 891-901;

Deng WM., Schneider M., Frock R., Castillejo-Lopez C., Gaman EA., Baumgartner S., Ruohola-Baker H., 2003 Dystroglycan is required for polarizing the epithelial cells and the oocyte in Drosophila. *Development*, 130(1):173-84;

Dobens LL., Raftery LA., 2000 Integration of epithelial patterning and morphogenesis in Drosophila ovarian follicle cells. *Dev Dyn.*, 218(1):80-93;

Dubreuil RR., Yu J., 1994 Ankyrin and beta-spectrin accumulate independently of alpha-spectrin in Drosophila. *Proc Natl Acad Sci,* 91(22):10285-9;

Duffy J.B., Harrison D.A., Perrimon N., 1998 Identifying loci required for follicular patterning using directed mosaics. *Development*., 125(12):2263-71;

Epstein A.C., Gleadle J.M., McNeill L.A., Hewitson K.S., O'Rourke J., Mole D.R., Mukherji M., Metzen E., Wilson M.I., Dhanda A., Tian Y.M., Masson N., Hamilton D.L., Jaakkola P., Barstead R., Hodgkin J., Maxwell P.H., Pugh C.W., Schofield C.J., Ratcliffe P.J., 2001 C. elegans EGL-9 and mammalian homologs define a family of dioxygenases that regulate HIF by prolyl hydroxylation. *Cell*, (1):43-54;

Esteban M.A., Tran M.G., Harten S.K., Hill P., Castellanos M.C., Chandra A., Raval R., O'brien T.S., Maxwell P.H., 2006 Regulation of E-cadherin expression by VHL and hypoxia-inducible factor. *Cancer Res.,* 66(7):3567-75;

Esteban-Barragán M.A., Avila P., Alvarez-Tejado M., Gutiérrez M.D., García-Pardo A., Sánchez-Madrid F., Landázuri M.O., 2002 Role of the von Hippel-Lindau tumor suppressor gene in the formation of beta1-integrin fibrillar adhesions. *Cancer Res*., (10):2929-36;

Etienne-Manneville S., Hall A., 2003 Cell polarity: Par6, aPKC and cytoskeletal crosstalk. *Curr Opin Cell Biol*., 15(1):67-72;

Evans A.J., Russell R.C., Roche O., Burry T.N., Fish J.E., Chow V.W., Kim W.Y., Saravanan A., Maynard M.A., Gervais M.L., Sufan R.I., Roberts A.M., Wilson L.A., Betten M., Vandewalle C., Berx G., Marsden P.A., Irwin M.S., Teh B.T., Jewett M.A., Ohh M., 2007 VHL promotes E2 box-dependent E-cadherin transcription by HIF-mediated regulation of SIP1 and snail. *Mol. Cell Biol*., 27(1):157-69;

Fakhouri M., Elalayli M., Sherling D., Hall JD., Miller E., Sun X., Wells L., LeMosy EK., 2006 Minor proteins and enzymes of the Drosophila eggshell matrix. *Dev Biol*, 293: 127-141;

Fernández-Miñán A., Martín-Bermudo MD., González-Reyes A., 2007 Integrin signaling regulates spindle orientation in Drosophila to preserve the follicular-epithelium monolayer. *Curr Biol.*, 17(8):683-8;

Fernández-Miñán A., Cobreros L., González-Reyes A., Martín-Bermudo MD., 2008 Integrins contribute to the establishment and maintenance of cell polarity in the follicular epithelium of the Drosophila ovary. *Int J Dev Biol.,* 52(7):925-32;

Fessler JH., Fessler LI., 1989 Drosophila extracellular matrix. *Annu Rev Cell Biol*, 5:309-39;

Foley and Cooley, 1998 Apoptosis in late stage *Drosophila* nurse cells does not require genes within the H99 deficiency. *Development*, 125:1075-1082;

Gargiulo G., Gigliotti S., Malva C., Graziani F., 1991 Cellular specificity of expression and regulation of Drosophila vitelline membrane protein 32E gene in the follicular epithelium: identification of cis-acting elements. *Mech Dev*, 35: 193-203;

Gigliotti S., Graziani F., de Ponti L., Rafti F., Manzi A., Lavorgna G., Gargiulo G. and Malva C., 1989 Sex-, tissue-, and stage-specific expression of a vitelline membrane protein gene from region 32 of the second chromosome of *Drosophila melanogaster*. *Dev. Genet.,* 10:33-41;

Gnarra JR., Tory K., Weng Y., Schmidt L., Wei MH., Li H., Latif F., Liu S., Chen F., Duh FM., et al. 1994 Mutations of the VHL tumour suppressor gene in renal carcinoma. *Nat Genet.*, 7(1):85-90;

Godt D., Tepass U., 1998 *Drosophila* oocyte localization is mediated by differential cadherin-based adhesion. *Nature*, 395:387-391;

Golic KG., 1991 Site-specific recombination between homologous chromosomes in Drosophila. *Science*, 252(5008):958-61;

Gonzalez-Reyes A., Elliott H., St. Johnston R. D., 1995 Polarization of both major body axes in *Drosophila* by gurken-torpedo signalling. *Nature*, 375:654-658;

Gonzalez-Reyes A., St. Johnston D., 1998 The *Drosophila* AP axis is polarised by the cadherin-mediated positioning of the oocyte. *Development*, 125:3635-3644;

Goode S., Melnick M., Chou T.B., Perrimon N., 1996 The neurogenic genes egghead and brainiac define a novel signaling pathway essential for epithelial morphogenesis during Drosophila oogenesis. *Development*., 122(12):3863-79;

Grammont M., Irvine KD., 2002 Organizer activity of the polar cells during Drosophila oogenesis. *Development*,129(22):5131-40;

Grifoni D., Garoia F., Schimanski CC., Schmitz G., Laurenti E., Galle PR., Pession A., Cavicchi S., Strand D., 2004 The human protein Hugl-1 substitutes for Drosophila lethal giant larvae tumour suppressor function in vivo. *Oncogene*, 23(53):8688-94;

Grünert S., St Johnston D., 1996 RNA localization and the development of asymmetry during Drosophila oogenesis. *Curr Opin Genet Dev*., 6(4):395-402;

Gutzeit H.O., Eberhardt W., Gratwohl E., 1991 Laminin and basement membrane-associated microfilaments in wild-type and mutant Drosophila ovarian follicles. *J. Cell. Sci*., 100(Pt 4):781-8:

Harris TJ., Peifer M., 2007 aPKC controls microtubule organization to balance adherens junction symmetry and planar polarity during development. *Dev Cell*., 12(5):727-38;

Hendzel M.J., Wei Y., Mancini M.A., Van Hooser A., Ranalli T., Brinkley B.R., Bazett-Jones D.P., Allis C.D., 1997 Mitosis-specific phosphorylation of histone H3 initiates primarily within pericentromeric heterochromatin during G2 and spreads in an ordered fashion coincident with mitotic chromosome condensation. *Chromosoma*., 106(6):348-60;

Hergovich A., Lisztwan J., Barry R., Ballschmieter P., Krek W., 2003 Regulation of microtubule stability by the von Hippel-Lindau tumour suppressor protein pVHL. *Nat. Cell Biol*., 5(1):64-70;

Hergovich A., Lisztwan J., Thoma C.R., Wirbelauer C., Barry R.E., Krek W., 2006 Priming-dependent phosphorylation and regulation of the tumor suppressor pVHL by glycogen synthase kinase 3. *Mol. Cell Biol*., 26(15):5784-96;

Higgins MJ., Walker VK., Holden JA., White BN., 1984 Isolation of two Drosophila melanogaster genes abundantly expressed in the ovary during vitelline membrane synthesis. *Dev Biol*, 105: 155-165;

Horne-Badovinac S. and Bilder D., 2005 Mass transit: epithelial morphogenesis in the Drosophila egg chamber. Dev Dyn., 232:559-74;

Hrdlicka L., Gibson M., Kiger A., Micchelli C., Schober M., Schöck F., Perrimon N., 2002 Analysis of twenty-four Gal4 lines in Drosophila melanogaster. Genesis., 34(1-2):51-7;

Hsu T., Adereth Y., Kose N., Dammai V., 2006 Endocytic function of von Hippel-Lindau tumor suppressor protein regulates surface localization of fibroblast growth factor receptor 1 and cell motility. *J. Biol. Chem*., 281(17):12069-80;

Hutterer A., Betschinger J., Petronczki M., Knoblich JA., 2004 Sequential roles of Cdc42, Par-6, aPKC, and Lgl in the establishment of epithelial polarity during Drosophila embryogenesis. *Dev Cell.*, 6(6):845-54;

Huynh JR., St Johnston D., 2004 The origin of asymmetry: early polarisation of the Drosophila germline cyst and oocyte. *Curr Biol.*, 8;14(11):R438-49;

Iliopoulos O., Kibel A., Gray S., Kaelin W.G. Jr., 1995 Tumour suppression by the human von Hippel-Lindau gene product. *Nat. Med*., 1(8):822-6;

Iliopoulos O., Ohh M. Kaelin WG Jr., 1998 pVHL19 is a biologically active product of the von Hippel-Lindau gene arising from internal translation initiation. *Proc Natl Acad Sci U S A.* 95(20):11661-6;

Isaac D.D. and Andrew D.J., 1996 Tubulogenesis in Drosophila: a requirement for the trachealess gene product. *Genes Dev*., 10(1):103-17;

Iturrioz X., Durgan J., Calleja V., Larijani B., Okuda H., Whelan R., Parker PJ., 2006 The von Hippel-Lindau tumour-suppressor protein interaction with protein kinase Cdelta. *Biochem J.,* 397(1):109-20;

Ivan M., Kaelin WG Jr., 2001 The von Hippel-Lindau tumor suppressor protein. *Curr Opin Genet Dev*.,11(1):27-34;

Iwai K., Yamanaka K., Kamura T., Minato N., Conaway RC., Conaway JW., Klausner RD., Pause A., 1999 Identification of the von Hippel-lindau tumor-suppressor protein as part of an active E3 ubiquitin ligase complex. *Proc Natl Acad Sci U S A*., 96(22):12436-41;

Jang AC., Starz-Gaiano M., Montell DJ., 2007 Modeling migration and metastasis in Drosophila. *J Mammary Gland Biol Neoplasia*, 12(2-3):103-14;

Jékely G., Rørth P., 2003 Hrs mediates downregulation of multiple signalling receptors in Drosophila. *EMBO Rep*., 4(12):1163-8;

Kaelin W.G. Jr., 2002 Molecular basis of the VHL hereditary cancer syndrome. *Nat. Rev. Cancer*., 2(9):673-82;

Kaelin WG., 2007 Von Hippel-Lindau disease. *Annu Rev Pathol.;*2:145-73;

Kaelin WG Jr., 2008 The von Hippel-Lindau tumour suppressor protein: O2 sensing and cancer. *Nat Rev Cancer*, 8(11):865-73;

Kamura T., Koepp DM., Conrad MN., Skowyra D., Moreland RJ., Iliopoulos O., Lane WS., Kaelin WG. Jr, Elledge SJ., Conaway RC., Harper JW., Conaway JW., 1999 Rbx1, a component of the VHL tumor suppressor complex and SCF ubiquitin ligase. *Science*, 284(5414):657-61;

Kibel A., Iliopoulos O., DeCaprio J.A., Kaelin W.G. Jr., 1995 Binding of the von Hippel-Lindau tumor suppressor protein to Elongin B and C. *Science*, 269(5229):1444-6;

King R. C., 1970 Ovarian development in *Drosophila melanogaster*. *Academic Press, New York, London and San Francisco*;

Knust E. and Bossinger O., 2002 Composition and formation of intercellular junctions in epithelial cells. *Science*, 298(5600):1955-9;

Knust E., 2000 Control of epithelial cell shape and polarity. *Curr Opin Genet Dev*, 10(5):471-5;

Kovac J., Oster H., Leitges M., 2007 Expression of the atypical protein kinase C (aPKC) isoforms iota/lambda and zeta during mouse embryogenesis. *Gene Expr Patterns*., 7(1-2):187-96;

Krishnamachary B., Zagzag D., Nagasawa H., Rainey K., Okuyama H., Baek J.H., Semenza G.L., 2006 Hypoxia-inducible factor-1-dependent repression of E-cadherin in von Hippel-Lindau tumor suppressor-null renal cell carcinoma mediated by TCF3, ZFHX1A, and ZFHX1B. *Cancer Res*., 66(5):2725-31;

Kuehn EW., Walz G., Benzing T., 2007 Von hippel-lindau: a tumor suppressor links microtubules to ciliogenesis and cancer development. *Cancer Res.*, 67(10):4537-40;

Latif F., Duh FM., Gnarra J., Tory K., Kuzmin I., Yao M., Stackhouse T., Modi W., Geil L., Schmidt L., et al., 1993 von Hippel-Lindau syndrome: cloning and identification of the plasma membrane Ca(++)-transporting ATPase isoform 2 gene that resides in the von Hippel-Lindau gene region. *Cancer Res*., 53(4):861-7;

Le Bivic A., 2005 E-cadherin-mediated adhesion is not the founding event of epithelial cell polarity in Drosophila. *Trends Cell Biol.,* 15(5):237-40;

Lecuit T., 2004 Junctions and vesicular trafficking during Drosophila cellularization. *J Cell Sci,* 117(Pt 16):3427-33;

Lee J.K., Brandin E., Branton D., Goldstein L.S., 1997 Alpha-Spectrin is required for ovarian follicle monolayer integrity in Drosophila melanogaster. *Development*., 124(2):353-62;

Lee C. Y., Robinson K. J., Doe C. Q., 2006 Lgl, Pins and aPKC regulate neuroblast self-renewal versus differentiation. *Nature* 439,594 -598;

Lee SJ., Lattouf JB., Xanthopoulos J., Linehan WM., Bottaro DP., Vasselli JR., 2008 Von Hippel-Lindau tumor suppressor gene loss in renal cell carcinoma promotes oncogenic epidermal growth factor receptor signaling via Akt-1 and MEK-1. *Eur Urol*., 54(4):845-53;

Leung DW., Cachianes G., Kuang WJ., Goeddel DV., Ferrara N., 1989 Vascular endothelial growth factor is a secreted angiogenic mitogen. *Science,* 246(4935):1306-9;

Levine E., Lee CH., Kintner C., Gumbiner BM., 1994 Selective disruption of E-cadherin function in early Xenopus embryos by a dominant negative mutant. *Development*, 120:901-909;

Lieubeau-Teillet B., Rak J., Jothy S., Iliopoulos O., Kaelin W., Kerbel R.S., 1998 Von Hippel-Lindau gene-mediated growth suppression and induction of differentiation in renal cell carcinoma cells grown as multicellular tumor spheroids. *Cancer Res*., 58(21):4957-62;

Lin H. and Spradling A., 1993 Germ line stem cell division and egg chamber development in transplanted *Drosophila* germaria. *Dev. Biol.,* 159:140-152;

Lisztwan J., Imbert G., Wirbelauer C., Gstaiger M., Krek W., 1999 The von Hippel-Lindau tumor suppressor protein is a component of an E3 ubiquitin-protein ligase activity. *Genes Dev*., 13(14):1822-33;

Liu Y. and Montell D.J., 1999 Identification of mutations that cause cell migration defects in mosaic clones. Development., 126(9):1869-78;

Lolkema MP., Mehra N., Jorna AS., van Beest M., Giles RH., Voest EE., 2004 The von Hippel-Lindau tumor suppressor protein influences microtubule dynamics at the cell periphery. *Exp Cell Res.*, 301(2):139-46;

Lolkema M.P., Gervais M.L., Snijckers C.M., Hill R.P., Giles R.H., Voest E.E., Ohh M., 2005 Tumor suppression by the von Hippel-Lindau protein requires phosphorylation of the acidic domain. *J. Biol. Chem*., 280(23):22205-11;

Lolkema MP., Mans DA., Snijckers CM., van Noort M., van Beest M., Voest EE., Giles RH., 2007 The von Hippel-Lindau tumour suppressor interacts with microtubules through kinesin-2. *FEBS Lett*., 581(24):4571-6;

Lonergan K.M., Iliopoulos O., Ohh M., Kamura T., Conaway R.C., Conaway J.W., Kaelin W.G. Jr., 1998 Regulation of hypoxia-inducible mRNAs by the von Hippel-Lindau tumor suppressor protein requires binding to complexes containing elongins B/C and Cul2. *Mol. Cell Biol*., 18(2):732-41;

López-Schier H., 2003 The polarisation of the anteroposterior axis in Drosophila. *Bioessays*., 25(8):781-91;

Margaritis L. H., Kafatos F. C. and Petri W. H., 1980 The eggshell of *Drosophila melanogaster*. *J. Cell Sci.*, 43:1-35;

Margaritis LH., 1984 Microtubules during formation of the micropylar canal in Drosophila melanogaster. *Cell Biol Int Rep.*, 8(4):317-21;

Margaritis LH., 1985 The egg-shell of drosophila melanogaster III. Covalent crosslinking of the chorion proteins involves endogenous hydrogen peroxide. *Tissue Cell*., 17(4):553-9;

Margaritis LH., Mazzini M.,1998 Structure of the egg. In: Harrison FW, Locke M (eds) Microscopic anatomy of invertebrates. vol 11C "Insecta". Wiley-Liss, New York, pp 995-1037;

Maxwell PH., Wiesener MS., Chang GW., Clifford SC., Vaux EC., Cockman ME., Wykoff CC., Pugh CW., Maher ER., Ratcliffe PJ., 1999 The tumour suppressor protein VHL targets hypoxia-inducible factors for oxygen-dependent proteolysis. *Nature*, 399(6733):271-5;

Maxwell PH., Ferguson DJ., Nicholls LG., Johnson MH., Ratcliffe PJ., 1997 The interstitial response to renal injury: fibroblast-like cells show phenotypic changes and have reduced potential for erythropoietin gene expression. *Kidney Int*., 52(3):715-24;

Maxwell PH., 2005 The HIF pathway in cancer. *Semin Cell Dev Biol.,*16(4-5):523-30;

Min JH, Yang H., Ivan M., Gertler F., Kaelin WG Jr., Pavletich NP., 2002 Structure of an HIF-1alpha -pVHL complex: hydroxyproline recognition in signaling. *Science*, 296(5574):1886-9;

Mindrinos M. N., Scherer L. K., Garcini F. J., Kwan H., Jacobs K. A. and Petri W. H., 1985 Isolation and chromosomal location of putative vitelline membrane genes in *Drosophila melanogaster*. *EMBO J.*, 4:147-153;

Mooseker MS., 1985 Organization, chemistry, and assembly of the cytoskeletal apparatus of the intestinal brush border. *Annu Rev Cell Biol*, 1:209-41;

Müller H. A., 2000 Genetic control of epithelial cell polarity: lessons from Drosophila. *Dev Dyn.*, 218(1):52-67;

Müsch A., 2004 Microtubule organization and function in epithelial cells. *Traffic*, 5(1):1-9;

Nambu J.R., Chen W., Hu S., Crews S.T., 1996 The Drosophila melanogaster similar bHLH-PAS gene encodes a protein related to human hypoxia-inducible factor 1 alpha and Drosophila single-minded. *Gene*, 172(2):249-54;

Nambu J.R., Lewis J.O., Wharton K.A. Jr., Crews S.T., 1991 The Drosophila single-minded gene encodes a helix-loop-helix protein that acts as a master regulator of CNS midline development. *Cell*, 67(6):1157-67;

Naora H., Montell DJ., 2005 Ovarian cancer metastasis: integrating insights from disparate model organisms. *Nat Rev Cancer*, 5(5):355-66;

Nelson WJ., Hammerton RW., Wang AZ., Shore EM., 1990 Involvement of the membrane-cytoskeleton in development of epithelial cell polarity. *Semin Cell Biol,*. 1(5):359-71;

Nelson WJ., Yeaman C., 2001 Protein trafficking in the exocytic pathway of polarized epithelial cells. *Trends Cell Biol.*, 11(12):483-6;

Neuman-Silberberg FS., Schüpbach T., 1993 The Drosophila dorsoventral patterning gene gurken produces a dorsally localized RNA and encodes a TGF alpha-like protein. *Cell,* 75: 165-174;

Neuman-Silberberg FS., Schüpbach T., 1996 The Drosophila TGF-alpha-like protein Gurken: expression and cellular localization during Drosophila oogenesis. *Mech Dev*, 59: 105-113;

Nezis IP., Stravopodis DJ., Papassideri I., Robert-Nicoud M., Margaritis LH., 2002 Dynamics of apoptosis in the ovarian follicle cells during the late stages of Drosophila oogenesis. *Cell Tissue Res.*, 307(3):401-9;

Niewiadomska P., Godt D., Tepass U., 1999 DE-Cadherin is required for intercellular motility during Drosophila oogenesis. *J Cell Biol.,* 144(3):533-47;

Oda H., Uemura T., Takeichi M., 1997 Phenotypic analysis of null mutants for DE-cadherin and Armadillo in Drosophila ovaries reveals distinct aspects of their functions in cell adhesion and cytoskeletal organization. *Genes Cells*, 2(1):29-40;

Ohh M., Yauch R.L., Lonergan K.M., Whaley J.M., Stemmer-Rachamimov A.O., Louis D.N., Gavin B.J., Kley N., Kaelin W.G. Jr., Iliopoulos O., 1998 The von Hippel-Lindau tumor suppressor protein is required for proper assembly of an extracellular fibronectin matrix. *Mol. Cell*, 1(7):959-68;

Ohno S., 2001 Intercellular junctions and cellular polarity: the PAR-aPKC complex, a conserved core cassette playing fundamental roles in cell polarity. *Curr Opin Cell Biol*., 13(5):641-8;

Ohshiro T. and Saigo K., 1997 Transcriptional regulation of breathless FGF receptor gene by binding of TRACHEALESS/dARNT heterodimers to three central midline elements in Drosophila developing trachea. *Development*, 124(20):3975-86;

Ohshiro T., Yagami T., Zhang C., Matsuzaki F., 2000 Role of cortical tumour-suppressor proteins in asymmetric division of Drosophila neuroblast. *Nature*, 408(6812):593-6;

Orr-Weaver TL., 1991 *Drosophila* chorion genes: cracking the eggshell's secrets. *BioEssays*, 13: 97-105;

Okuda H., Hirai S., Takaki Y., Kamada M., Baba M., Sakai N., Kishida T., Kaneko S., Yao M., Ohno S., Shuin T., 1999 Direct interaction of the beta-domain of VHL tumor suppressor protein with the regulatory domain of atypical PKC isotypes. *Biochem. Biophys. Res. Commun*., 263(2):491-7;

Okuda H., Saitoh K., Hirai S., Iwai K., Takaki Y., Baba M., Minato N., Ohno S., Shuin T., 2001 The von Hippel-Lindau tumor suppressor protein mediates ubiquitination of activated atypical protein kinase C. *J. Biol. Chem*., 276(47):43611-7;

Pal S., Claffey K.P., Dvorak H.F., Mukhopadhyay D., 1997 The von Hippel-Lindau gene product inhibits vascular permeability factor/vascular endothelial growth factor expression in renal cell carcinoma by blocking protein kinase C pathways. *J. Biol Chem*., 272(44):27509-12;

Parks S, Spradling A., 1987 Spatially regulated expression of chorion genes during *Drosophila* oogenesis. Genes Dev, 1: 497-509;

Parks A.L., Cook K.R., Belvin M., Dompe N.A., Fawcett R., Huppert K., Tan L.R., Winter C.G., Bogart K.P., Deal J.E., Deal-Herr M.E., Grant D., Marcinko M., Miyazaki W.Y., Robertson S., Shaw K.J., Tabios M., Vysotskaia V., Zhao L., Andrade R.S., Edgar K.A., Howie E., Killpack K., Milash B., Norton A., Thao D., Whittaker K., Winner M.A., Friedman L., Margolis J., Singer M.A., Kopczynski C., Curtis D., Kaufman T.C., Plowman G.D., Duyk G., Francis-Lang H.L., 2004 Systematic generation of high-resolution deletion coverage of the Drosophila melanogaster genome. *Nat. Genet*., 36(3):211-2.

Pascucci T., Perrino J., Mahowald AP., Waring GL., 1996 Eggshell assembly in Drosophila: processing and localization of vitelline membrane and chorion proteins. *Dev Biol.*, 177(2):590-8;

Pause A., Lee S., Worrell R.A., Chen D.Y., Burgess W.H., Linehan W.M., Klausner R.D., 1997 The von Hippel-Lindau tumor-suppressor gene product forms a stable complex with human CUL-2, a member of the Cdc53 family of proteins. *Proc. Natl. Acad. Sci. U.S.A*., 94(6):2156-61;

Peifer M., Orsulic S., Sweeton D., Wieschaus E., 1993 A role for the Drosophila segment polarity gene armadillo in cell adhesion and cytoskeletal integrity during oogenesis. *Development*., 118(4):1191-207;

Peng CY., Manning L., Albertson R., Doe CQ., 2000 The tumour-suppressor genes lgl and dlg regulate basal protein targeting in Drosophila neuroblasts. *Nature*, 408(6812):596-600;

Peri F., Bokel C., Roth S., 1999 Local gurken signaling and dynamic MAPK activation during Drosophila oogenesis. *Mech Dev*, 81: 75-88;

Perrimon N., Perkins LA., 1997 There must be 50 ways to rule the signal: the case of the Drosophila EGF receptor. *Cell*, 89: 13-16;

Peterson JS., Barkett M., McCall K., 2003 Stage-specific regulation of caspase activity in drosophila oogenesis. *Dev Biol.* Aug 1;260(1):113-23;

Petronczki M. Knoblich JA., 2001 DmPAR -6 directs epithelial polarity and asymmetric cell division of neuroblasts in Drosophila. *Nat Cell Biol*., 3(1):43-9;

Plant PJ., Fawcett JP., Lin DC., Holdorf AD., Binns K., Kulkarni S., Pawson T., 2003 A polarity complex of mPar-6 and atypical PKC binds, phosphorylates and regulates mammalian Lgl. *Nat Cell Biol.,* 5(4):301-8;

Popodi E., Minoo P., Burke T. and Waring G. L., 1988 Organization and expression of a second chromosome follicle cell gene cluster in *Drosophila*. *Dev. Biol.*, 127:248-256;

Prasad M., Jang AC., Starz-Gaiano M., Melani M., Montell DJ., 2007 A protocol for culturing Drosophila melanogaster stage 9 egg chambers for live imaging. *Nat Protoc*., 2(10):2467-73;

Poulton J.S. and Deng W.M., 2006 Dystroglycan down-regulation links EGF receptor signaling and anterior-posterior polarity formation in the Drosophila oocyte. *Proc. Natl. Acad. Sci. U.S.A*., 103(34):12775-80;

Queenan AM., Ghabrial A., Schüpbach T., 1997 Ectopic activation of torpedo/Egfr, a Drosophila receptor tyrosine kinase, dorsalizes both the eggshell and the embryo. *Development*, 124(19):3871-80;

Quondamatteo F., 2002 Assembly, stability and integrity of basement membranes in vivo. *Histochem J.,* 34(8-9):369-81;

Ray R. P. and Schüpbach T., 1996 Intercellular signalling and the polarization of body axes during *Drosophila* oogenesis. *Genes Dev.*, 10:1711-1723;

Rittenhouse KR., Berg CA., 1995 Mutations in the Drosophila gene bullwinkle cause the formation of abnormal eggshell structures and bicaudal embryos. *Development*, 121(9):3023-33;

Rodriguez-Boulan E., Kreitzer G., Müsch A., 2005 Organization of vesicular trafficking in epithelia. *Nat Rev Mol Cell Biol.,* 6(3):233-47;

Roe J.S., Kim H., Lee S.M., Kim S.T., Cho E.J., Youn H.D., 2006 p53 stabilization and transactivation by a von Hippel-Lindau protein. *Mol. Cell*, 22(3):395-405;

Rogers SL., Rogers GC., Sharp DJ., Vale RD., 2002 Drosophila EB1 is important for proper assembly, dynamics, and positioning of the mitotic spindle. *J Cell Biol*., 158(5):873-84;

Rolls MM., Albertson R., Shih HP., Lee CY., Doe CQ., 2003 Drosophila aPKC regulates cell polarity and cell proliferation in neuroblasts and epithelia. *J Cell Biol.*, 163(5):1089-98;

Rübsam R., Hollmann M., Simmerl E., Lammermann U., Schäfer M.A., Büning J., Schäfer U., 1998 The egghead gene product influences oocyte differentiation by follicle cell-germ cell interactions in Drosophila melanogaster *Mech Dev.*, 7:131-40;

Ruohola H., Bremer KA., Baker D., Swedlow JR., Jan LY., Jan YN., 1991 Role of neurogenic genes in establishment of follicle cell fate and oocyte polarity during oogenesis in Drosophila. *Cell*, 66(3):433-49;

Schermer B., Ghenoiu C., Bartram M., Müller R.U., Kotsis F., Höhne M., Kühn W., Rapka M., Nitschke R., Zentgraf H., Fliegauf M., Omran H., Walz G., Benzing T., 2006 The von Hippel-Lindau tumor suppressor protein controls ciliogenesis by orienting microtubule growth. *J. Cell Biol*., 175(4):547-54;

Schneider I., 1972 Cell lines derived from late embryonic stages of Drosophila melanogaster. *J Embryol Exp Morphol*., 27(2):353-65;

Schober M., Rebay I., Perrimon N., 2005 Function of the ETS transcription factor Yan in border cell migration. *Development*, 132(15):3493-504;

Schüpback T., 1987 Germ line and soma co-operate during oogenesis to establish the dorsoventral pattern of egg shell and embryo in *Drosophila melanogaster*. *Cell,* 49:699-707;

Semenza GL., 1999 Regulation of mammalian O2 homeostasis by hypoxia-inducible factor 1. *Annu Rev Cell Dev Biol*., 15:551-78;

Sen J., Goltz JS., Stevens L., Stein D., 1998 Spatially restricted expression of pipe in the Drosophila egg chamber defines embryonic dorsal-ventral polarity. *Cell*, 95: 471-481;

Shcherbata HR., Althauser C., Findley SD., Ruohola-Baker H., 2004 The mitotic-to-endocycle switch in Drosophila follicle cells is executed by Notch-dependent regulation of G1/S, G2/M and M/G1 cell-cycle transitions. *Development,* 131(13):3169-81;

Shweiki D., Itin A., Soffer D., Keshet E., 1992 Vascular endothelial growth factor induced by hypoxia may mediate hypoxia-initiated angiogenesis. *Nature,* 359(6398):843-5;

Sikora S., Godzik A., 2004 Combination of multiple alignment analysis and surface mapping paves a way for a detailed pathway reconstruction--the case of VHL (von Hippel-Lindau) protein and angiogenesis regulatory pathway. *Protein Sci.*, 13(3):786-96;

Sonnenfeld M., Ward M., Nystrom G., Mosher J., Stahl S., Crews S., 1997 The Drosophila tango gene encodes a bHLH-PAS protein that is orthologous to mammalian Arnt and controls CNS midline and tracheal development. *Development*, 124(22):4571-82;

Sotillos S., Díaz-Meco MT., Caminero E., Moscat J., Campuzano S., 2004 DaPKC-dependent phosphorylation of Crumbs is required for epithelial cell polarity in Drosophila. *J Cell Biol.*, 166(4):549-57;

Spradling A. C., 1993 Developmental genetics of oogenesis. In the development of *Drosophila melanogaster*. Volume 1 (M. Bate and A. Martinez Arias, eds.). *Cold Spring Harbor, New York: Cold Spring Harbor Laboratory Press,* pp. 1-70;

Stebbins C.E., Kaelin W.G. Jr., Pavletich N.P., 1999 Structure of the VHL-ElonginC-ElonginB complex: implications for VHL tumor suppressor function. *Science*, 284(5413):455-61;

Sutovsky H. and Gazit E., 2004 The von Hippel-Lindau tumor suppressor protein is a molten globule under native conditions: implications for its physiological activities. *J. Biol. Chem*., 279(17):17190-6;

Suzuki A., Yamanaka T., Hirose T., Manabe N., Mizuno K., Shimizu M., Akimoto K., Izumi Y., Ohnishi T., Ohno S., 2001 Atypical protein kinase C is involved in the evolutionarily conserved PAR protein complex and plays a critical role in establishing epithelia-specific junctional structures. *J Cell Biol,* 152, 1183–1196;

Szafranski P. and Goode S., 2007 Basolateral junctions are sufficient to suppress epithelial invasion during Drosophila oogenesis. *Dev Dyn.*: 236(2):364-73;

Tanentzapf G., Smith C., McGlade J., Tepass U., 2000 Apical, lateral, and basal polarization cues contribute to the development of the follicular epithelium during Drosophila oogenesis. *J. Cell Biol*., 151(4):891-904;

Tanentzapf G. and Tepass U., 2003 Interactions between the crumbs, lethal giant larvae and bazooka pathways in epithelial polarization. *Nat. Cell. Biol*., 5(1):46-52;

Tepass U., Theres C., Knust E., 1990 Crumbs encodes an EGF-like protein expressed on apical membranes of Drosophila epithelial cells and required for organization of epithelia. *Cell*, 61(5):787-99;

Tepass U., 1997 Epithelial differentiation in Drosophila. *Bioessays*, 19(8):673-82;

Tepass U., 1999 Genetic analysis of cadherin function in animal morphogenesis. *Curr Opin Cell Biol*., 11(5):540-8;

Tepass U., Tanentzapf G., Ward R., Fehon R., 2001 Epithelial cell polarity and cell junctions in Drosophila. *Annu Rev Genet*, 35:747-84;

Theurkauf W. E., Smiley S., Wong M. L. and Alberts B. M., 1992 Reorganization of the cytoskeleton during *Drosophila* oogenesis: implications for axis specification and intercellular transport. *Development*, 115(4):923-936;

Thiery JP., 2002 Epithelial-mesenchymal transitions in tumour progression. *Nat Rev Cancer*, 2(6):442-54;

Tian AG., Deng WM., 2008 Lgl and its phosphorylation by aPKC regulate oocyte polarity formation in Drosophila. *Development,* 135(3):463-71;

Tsukita S., Furuse M., Itoh M., 2001 Multifunctional strands in tight junctions. *Nat. Rev. Mol. Cell Biol.,* 2:285–293;

Uemura T., Oda H., Kraut R., Hayashi S., Kotaoka Y., Takeichi M., 1996 Zygotic Drosophila E-cadherin expression is required for processes of dynamic epithelial cell rearrangement in the Drosophila embryo. *Genes Dev*.,10:659–67;

Vasioukhin V., 2006 Lethal giant puzzle of Lgl. *Dev Neurosci.,* 28(1-2):13-24;

Wang GL., Semenza GL., 1995 Purification and characterization of hypoxia-inducible factor 1. *J Biol Chem*., 270(3):1230-7;

Waring GL., 2000 Morphogenesis of the eggshell in Drosophila. *Int Rev Cytol.*, 198:67-108;

Wasserman JD., Freeman M., 1998 An autoregulatory cascade of EGF receptor signaling patterns the Drosophila egg. *Cell*, 95: 355-364;

Wilk R., Weizman I., Shilo B.Z., 1996 Trachealess encodes a bHLH-PAS protein that is an inducer of tracheal cell fates in Drosophila. *Genes Dev*., 10(1):93-102;

Wirtz-Peitz F., Knoblich JA., 2006 Lethal giant larvae take on a life of their own. *Trends Cell Biol.*, 16(5):234-41;

Wodarz A., Hinz U., Engelbert M., Knust E., 1995 Expression of crumbs confers apical character on plasma membrane domains of ectodermal epithelia of Drosophila. *Cell.*, 14;82(1):67-76;

Wodarz A., Ramrath A., Grimm A., Knust E., 2000 Drosophila atypical protein kinase C associates with Bazooka and controls polarity of epithelia and neuroblasts. *J. Cell Biol*., 150(6):1361-74;

Woods D.F., Wu J.W., Bryant P.J., 1996 Localization of proteins to the apico-lateral junctions of Drosophila epithelia. *Dev Genet*., 20(2):111-8;

Wu PS., Egger B., Brand AH., 2008 Asymmetric stem cell division: lessons from Drosophila. *Semin Cell Dev Biol,*19(3):283-93;

Xi R., McGregor JR., Harrison DA., 2003 A gradient of JAK pathway activity patterns the anterior-posterior axis of the follicular epithelium. *Dev Cell.*, 4(2):167-77;

Xu T., Rubin GM., 1993 Analysis of genetic mosaics in developing and adult Drosophila tissues. *Development*, 117(4):1223-37;

Xu T., Harrison SD., 1994 Mosaic analysis using FLP recombinase. *Methods Cell Biol.*, 44:655-81;

Yamanaka T., Horikoshi Y., Sugiyama Y., Ishiyama C., Suzuki A., Hirose T., Iwamatsu A., Shinohara A., Ohno S., 2003 Mammalian Lgl forms a protein complex with PAR-6 and aPKC independently of PAR-3 to regulate epithelial cell polarity. *Curr Biol*., 13(9):734-43;

Yamanaka T., Ohno S., 2008 Role of Lgl/Dlg/Scribble in the regulation of epithelial junction, polarity and growth. *Front Biosci*., 13:6693-707;

Yap AS., Brieher WM., Pruschy M., Gumbiner BM., 1997 Lateral clustering of the adhesive ectodomain: a fundamental determinant of cadherin function. *Curr Biol.*, 7(5):308-15;

Yee GH., Hynes RO., 1993 A novel, tissue-specific integrin subunit, beta nu, expressed in the midgut of Drosophila melanogaster. *Development*, 118(3):845-58;

Yu, J., Starr, D.A., Wu, X., Parkhurst, S.M., Zhuang, Y., Xu, T., Xu, R., Han, M., 2006 The KASH domain protein MSP-300 plays an essential role in nuclear anchoring during Drosophila oogenesis. *Dev. Biol.,* 289(2): 336-345;

Zahraoui A., Louvard D., Galli T., 2000 Tight junction, a platform for trafficking and signaling protein complexes. *J. Cell Biol.,* 151:F31–F36;

Zarnescu DC., Thomas GH., 1999 Apical spectrin is essential for epithelial morphogenesis but not apicobasal polarity in Drosophila. *J Cell Biol*., 146(5):1075-86.

7. SUMMARY

In *Drosophila melanogaster* the follicle cells form the follicular epithelium that surrounds the egg chamber and this epithelium is a powerful model system in which to study mechanisms underlying biological processes relevant to epithelial morphogenesis such as cell proliferation, cell growth, cell polarity, cell motility and cell death. The follicular epithelium shares morphological and molecular features with vertebrate's epithelia, so represents an excellent model system for studying signaling pathways involved in the correct differentiation of the subpopulation that compose it. Moreover follicular epithelium forms through a mesenchymal–epithelial transition (Tanentzapf et al, 2000) and indeed represents a powerful model for studying the EMT transition. Epithelial to mesenchymal transition (EMT), as well as the reverse process (MET), are extremely important for normal development. In addition, these transitions are important in wound healing, and tumor cells that develop from epithelial cells must transform into motile cells in order to metastasize. Importantly, loss of apicobasal cell polarity and cell adhesion, cytoskeleton reorganization, microtubule dynamics, disruption of basement membrane are some of the processes required for epithelial–mesenchymal transition (EMT), and they represent critical steps in cellular motility and invasiveness (Thiery, 2002).

During my PhD I have been involved in several projects regarding the morphogenesis of the follicular epithelium, such as the analysis of the pathways that correlate follicular epithelium patterning and eggshell gene expression. Moreover, during my PhD I used the follicular epithelium as a model system to analyze the function of the *Drosophila* homolog of the human von Hippel-Lindau (d-VHL*)* during oogenesis in order to gain insight into the role of h-VHL for the pathogenesis of VHL disease. h-VHL is implicated in a variety of processes and there is now a greater

appreciation of HIF-independent h-VHL functions that are relevant to tumour development, including maintenance and organization of the primary cilium, maintenance of the differentiated phenotype in renal cells and regulation of EMT (Kaelin, 2008). However, the function of *h-VHL* gene during development has not been fully understood. Adryan et al (2000) studied the *d-VHL* function during *Drosophila* embryogenesis and they showed that beside the highly conservation of *d-VHL* compared to the human counterpart, it has a role in the development of the *Drosophila* vasculature. Therefore, to examine whether d-VHL has a role in epithelial morphogenesis and maintenance, I performed genetic and molecular analyses by using *in vivo* and *in vitro* approaches. From my analysis, results evident that d-VHL binds to and stabilizes microtubules. Loss of d-VHL depolymerizes microtubules during oogenesis, leading to a possible deregulation in the subcellular trafficking transport of polarity markers from Golgi apparatus to the different domains in which follicle cells are divided (Nelson and Yeaman, 2001; Szafranski and Goode, 2007). As a consequence, aPKC complex, Armadillo, basolateral junction and basal junction components localization appears strongly affected, and the major defects are observed after stage 7 of oogenesis. Perturbation of d-VHL function in follicle cells clones causes indeed altered cell shape and distribution without affecting cell proliferation.

By analyzing the precise timing of synthesis of the *VM32E* eggshell component which relies on a fine regulation of gene expression, it is possible to assume an involvement of Egfr in d-VHL mechanism. Through clonal analysis I showed that loss of d-VHL causes an increase in VM32E protein levels comparable to the increment observed in Egfr loss of function clones (Bernardi et al., 2007). Moreover loss of Egfr activity affects the epithelium morphology and Dystroglycan localization. Interestingly,

the alteration in follicle cell shape and DG accumulation are similar to the phenotypic effect caused by the loss of d-VHL. Giving that, loss of d-VHL function could lead to the loss of Egfr activity, defects in microtubule reorganization and consequently to a failure in the downregulation of DG. The hypothesis I proposed in my model is that Egfr in d-VHL follicle cell clones accumulates on follicle cell surface and loses its activity as a consequence of MTs depolymerization and defects in endocytosis mechanisms.

The analysis carried out on d-VHL function during follicular epithelium development has allowed to establish a significant role of d-VHL in the maintenance of the follicular epithelium integrity.

8. ACKNOWLEDGEMENTS

These last pages of a PhD thesis are the most widely read pages of the entire publication. It is here where you will find out whether you have meant something in the life of the PhD candidate. And it is here were you'll figure out whether you have contribute to the low level of sanity left in this PhD candidate, after several years of studying eggshells and modifying flies genotypes!

First of all, I would like to express all my gratitude to Prof. Giuseppe Gargiulo and Prof. Valeria Cavaliere: you have believed in me since 2003 and you gave me the chance to become a "philosophy doctor". You provided me with direction, technical support, constantly teaching and writing assistance.

Many many many thanks to my colleagues! In alphabetical order: Doc. Fabio Zoccoletta Bernardi, for your patience and your invaluable mind. Doc. Alessandra Donati, because you taught me there are many options to avoid the frustrating life of researcher. Doc. Luca Toro Fagnocchi for your priceless technical and spiritual support. Doc. Patrizia Chinese Romani, for be my "fren" and my MacGyver everytime and anytime. Without all of you I would not have finished this thesis.

I really must to express my gratitude to Prof. Tien Hsu, to gave me the chance to spend 9 professionally wonderful and invaluable months in USA. His expertise, understanding, and patience, added considerably to my graduate experience. A very special thanks goes to Anita, Julie, Nurgun, Gouthami and Maria, without whose motivation, encouragement and help in molecular biology I wouldn't have considered to graduate so fast. Thank you to Doc. Stefania Lenna, for reagents supply, patience, real time PCR and…whatever! Thanks to "Sté and Paul" to make my stay in Charleston so unforgettable…hoping to be your Little One for the rest of your life. Thanks to Daniela Grifoni and her staff: Marcello, Francesca and Carmine. Thanks for feeding me with your holy coffee! And thanks Fede…I'll never forget our PS1 nights @ NYC.

I must also acknowledge Prof. Marialuisa Melli to share her invaluable expertises in cell culture with me. Many thanks to Franco Graziani to support me and to be an irreplaceable member of my committee.

How to forget all the people I met in South Carolina that directly or indirectly helped me to realize my thesis work. So, many thanks to Julia, Bridget and Kavin for gave me an home, Fabio, Joshua, Nate, Javier, Victor, Vincent, Carmine…to many to remember!

A special thanks to Elisa, because best friends share everything…a damn PhD as well!

Another special thanks to Stefy for your advices and your brave heart. Thanks to Tony Gorilla, because dreams are the answer and you make me feel so valuable in spite of everything. Thanks to Anna, because life without Rabbit is a boring and empty life, even I doubt that I will ever be able to convey my appreciation fully. Thanks to India and Tenzin, because you make me think that my rational and scientific lifestyle is often a flop! Thanks to Zapatero, because another politically school of thought is possible! Many thanks to my iPod who has been my best mentor in the long lonely days of writing! Thanks to Corona beers to be a cure for "certain injuries".

And last but not least, I need to acknowledge my family. Oscar and Lucy, you provide me the power and the proofs to believe in myself and science. Without your advices and love I wouldn't have follow my dreams and I would have never know how wonderful is world! And…thank you Massimo, because we believe in our future and we will always run after our wishes.